Appendix F
Hydrogeology

Klohn Crippen Berger

Ashurst Australia

ITRB Report on NTSF Embankment Failure

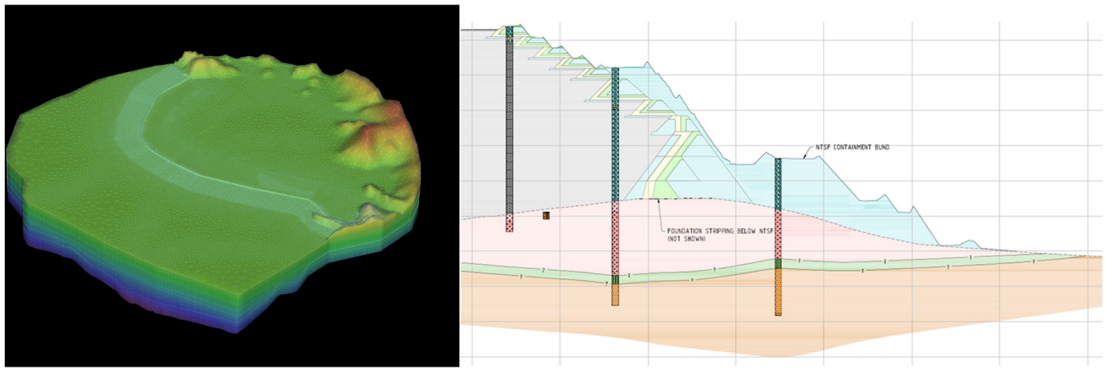

Hydrogeology Assessment Report

CANADA'S BEST MANAGED COMPANIES Platinum member

ISO 9001
ISO 14001
OHSAS 18001

D03353A02

March 2019

EXECUTIVE SUMMARY

A three-dimensional groundwater flow model has been constructed to replicate performance of the NTSF in the period leading up to the slump event that occurred in March of 2018. The model was constructed based on the conceptual understanding of the site, and the construction detail of the NTSF as it relates to internal management of seepage and phreatic conditions. There are four broad groundwater systems beneath the NTSF, being:

- Low permeability Ordovician volcanics;
- Low permeability Silurian sediments;
- Moderate to high permeability Tertiary basalt, which may include a buried palaeo channel;
- Quaternary alluvium, which in the immediate study area is poorly developed.

Structurally, the Werribee Fault underlies the NTSF and is a regionally mapped N to NNE- trending, westerly dipping thrust with a strike-slip component. Groundwater recharge of the basalt is most likely through rainfall recharge. Recharge of alluvium will be a combination of rainfall, creek flow and spring / seep contributions. Recharge into the Silurian / Ordovician will be via rainfall recharge and will also occur where saturated Tertiary basalt overlies these systems. Springs are noted throughout the area although do not appear to be deep seated in the area of the NTSF.

The NTSF design recognised, and construction had accounted for, the presence of springs and the potential impacts of a high permeability aquifer beneath the western embankment. Performance monitoring has indicated the underdrain installed during Stage 3 construction has performed as intended. Phreatic conditions within the tailings indicate downward drainage, and unsaturated tailings conditions of up to 8m below tailings elevation at the upstream of the embankment. Foundation seepage loss appears to be low and does not appear to have pressurised the contrastingly permeable underlying basalt.

The 3D model construction process was based on this conceptual and construction understanding and was also informed through 2D modelling to assess prominent hydraulic concepts of greatest relevance to prediction of conditions inside the NTSF. Model calibration was to three primary criteria determined to be most influential to NTSF seepage conditions:

- piezometric conditions of the tailings;
- vertical gradients within the tailings derived from CPtu testing; and,
- estimation of drain flow emerging from the Stage 3 underdrain.

Model calibration was able to replicate each of these criteria, and the model was set up to simulate Stage 10 construction to the time of the slump event under transient conditions. During the period of simulation, no significant rainfall was noted, pressure conditions within the tailings did not exhibit abnormal trends compared with prior or recent data, and the decant pond elevation was not substantially increased.

Model simulated conditions for the time of failure do not indicate occurrence of new or abnormal seepage emergence on the dam face, and the effect of the Stage 3 underdrain maintained phreatic conditions upstream of the dam lifts.

TABLE OF CONTENTS

TABLE OF CONTENTS
(continued)

List of Tables

List of Figures

TABLE OF CONTENTS

(continued)

TABLE OF CONTENTS

(continued)

1 INTRODUCTION

1.1 Project Background

1.1.1 Cadia Mine

Cadia Valley Operations (CVO) is a gold/copper mining and processing complex 25 km south of Orange in NSW (Figure 1). Cadia Holdings Pty Ltd (CHPL), a wholly owned subsidiary of Newcrest Mining Limited (NML), is the owner and operator of CVO. The CVO complex comprises the Cadia Hill, Ridgeway and Cadia East mines, minerals processing facilities and associated infrastructure. Mining commenced in 1998, with current approvals taking the project to 2031 (Hatch, 2018).

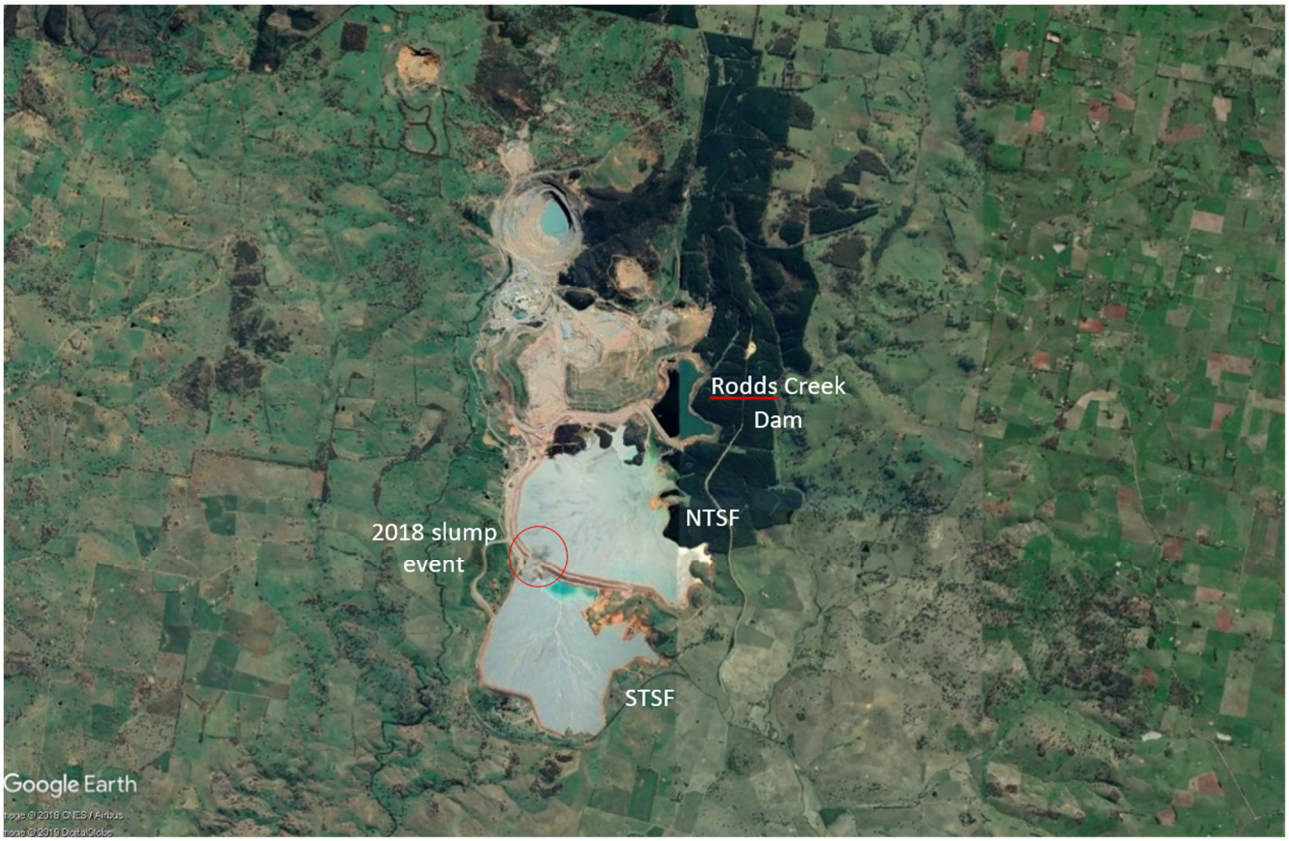

Figure 1: Cadia Mine General Layout (May 2018)

1.1.2 The NTSF Slump Event

There are two operational tailings storage facilities (TSF) at CVO; the Northern TSF (NTSF) and the Southern TSF (STSF) (Figure 1). Both TSF embankments were constructed across the former Rodds Creek. Construction of Stage 1 of the NTSF was completed in 1998, while construction of Stage 1 of the STSF was completed in November 2001. By mid-2007, tailings and decant water impounded by the STSF had commenced to encroach on the downstream toe of the NTSF (Hatch, 2018).

The NTSF is a Prescribed Dam under the requirements of the NSW Dams Safety Act 1978, with the NSW Dam Safety Committee (DSC) being the administering authority. At the time of the failure (March 2018), the NTSF was assigned a Consequence Category of Significant with an environmental approval for a final crest level of 779 mAHD. In the late afternoon of Friday 9th

March 2018, following the identification of cracks on the dam crest earlier in the day, a slump occurred on the western side of the southern embankment of the NTSF (Figure 2). The NTSF has been in operation for approximately 20 years and has been raised on average every two years (Hatch, 2018).

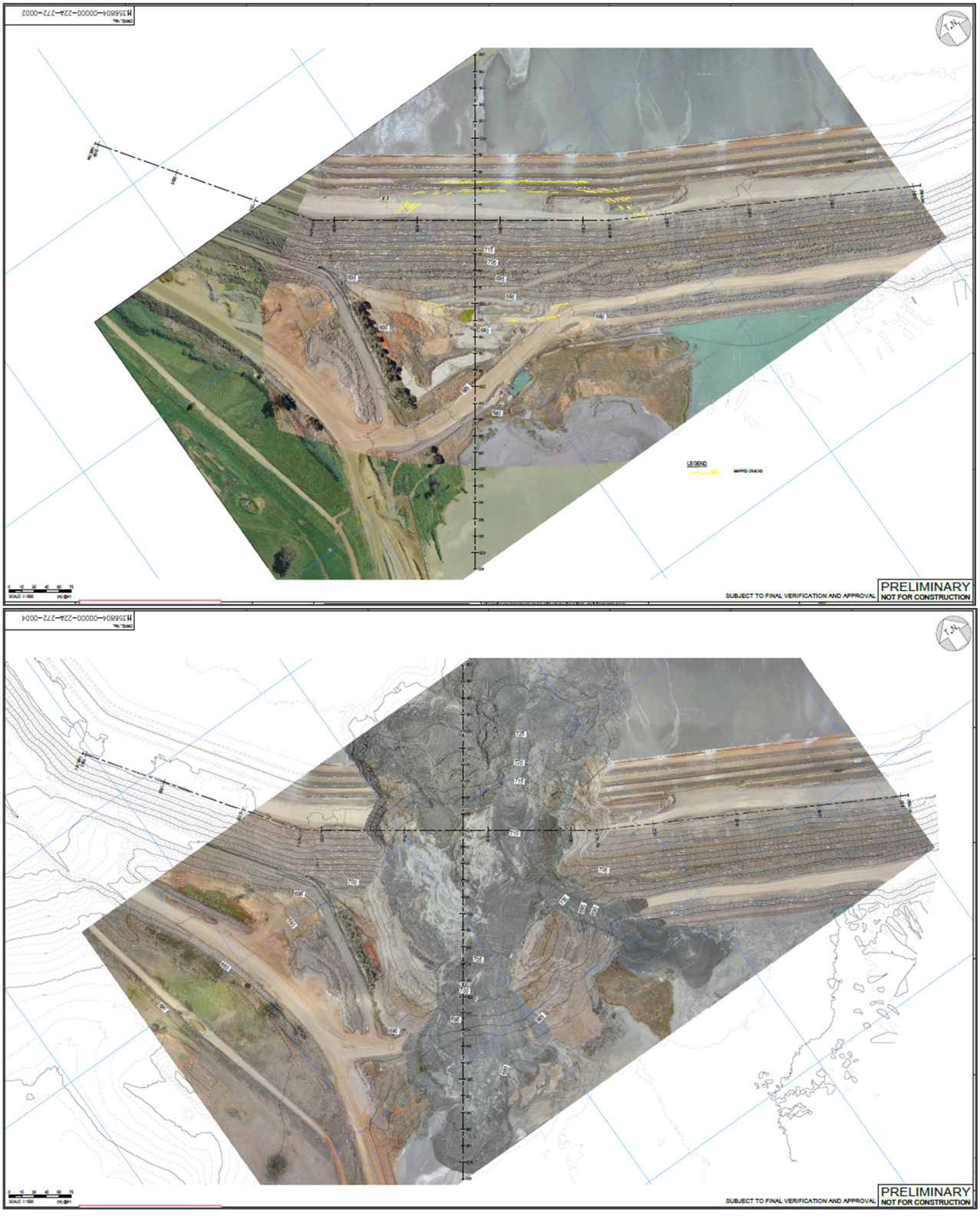

Figure 2: NTSF Area of Slump, Pre-slump (above), and Post-slump (below) (Hatch, 2018)

1.1.3 Intent of this Report

This report provides a technical assessment of pressure and seepage conditions in the period leading up to the slump event. This work is to provide key input to deformation and stability analysis being undertaken independently.

2 CONCEPTUAL HYDROGEOLOGY OF THE NTSF AREA

2.1 Regional Setting

2.1.1 Geological Framework

The project area lies within the eastern Lachlan Fold Belt of NSW. The Lachlan Fold Belt (the Belt) is divided into northerly trending metamorphic, volcanic, and sedimentary belts intruded by numerous igneous rocks. The rocks of the Belt are primarily of Ordovician, Silurian and Devonian age (AGE, 2009). A simplified summary of the Ordovician geology of the study area is provided in Figure 3, after (Wilson, 2003). The major Ordovician sequences of relevance to this assessment and which form part of the Belt are the mid Ordovician Weemalla Formation, and the late Ordovician Forest Reefs Volcanics.

Overlying the Ordovician across a large proportion of the NTSF and STSF footprint are rocks of the Silurian Ashburnia Group. Tertiary basalt and Quaternary alluvium conformably overlie Silurian and Ordovician units where they outcrop.

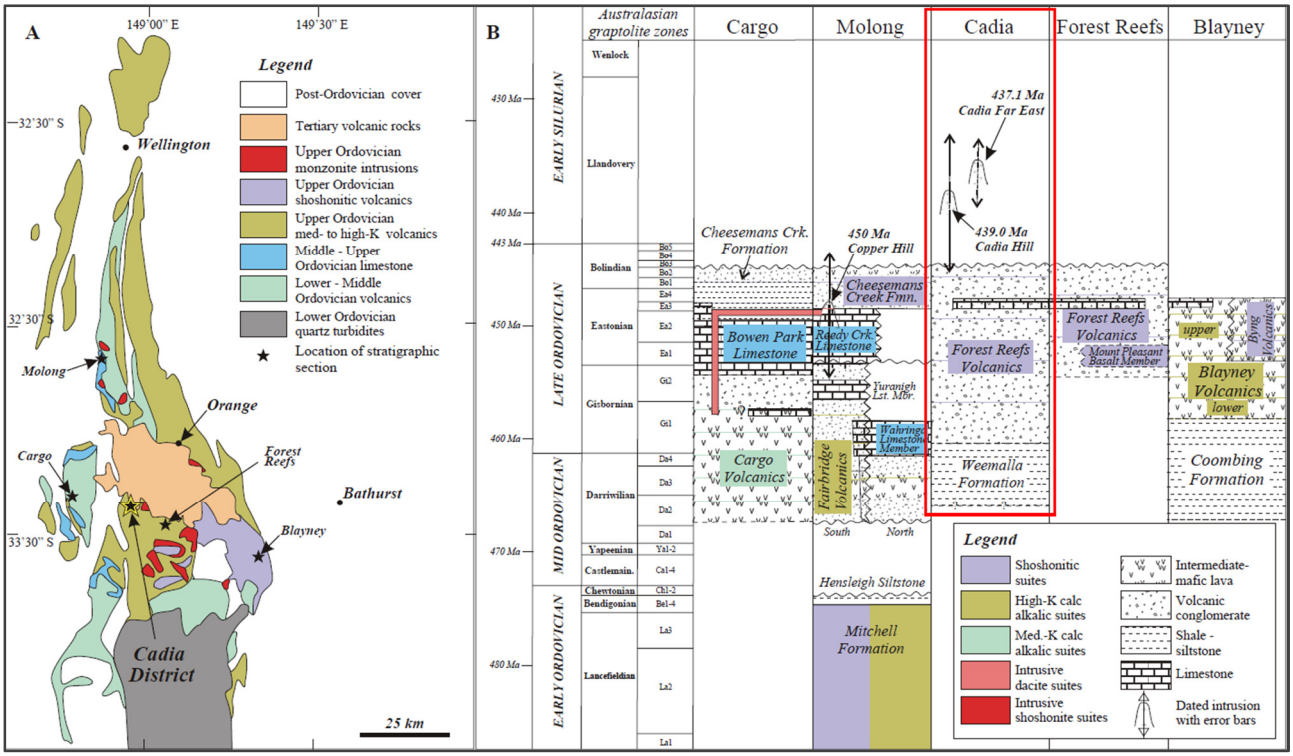

Figure 3: Simplified Ordovician Geology of the Molong Volcanic Belt after (Wilson, 2003), (Figure 2.4) (modified from Glen et al, 1998), Cadia area marked

The dominant regional structural features are a series of north trending reverse faults and related splays. Faults can form barriers to groundwater flow or can act as more transmissive conduits for water (AGE, 2009). The regional geology of the area is shown in Figure 4.

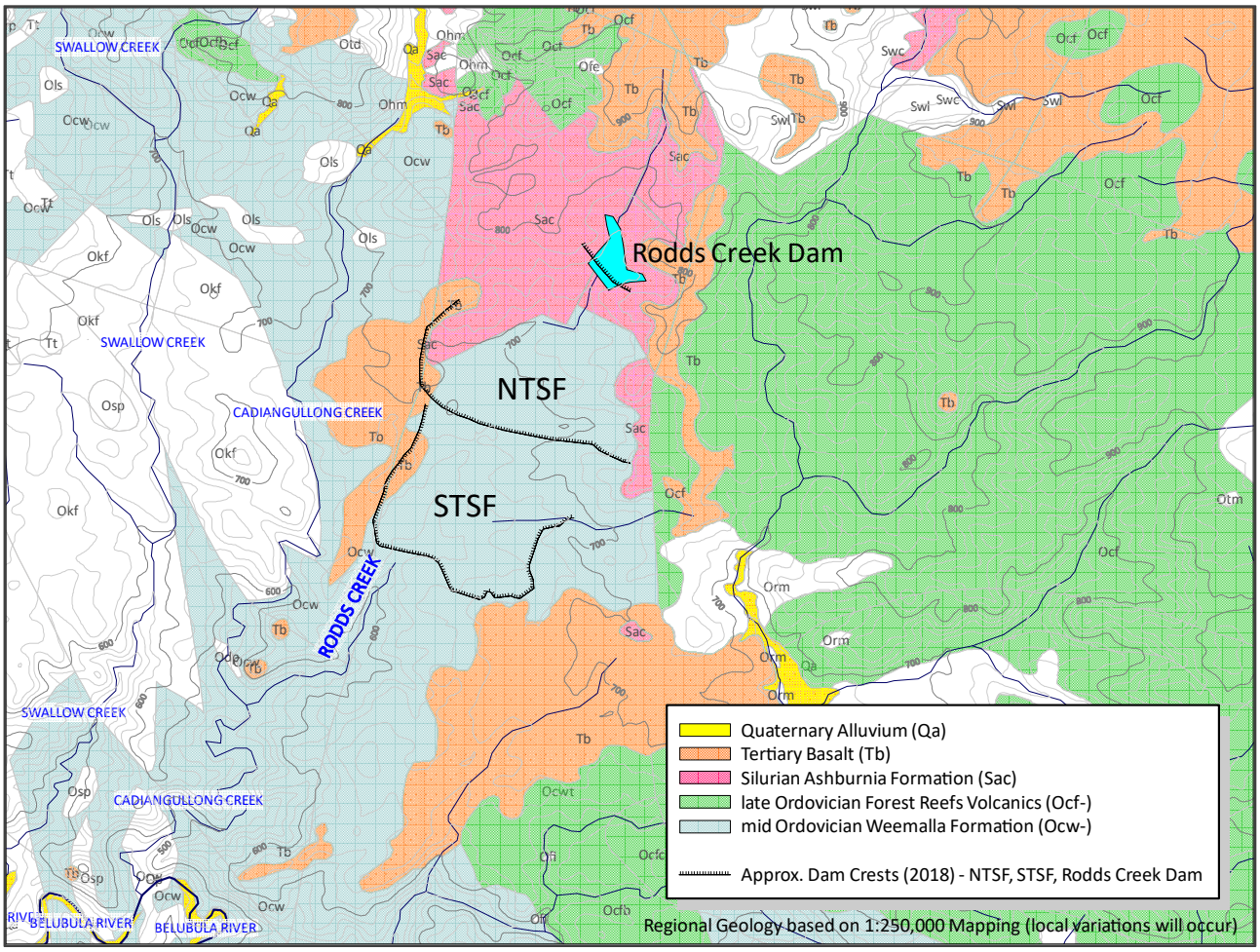

Figure 4: Regional Geology of the NTSF / STSF Area

2.2 Hydrology & Meteorology

Rainfall and creek flow monitoring data from five locations have been used to assess hydrology and rainfall conditions in the period before the slump. The location of these stations is provided in Figure 5, and the data are discussed in the following sections. The stations are:

Rainfall (daily, and long term CRD)

- 063133 Angullong, ~7.5 km southwest of the STSF
- 063254 Orange Agricultural Institute, ~25 km north-northeast of the NTSF

Creek Flow (gauge height and flow) for three stations, all within a few km of the NTSF, being:

- 412702 Cadiangullong Creek, upstream and west of the NTSF.
- 412161 Cadiangullong Creek, downstream and southwest of the STSF.
- 412147 South flowing creek northeast of the NTSF and upstream of Errowanbang.

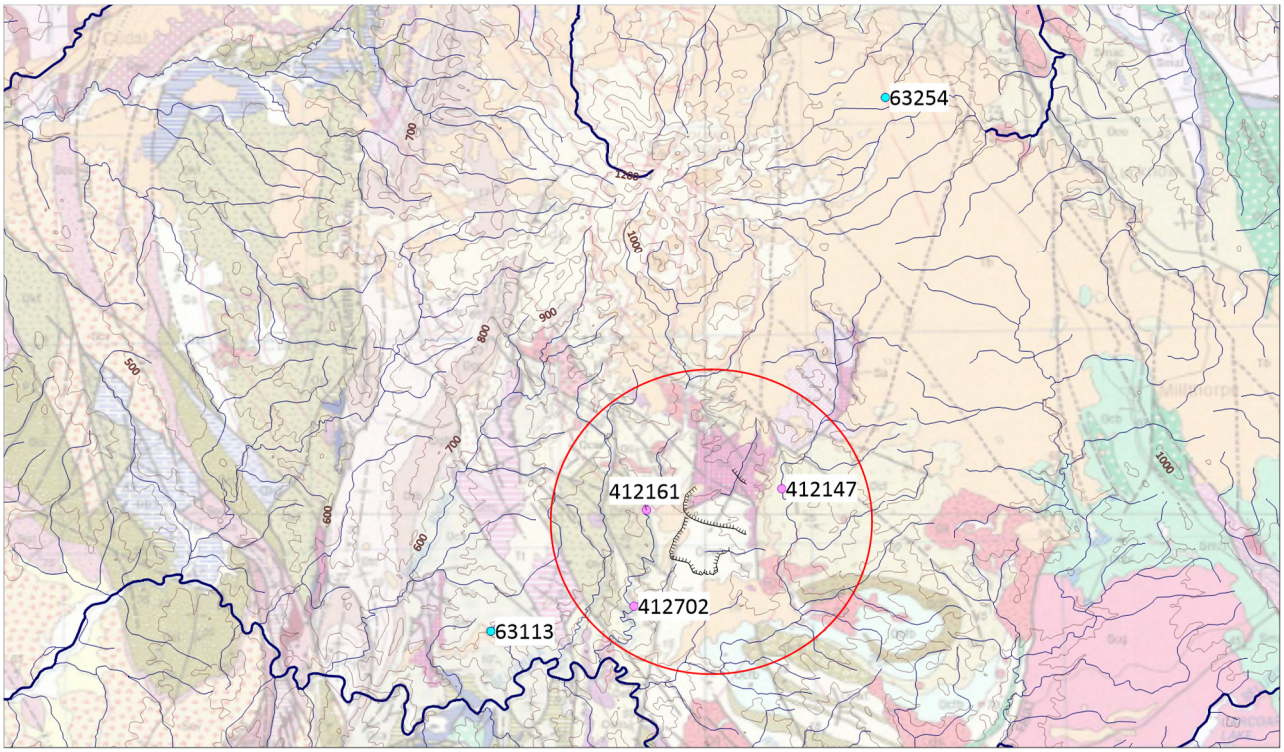

Figure 5: Location of Rainfall and Creek Flow Monitoring Stations

2.2.1 Meteorology

CRD (Cumulative Rainfall Departure) trend analyses has been applied in most of the recent hydrogeological reports for the mine. This data has been updated to after the slump for station 063254 (Orange Agricultural Station), which is applied in the recent works of AGE. This update is presented in Figure 6, and shows that rainfall has been below average for the 15 months preceding the slump event. A brief period of above average conditions producing an excess of about 500mm occurred between May and November 2016. Conditions were below average before this period, as far back as 2011.

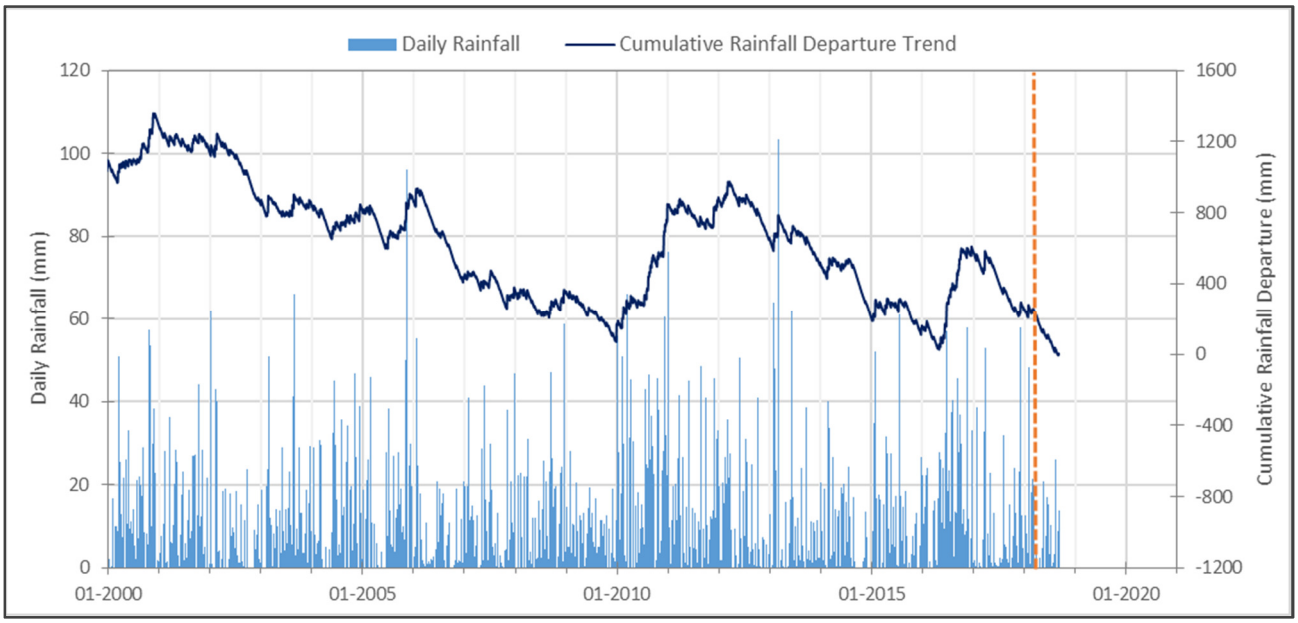

Figure 6: Long Term Rainfall (Daily Totals) and Daily CRD Trend for the Orange Agricultural Institute (063254), for the Period 2000 to 2020

Figure 7 shows daily rainfall totals for Stations 063133 and 063254 for the period leading up to the slump, marked as an orange bar for readability. Both stations observe good rainfall events in late January and late February as well as mid-May 2018. Stations 063254 observed ~20 mm rainfall ~3 days prior to the slump, although this event appears more local in nature with no rainfall recorded at Station 063133.

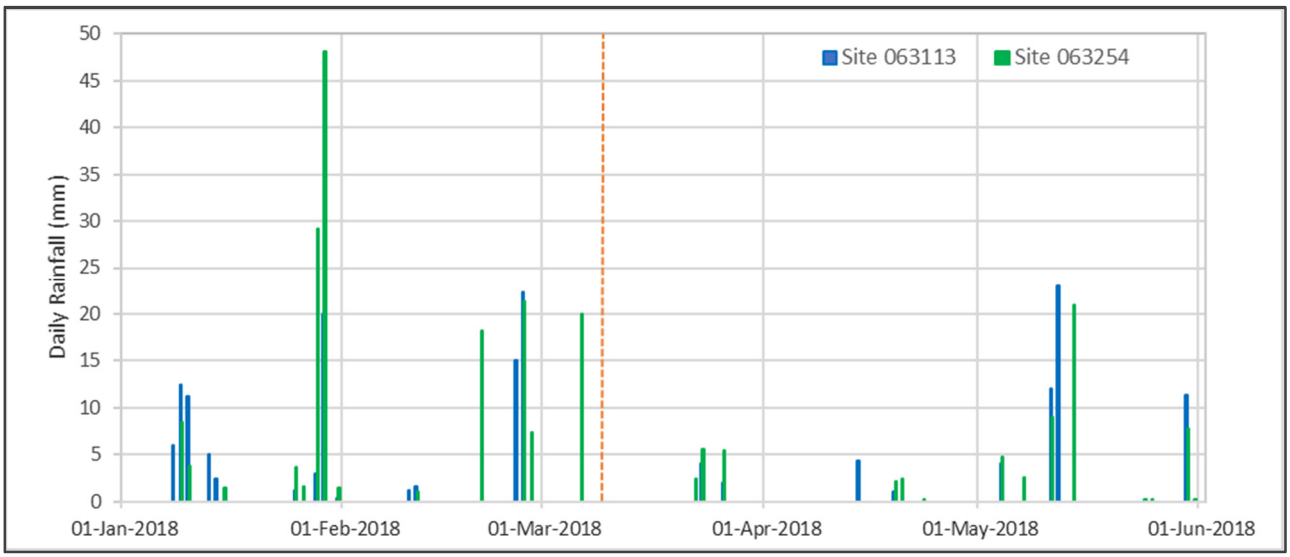

Figure 7: Daily Rainfall Totals Stations 063254 (Orange Agricultural Institute) and 063133 Angullong for the Period 2010 to 2015

2.2.2 Drainage

The NTSF and STSF (and the Rodds Creek Dam) each lie in the original Rodds Creek drainage (Figure 4). There are two stream gauging locations to the west of the NTSF/STSF complex located on Cadiangullong Creek, being stations 412702 and 412161. In the east, there is one location on

the southerly flowing Flyers Creek. All three stations (Figure 8) show similar response to rainfall for the 2018 period of record surrounding the slump event (Figure 7).

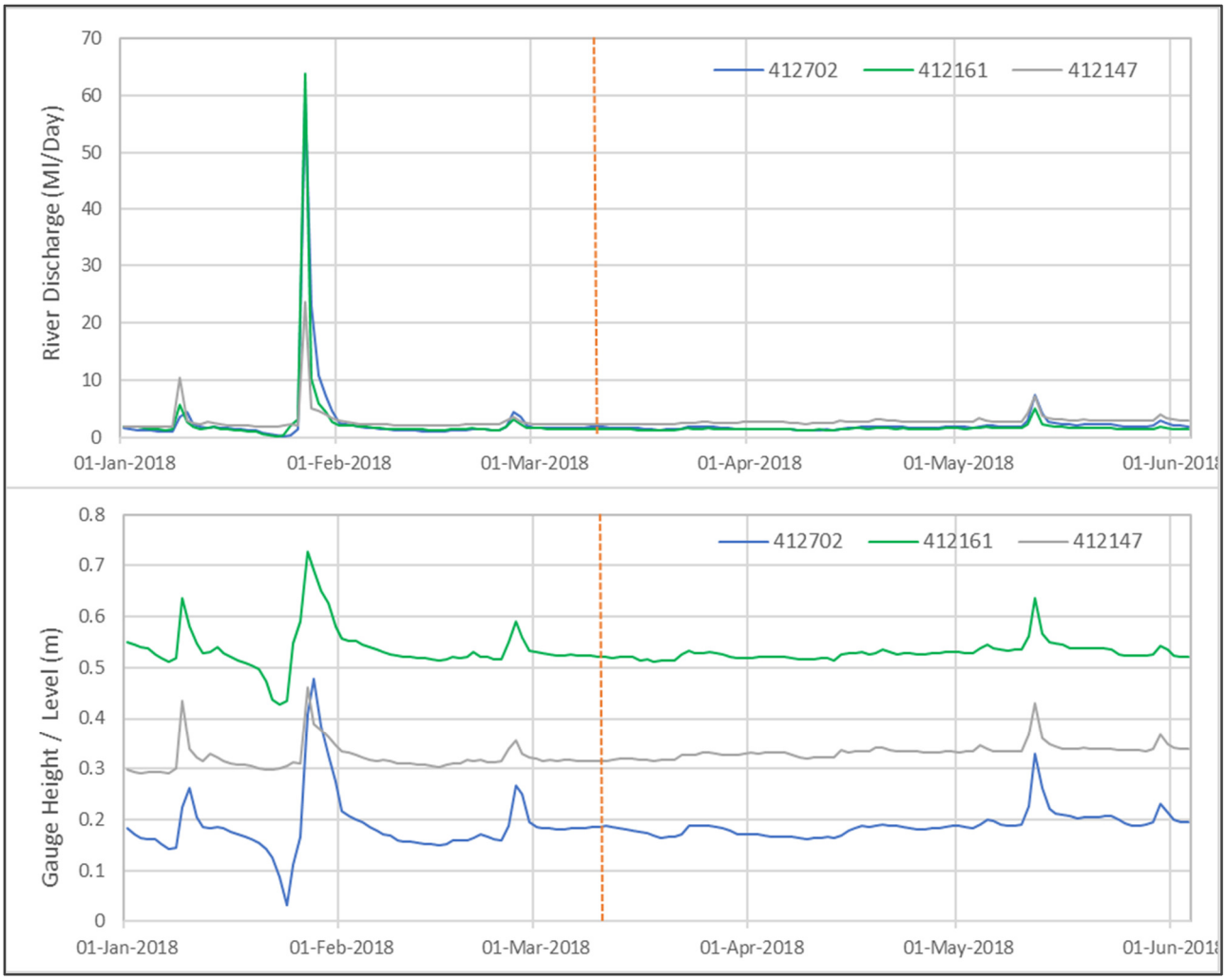

Figure 8: Stream Gauge Height and Discharge, Period of Slump Event

2.3 Geology & Structure

2.3.1 Main Geological Units

A simplified geological map showing only units described in this report is provided in Figure 4. Each of the units shown are discussed in the following section.

Quaternary Alluvium

Quaternary alluvium is common throughout the region, although only significant sequences are regionally mapped. Alluvium generally comprises clays, sands and gravels deposited by modern meandering fluvial systems which are generally well incised with poorly developed backplains (Pogson D.J. & Watkins J.J., 1998). Alluvium may be present in the form of buried palaeo-channels beneath valley fill Tertiary basalt. Local logs indicate these may be several metres thick in some locations. Hydrogeological conditions of alluvium would be expected to be highly variable

depending on the nature of sediment, depositional conditions and post-deposition impacts such as weathering, reworking, and deposition under basalt.

Recharge of alluvium will be a combination of rainfall infiltration, creek (and flood / overbank) flow and spring / seep contributions from underlying basement geology or flanking Tertiary basalt. Discharge from alluvium may occur via losses to reaches of gaining streams, losses to underlying geology and in areas where the aquifer is sufficiently developed, abstraction from bores.

Tertiary Basalt

Prominent outcrop of Tertiary basalt is expressed as lava plains resulting from the outpouring of several basalt flows from Mount Canobolas to the southeast, south and west of Orange (Pogson D.J. & Watkins J.J., 1998).

Tertiary basalt crops out along elevated ridgelines adjacent to both the NTSF and STSF. The basalts are typically olivine basalt and are part of the now dissected Conobolas Volcanic Complex. The basalts are up to 80m thick at Cadia East and comprise at least six separate flows (Wilson, 2003). Potassium-Argon dating of the Canobolas Basalt (Gibson,2007) provides a Middle Miocene age of 12.7 to 11.2 Ma. The basalts were extruded over a paleo terrain and initial flows would have been along paleo drainage channels which now occupy the thickest accumulations of basalt (Hatch, 2019).

In the south west corner of the NTSF, a remnant sequence of valley fill basalt exists and underlies a portion of the western embankment. The portion underlying the western embankment was reviewed and re-interpreted, with an updated isopach assessment and a sectional assessment of the unit provided in Figure 9. All drill control available were used (partial and fully penetrating sites), underlying palaeo-alluvium of up to 4m thickness was identified. Red contours represent elevation of the base of the basalt, while blue contours represent unit thickness. The base of the Tertiary basalt varies from a high of 710m in the north, to 655m in the south.

Groundwater recharge of the Tertiary basalt is most likely through rainfall infiltration and may also occur where drainages flow over the unit and surface water is able to infiltrate to the basalt. Discharge occurs though bore abstraction, discharge into creeks, seepage to underlying rock formations (AGE, 2009) and through contact spring losses.

The basalts and covered palaeo-alluvium which underlie them are recognised aquifers of significance. (AGE, 2013) notes that Tertiary basalt forms a productive aquifer with variable yields and consistently good quality water suitable for potable use. Local permeability and storage characteristics can be highly variable depending on the nature, thickness and continuity of the basalt and the extent and inter-connectivity of primary and secondary permeability features. The basalts have the ability to store and transmit water and will also provide active drainage depending on system geometry and connectivity. Springs are often located along the margins of Tertiary basalts.

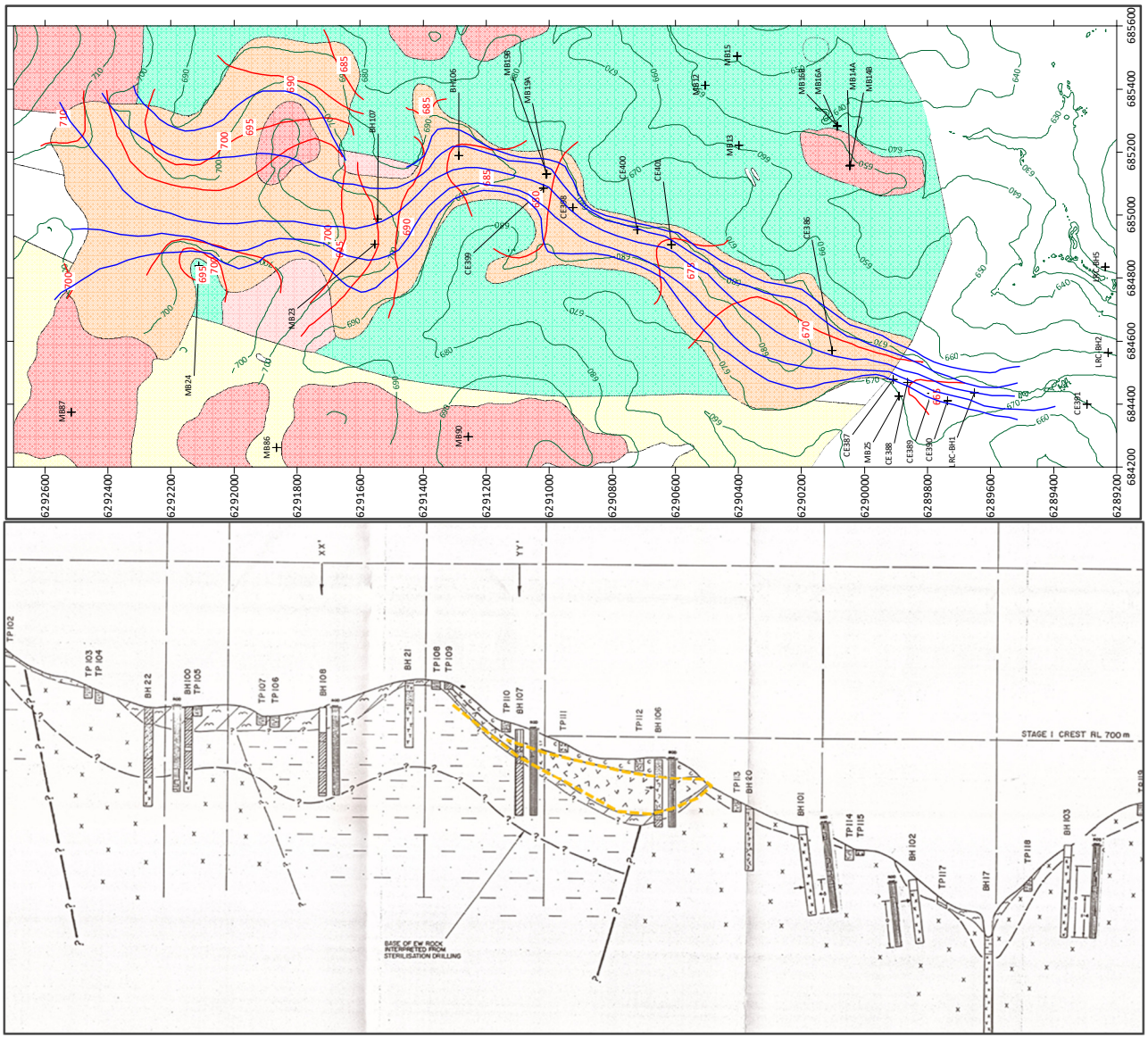

Figure 9: **Local Interpretation of the Tb Flanking the Southwest of the NTSF: Upper Image represents Isopach of the Tb (rotated), Lower image is an Earlier Sectional Interpretation of the unit for a section located along the approximate centreline near the western embankment**

(AGE, 2013) apply a K_h and K_v value of $1.6x10^{-6}$ m/sec, with a specific yield (Sy) of 0.2% and a specific storage (Ss) of $1x10^{-6}$. Of note, the vertical permeability is around three orders of magnitude higher than the vertical permeability of the underlying Silurian sediments and Ordovician volcaniclastics (under fresh conditions).

Early Silurian Ashburnia Formation

The Ashburnia Group comprises Silurian limestones, mudstones, siltstones, sandstones and shales. The unit represents fluctuating transgressive / regressive depositional conditions in a variable supratidal to sublittoral depositional environment. Rapid deepening provided relatively quiet conditions for the accumulation of the turbidite and muds of the Cadia Coach Shale (Pogson D.J. & Watkins J.J., 1998).

(AGE, 2013) divide the Silurian sediment sequence into three sub units – an upper sandstone comprising interbedded siltstone and sandstones, and an overlying massive sandstone, a lower siltstone, and a basal unit which varies locally. The basal unit may be boulder conglomerate, limestone or oxidised siltstone. Groundwater depths vary between about 25m to 64m (depth below ground), and aquifer water quality is typically fresh, and calcium-bicarbonate dominated (AGE, 2009).

Recharge is expected to be dominated by two processes: rainfall infiltration to exposed areas of the sequence, and vertical leakage from the Tertiary basalt where this unit overlies the Silurian sediments. Groundwater discharge is likely where creek incision causes seeps and spring discharge.

(AGE, 2013) provides median hydraulic conductivity data for Silurian sediments, which are K_h $6.1x10^{-8}$ m/sec, and K_v $7.2x10^{-9}$ m/sec. Sy is estimated at 0.5% and Ss is estimated at $1x10^{-6}$ (unitless). Weathered Silurian sediments are estimated to have hydrogeological parameters two orders of magnitude higher than those of fresh rock.

Late Ordovician (to Early Silurian) Forest Reefs Volcanics

The Forest Reefs Volcanics comprise stratified clastic volcanic derived conglomerates and breccias, sandstones and siltstones. Rocks are high K calc-alkaline and vary in composition from basaltic to basaltic andesite (Harris, 2014). The volcanic and volcaniclastic components of this unit are formed by effusive and explosive processes. (Harris 2014). Volcanic eruptions appear to have occurred from a low relief, submarine volcanic complex with multiple vents, producing thickly stacked lava sequences. Explosive volcanism occurred during the later stages resulted in ash fall deposits in a shallow water environment (Hatch, 2019)). Rock types range from basaltic lava and breccia, matrix supported volcanic conglomerate, volcaniclastic sand and ash and other fractionated volcanic deposits (Pogson D.J. & Watkins J.J., 1998).

(AGE, 2009) notes that Ordovician volcaniclastic basement rocks appear to have a widely spaced and poorly interconnected fracture network beyond the major fault zones and form an aquitard with very low groundwater yields and slightly brackish water quality. (AGE, 2013) provides median hydraulic conductivity data for Ordovician volcaniclastics, which are K_h $5.4x10^{-8}$ m/sec, and K_v $2.8x10^{-9}$ m/sec. Sy is estimated at 0.1% and Ss is estimated at $1x10^{-5}$. Hydrogeological properties for weathered Ordovician are also presented in (AGE, 2013), estimated hydraulic conductivity around 2 orders of magnitude higher than fresh rock. Sy is estimated at 1%, and Ss remains unchanged at $1x10^{-5}$.

Ordovician Weemalla Formation

The Weemalla Formation comprises Ordovician aged laminated siltstone and lesser siliceous siltstone, mudstone and feldspar-rich sandstone that include pillow basalts. It has been suggested that the deposition of this unit occurred in a proximal to distal wedge of shallow marine volcanic debris developed on the slopes of a marine volcanic edifice (Pogson D.J. & Watkins J.J., 1998). The fine grained and well sorted nature of the Weemalla Formation and presence of abundant volcanic detritus is consistent with deposition in a deep low relief, marine sedimentary basin on the flank of an eroding volcanic arc (Hatch, 2019). In the study area the top of the Weemalla Formation is defined as the contact with the basal volcanic conglomerate of the overlying Forest Reefs Volcanics (Pogson D.J. & Watkins J.J., 1998). The upper contact of this unit has been

described as gradational and intercalated. Although the regional contact between the Weemalla Formation and overlying Forest Reef Volcanics is gradational, the contact in the vicinity of the NTSF is faulted, with the Weemalla lying to the west of the NTSF (Hatch, 2019).

Recharge and discharge conditions for each of the Ordovician sequences is the same as that expected for the Silurian. Recharge is expected to be dominated by rainfall infiltration to exposed areas of the sequence, and vertical leakage from the Tertiary basalt. Discharge is likely where creek incision causes seeps and spring discharge.

Most previous hydrogeological works differentiate between Silurian and Ordovician units, but do not differentiate between individual units. Hydrogeological conditions for the Weemalla Formation are therefore assumed to be similar to the Forest Reefs Volcanics.

2.3.2 Prominent Local Structure

Wyangala-Werribee Fault System

The Werribee Fault is a regionally mapped north to north-northeast trending, westerly dipping (60°-70°) thrust with a strike-slip component. In the north of its mapped extent and near to the Cadia Mine, it truncates several NNW trending faults indicating it may be a late stage feature. In the area of the mine the fault lies under cover of Tertiary basalt and passes close to the Cadia Mine juxtaposing Ordovician volcanics on the west against Silurian sediments on the east (Pogson D.J. & Watkins J.J., 1998). A regional scale section provided with 1:250,000 mapping (NGMA, 1998) passes across the Werribee Fault approximately 15 km south of the NTSF and shows the general nature of its influence on surrounding rock described above. A portion of this section is reproduced in Figure 10.

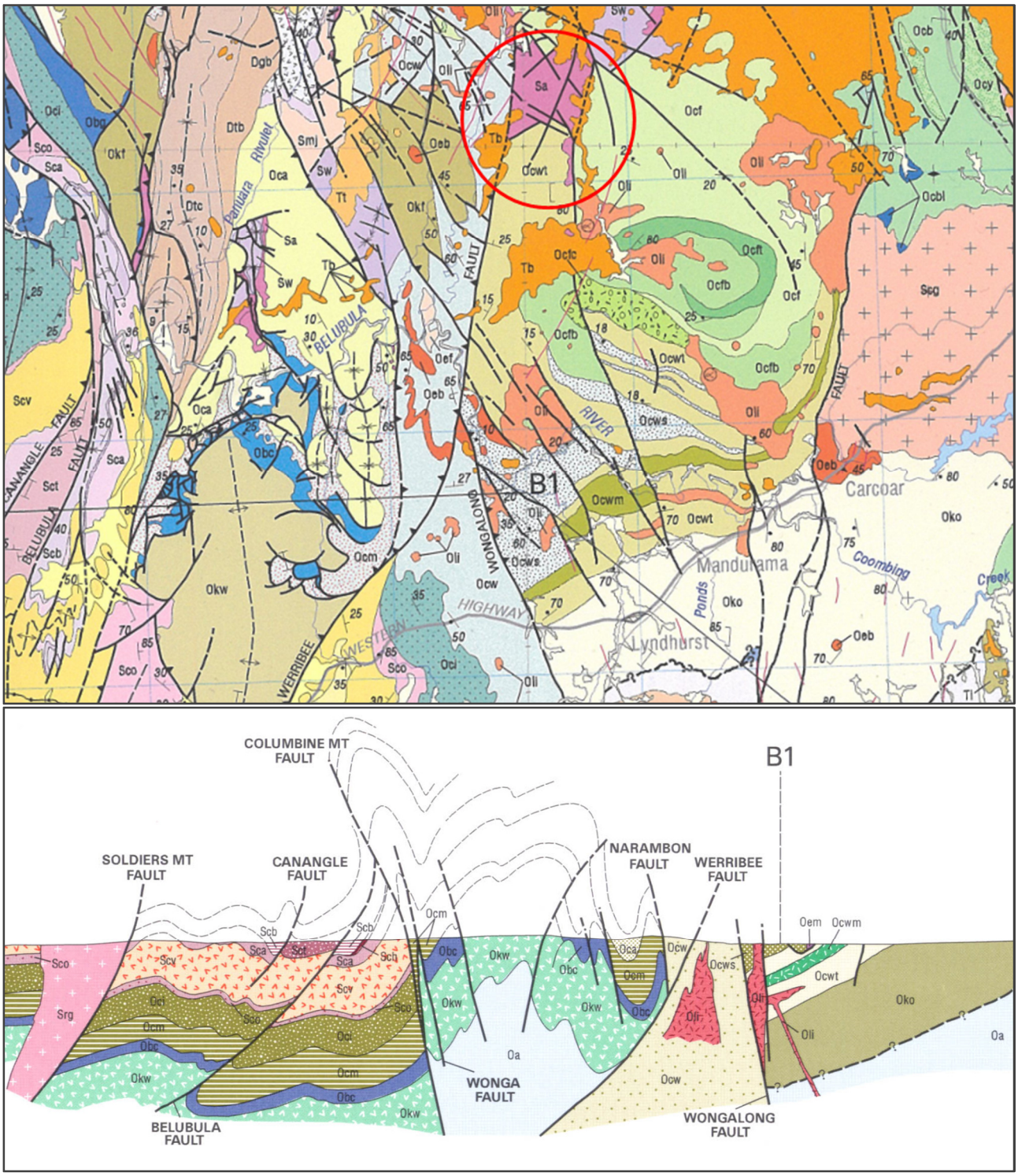

Figure 10: 1:250,000 Regional Geology, approximate NTSF Area (red circle) and Regional Cross Section of the Werribee Fault (NGMA, 1998) to the South of the NTSF

Newcrest have completed a more focussed evaluation of the structural architecture of the Wyangala-Werribee Fault System (Newcrest Mining Ltd., 2016?). This interpretation has been completed for the whole of the mine area including the tailings facilities to the south of the mine, and defines the structural feature as:

- About 30 km long (strike length)
- Well defined in geophysics and surface mapping;
- Represented as two-three parallel thrust faults
- Damage zone 200-400m wide
- Moderately dipping to the west
- Significant (vertical) offset, up to 300 m

Definition of the system is based on a number of data sources and fault mapping exercises. The colour coding of this structure shown in Figure 11 reflects these assessments, with the red being 1997 Geological Survey mapping, and the yellow and blue being project mapping completed in the 2000s and 2007 respectively. Tertiary basalt flows cover most of the fault architecture associated with the Wyangala-Werribee Fault System (Newcrest Mining Ltd., 2016?).

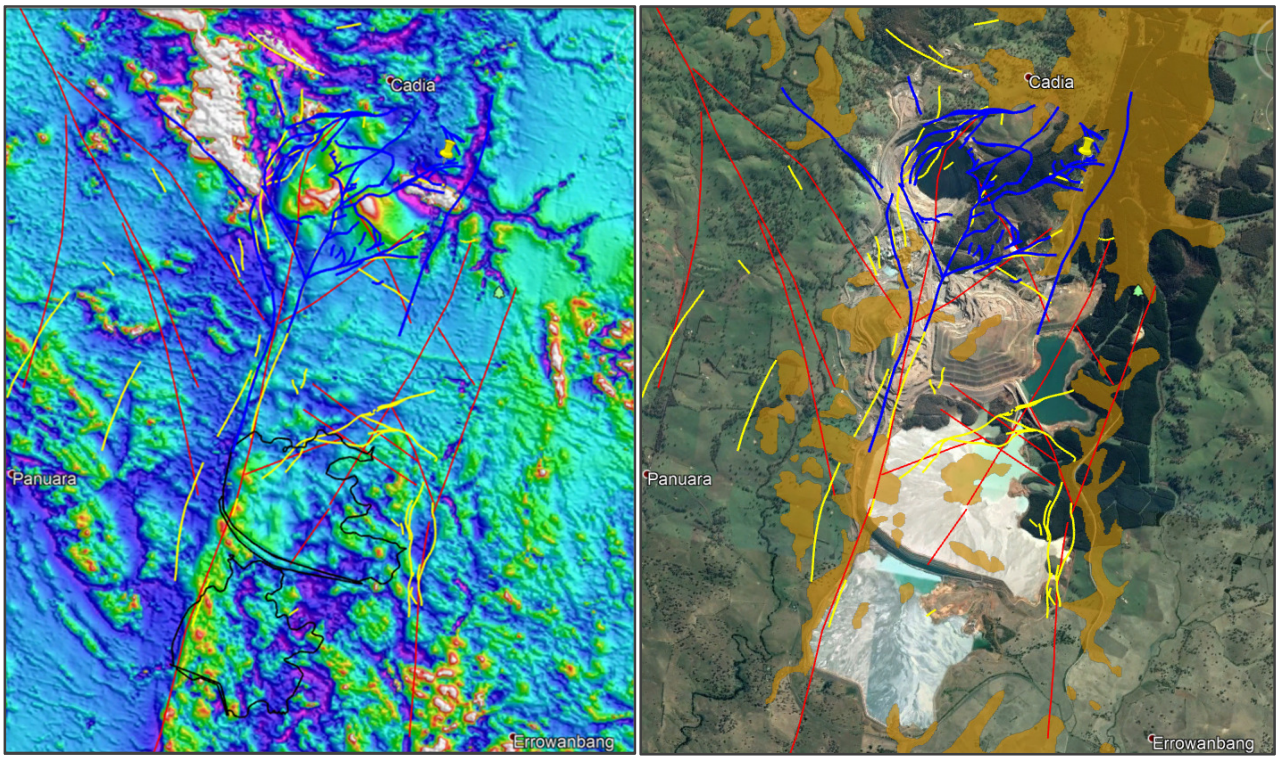

Figure 11: Geophysical Constraints (left) and Relevance of Basalt Cover (right) after (Newcrest Mining Ltd., 2016?)

In the immediate area of the NTSF, updated interpretation of the location of this fault system has been undertaken, with current interpretation of Hatch (Sep-2018) provided in Figure 12. This indicates a westerly displacement of the surface expression of the fault of about 150 m, immediately west and south west of the NTSF. Geologically, this interpretation also shows the late Ordovician Forest Reef Volcanics to the east, and middle Ordovician Weemalla Formation to the west, which is overlain by Quaternary alluvium and Tertiary basalt.

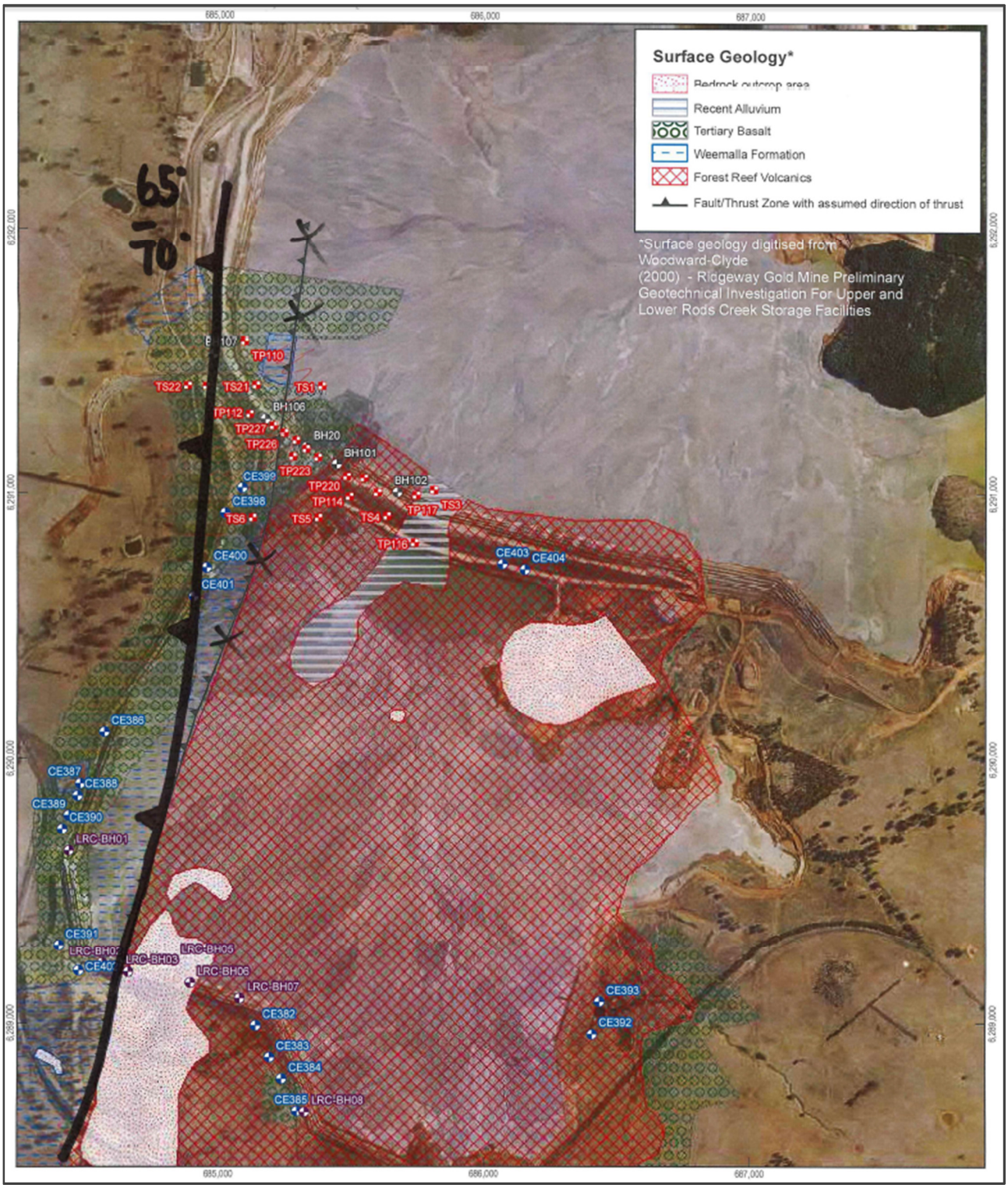

Figure 12: Hatch (2018) Revision to the Local Alignment of the Werribee Fault near the NTSF, using GHD Mapping (reference) as a Base Map

2.4 Hydrogeology of the NTSF

Description of the construction of the NTSF is provided in detail in (Hatch, 2019). Elements of construction relevant to seepage modelling are provided in the following section. This information is taken verbatim from Appendix B (NTSF TimeLine) of (Hatch 2019).

2.4.1 NTSF Construction Sequencing

Initial construction of the NTF commenced in August 1997 to a height of 50 m. Since then, the TSF has been raised eleven times, with the most recent raising being Stage 10 which commenced in 2017. A summary of the design and construction details of the NTSF is provided in Table 1.

Table 1: Summary of Design & Construction (after Hatch 2019, Appendix B)

Stage	Crest Level (mAHD)	Max Height (m)	Construction Type	Design By (1)	Construction Completed
1	700.0	50.0	Conventional	Knight Piesold	May 1998
2A	707.0	57.0	Downstream	Woodward Clyde	Aug 2000
2B/1	710.5	60.5	Downstream	URS	May 2002
2B/2	714.0	64.0	Downstream		Jun 2003
3	718.5	68.5	Centreline	URS	Nov 2005
4	723.0	73.0	Upstream	URS	Oct 2008
5	729.0	79.0	Upstream	URS	Aug 2011
6	732.0	82.0	Upstream	URS	Dec 2012
7	735.0	85.0	Upstream	URS	Feb 2014
8	738.0	88.0	Upstream	URS/AECOM	Oct 2015
9	741.0	91.0	Upstream	AECOM	Dec 2016
10	744.0	94.0	Upstream	ATC Williams	Mar 2018 (2)

(1) Woodward Clyde was acquired by URS who were subsequently acquired by AECOM.
(2) Stage 10 was incomplete at the time of the NTSF Failure

2.4.2 NTSF Construction Elements

Starter Embankment

The Stage 1 starter embankment is an earth and rockfill dam, with a 1,680 m long embankment and a 16 m wide crest at RL 700. A 5 m wide clay core is bounded by rockfill shoulders, with a 15 m wide transition / filter zone between the clay core and the downstream rockfill shoulder of the embankment.

Rodds Creek Diversion

Rodds creek was diverted through the dam foundation via a 1,350 mm concrete encased (through the clay core) steel conduit. A sediment dam was integrated into the upstream face to control runoff during construction and emergent groundwater from springs in the creek channel. The sediment dam includes a 10 m wide zone of drainage gravel between RL 661 and RL 665.

Clay Blanket

A 1 m thick clay blanket (permeability $1.0x10^{-9}$ m/sec) was constructed upstream of the dam in Rodds Creek and a 1 m thick clay layer was constructed between the sediment dam and the clay core at RL 658.

Any areas of exposed fractured rock or permeable soil on the storage floor were covered with low permeability clayey soil to provide an overall average base permeability equivalent to 1 m thickness of material with a permeability of $1x10^{-9}$ m/sec or better (ATC Williams, 2017).

Underdrain

During Stage 3 construction, an underdrain system consisting of a slotted collection pipe encapsulated within a filter blanket was provided over the full length of the upstream toe of the Stage 3 embankment. Outlet pipes were provided to the downstream rockfill batter at 200 m intervals, which were concrete encased through the clay core with a filter sand plug immediately downstream of the concrete encasement.

For drainage under the clay liner, ABS pipe was laid on the base of Rodds Creek channel and rock drainage material placed on top. All water collected by this system was returned back into the NTSF via a drainage collection pond, nor covered by tailings within the STSF (ATC Williams, 2017).

Tailings Deposition

Tailings deposition is sub aerial using multiple spigots. Deposition planning is achieved by splitting the dam embankment into zones, each containing five to seven discharge spigots. Modelled tailings rate of rise is ~1.9m/year prior to 2010 and ~2.4m/year after 2010. The NTSF has an average beach slope of 0.3%.

Buttressing

In mid-2007, a 35 m wide berm of igneous mine waste was placed at the toe of the NTSF. Over the following years, the berm was progressively raised and lengthened to keep it above the STSF decant pond level. As a consequence of cone penetration tests completed in 2017, ATCW recommended the construction of two buttresses (the Stage 1 buttress and the Stage 2 buttress). The Stage 1 buttress extends from the Stage 3 crest to the Stage 7 crest, the Stage 2 buttress extends from natural ground at the toe of the NTSF to the Stage 3 crest.

2.4.3 Drainage & Seepage

The Stage 3 underdrains have remained largely dry, except for the western drain. Although seepage from this drain was noted for some time, it was not until a pipe was attached that the measurements of flow rate were possible. Drain flow for the period 2015 to early 2018 range between 30 L/min and 50 L/min (Figure 13). Extension of a trend line through this data indicates flow may have commenced around mid-2006. Prior to the slump event, a 10 L/min increase in flow rate was observed for each 5 m rise in the decant pond level.

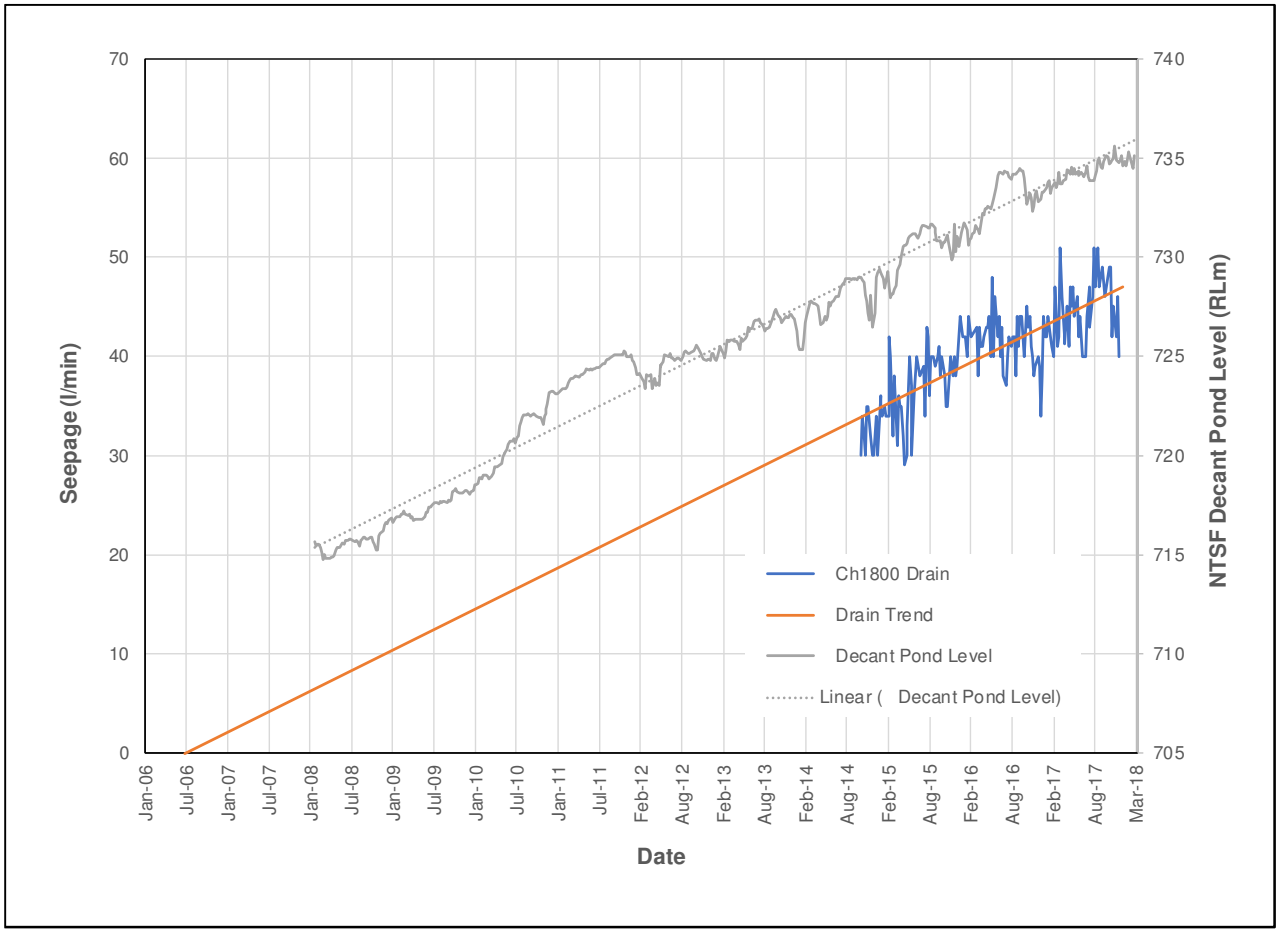

Figure 13: Ch.1800 Drain Flow and NTSF decant Pond level

Seepage observed as semi-permanent wet spots have been noted on a number of berms on both the Southern and Western Embankments. As most of the wet spots appear to dry out during dry weather, Hatch concluded that they most likely result from rainfall runoff and infiltration into the rockfill collecting at low points. This is consistent with the concept of shallow interflow discussed in the Ridgeway EIS (Kalf, 2000).

2.4.4 NTSF (& STSF) Decant Ponds

Stage 4 to Stage 10 elevation data for the NTSF and STSF dam crest and decant pond elevation, and the water elevation of the Rodds Creek Dam, is provided in Figure 14.

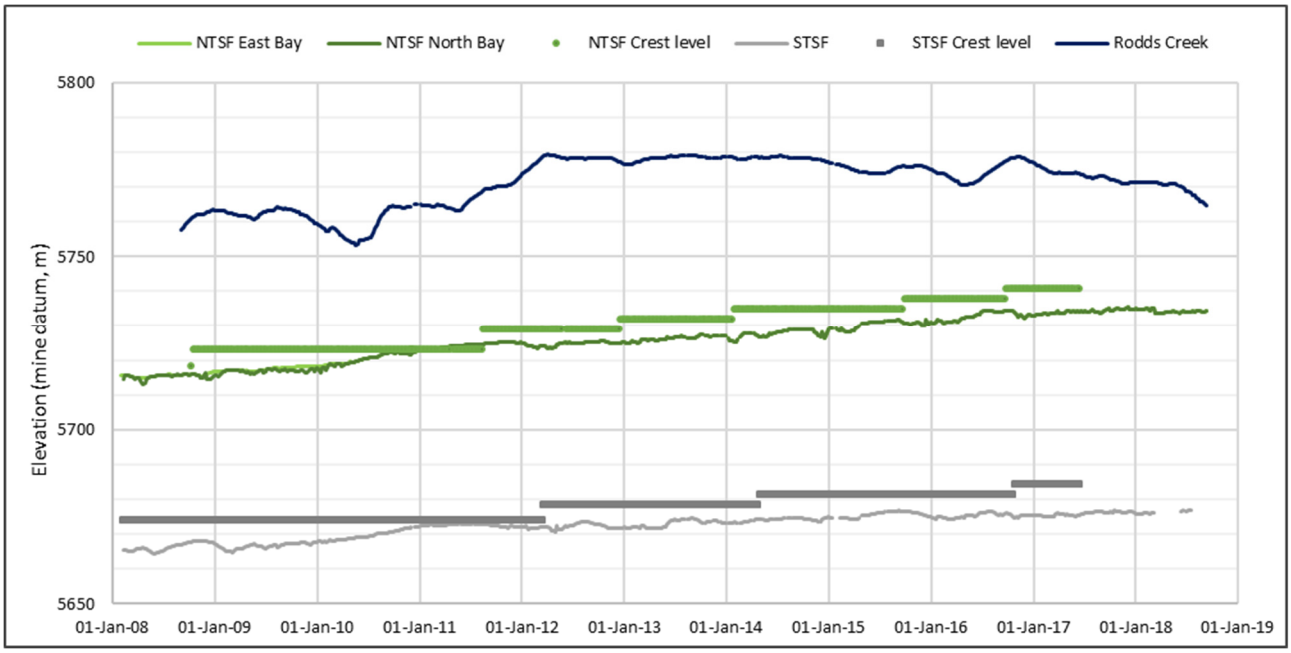

Figure 14: NTSF & STSF Dam Crest and Pond Elevations, Rodd Creek Dam Water Elevation

Spatial representation of pond location has been assessed by KCB using available air photography, from site held data and Google Earth imagery. A summary of this information is presented in Figure 15, observations include:

- For the three recent images, the pond sizes in each of the NTSF and the STSF are not large compared with the cluster image of longer-term pond records;
- The NTSF pond has generally maintained a lateral distance of 1,000 m or greater from the area of the slump, with exception of a period in late 2010 when both TSFs experienced large pond extents. Under these conditions the pond was still several hundred metres from the slump area.
- In 2010, the area experienced a year of above average rainfall which produced a CRD excess of about 800 mm. The period is also reflected in crest versus pond elevation data presented in Figure 14, which shows a brief period of merged elevations.
- Post slumping, pond sizes in each facility are comparatively very small.

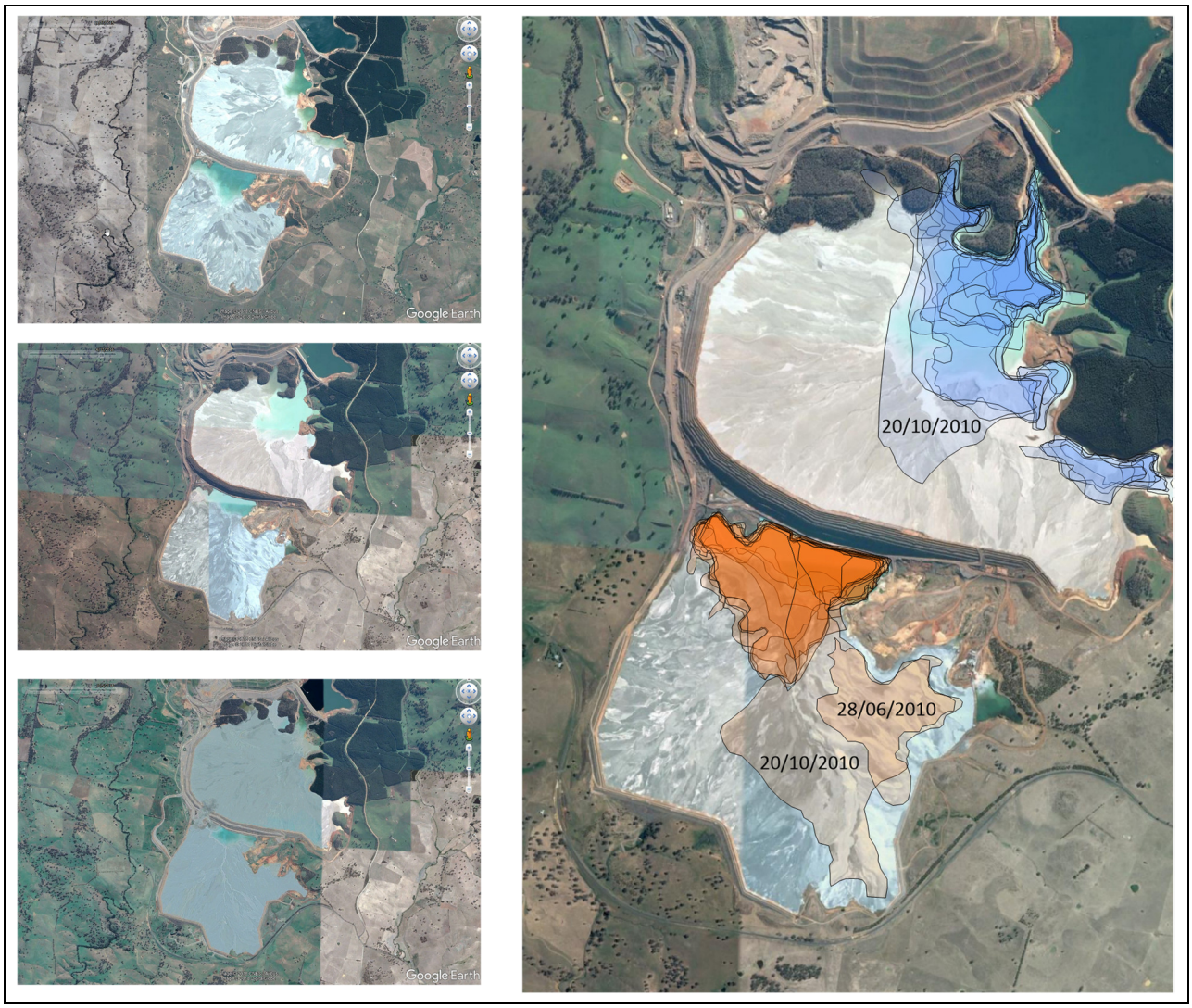

Figure 15: NTSF and STSF Pond Location (Upper Left Nov-2015, Centre Left Dec-2016, Lower Left May-2018, Right Cluster Map of All Data Available)

2.4.5 Piezometric Monitoring Data

There is a large inventory of monitoring established at the mine. With focus on the seepage performance of the NTSF for the period leading up to the slump event, a reduced subset of data is presented. Figure 16 provides a location map of monitoring facilities (bores and VWPs) used in this assessment. Table 2 provides a tabulated summary of these facilities.

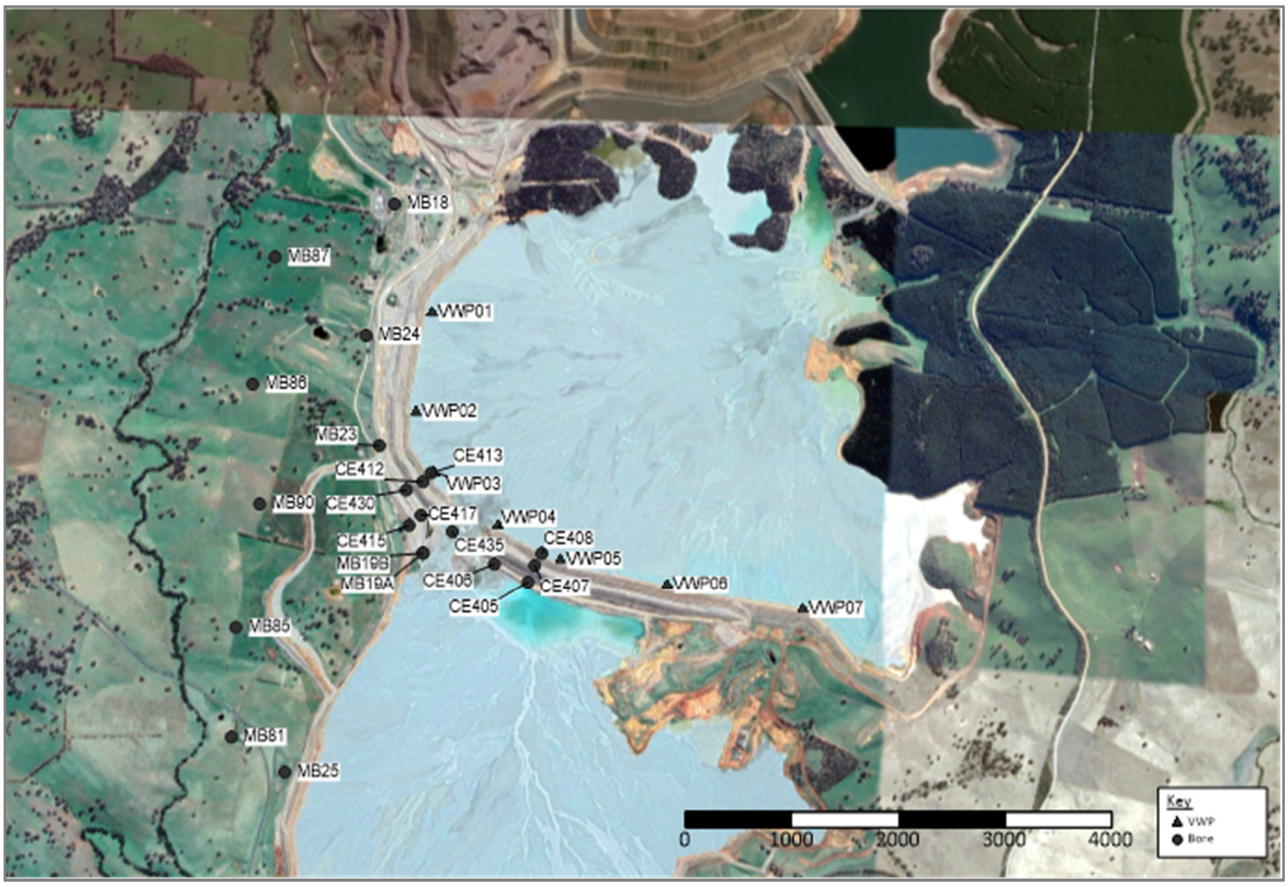

Figure 16: Location of Key Monitoring Locations (Bores and VWPs) (figure needs improvement / clarity)

Table 2: Bore & VWP Completion Details for Sites Used in Hydrograph Interpretations

Bore	Easting	Northing	RL (mAHD)	Total Depth (m)	Unit	Type
CE405	685,666	6,290,860	687.83	30.5	Fresh Volcanics	VWP
CE406	685,495	6,290,952	688.04	31.8	Fresh Volcanics	VWP
CE407	685,700	6,290,945	731.80	61.6	Core	VWP
CE408	685,737	6,291,006	743.80	57.0	Tailings	VWP
CE412	685,129	6,291,369	732.14	67.5	Basalt	VWP
CE413	685,171	6,291,414	743.85	58.4	Basalt	VWP
CE415	685,059	6,291,149	686.16	31.3	Fresh Volcanics	VWP
CE417	685,120	6,291,200	701.00	39.0	Basalt	VWP
CE430	685,045	6,291,328	706.32	44.5	Basalt	VWP
CE435	685,280	6,291,117	708.33	45.0	Fresh Volcanics	VWP
MB18	684,985	6,292,785	722.00	40.0	Silurian Sediments	Bore
MB19A	685,131	6,291,009	688.12	39.7	Ordovician Volcanics	Bore
MB19B	685,130	6,291,007	688.14	7.6	Soil/Clay	Bore
MB23	684,908	6,291,554	703.49	41.3	Ordovician Volcanics	Bore
MB24	684,839	6,292,112	696.44	30.9	Ordovician Volcanics	Bore

Bore	Easting	Northing	RL (mAHD)	Total Depth (m)	Unit	Type
MB25	684,425	6,289,890	668.90	30.5	Ordovician Volcanics	Bore
MB81	684,153	6,290,069	657.48	19.0	Silurian Siltstone	Bore
MB85	684,175	6,290,626	676.50	26.0	Silurian Sediments	Bore
MB86	684,261	6,291,865	685.65	22.0	Ordovician Volcanics	Bore
MB87	684,375	6,292,516	693.56	21.5	Ordovician Volcanics	Bore
MB90	684,297	6,291,257	644.00	60.0	Tertiary Basalt	Bore
N1-2	685,908	6,288,934	731.71	24.9	Tailings	VWP
N2-2	685,557	6,289,718	731.67	35.0	Tailings	VWP
N3-2	685,943	6,290,405	730.67	36.0	Tailings	VWP
VWP01(NO1)	685,177	6,292,229	740.68	10.0	Tailings	VWP
VWP02(NO2)	685,097	6,291,723	741.16	10.0	Tailings	VWP
VWP03(NO3)	685,188	6,291,417	740.86	10.0	Tailings	VWP
VWP04(NO4)	685,514	6,291,149	740.39	16.0	Tailings	VWP
VWP05(NO5)	685,833	6,290,973	740.08	16.0	Tailings	VWP
VWP06(NO6)	686,377	6,290,845	739.02	16.0	Tailings	VWP
VWP07(NO7)	687,069	6,290,719	738.96	16.0	Tailings	VWP
NTSF20001	685,472	6,291,067	705.50	10.0	Tailings	VWP
NTSF20002	685,472	6,291,067	719.77		Decommissioned	VWP
NTSF20003	685,472	6,291,067	720.69		Decommissioned	VWP
NTSF20004	685,472	6,291,067	726.64		Decommissioned	VWP
NTSF20017	685,472	6,291,067	721.10		Decommissioned	VWP

There are five hydrographs presented for bores completed in natural strata and proximal to the NTSF. These are MB18, MB19A/MB19B, MB23 and MB24 (Figure 17). The bores are located immediately west and south west of the NTSF, close to the abutment of the STSF into the southern NTSF embankment. All the bores are within 500 m of the toe of the western or southern embankment of the south west corner of the NTSF.

Long term trends for four of these bores are shown and indicate a consistent head increase of 0.35 m to 0.55 m per year. No unique spikes in the record due to sudden recharge events such as rainfall or creek flow are evident. The equivalent lineal trend on the NTSF and the STSF decant ponds are 2.0 m/year and 1.0 m/year respectively. These data indicate translation of the developing pressure response from raising of the NTSF into local groundwater conditions within the Silurian and Ordovician strata.

The absence of local peaks in the data (exception being MB19B which is the shallowest completion at 7.6 m) and the large difference in vertical elevations between the bores and the decant pond elevation in the NTSF (30 m-50 m), indicates that this trend is a muted pressure response to the TSF's presence rather than an indicator of direct and efficient hydraulic continuity. This is a relevant observation in considering the interaction between the NTSF and natural ground from a modelling context. If the efficiency of the interaction between these systems is represented too strongly, then the prediction of heads in natural ground will be dominated by the NTSF, and likely over-estimated to the order of 10's of metres.

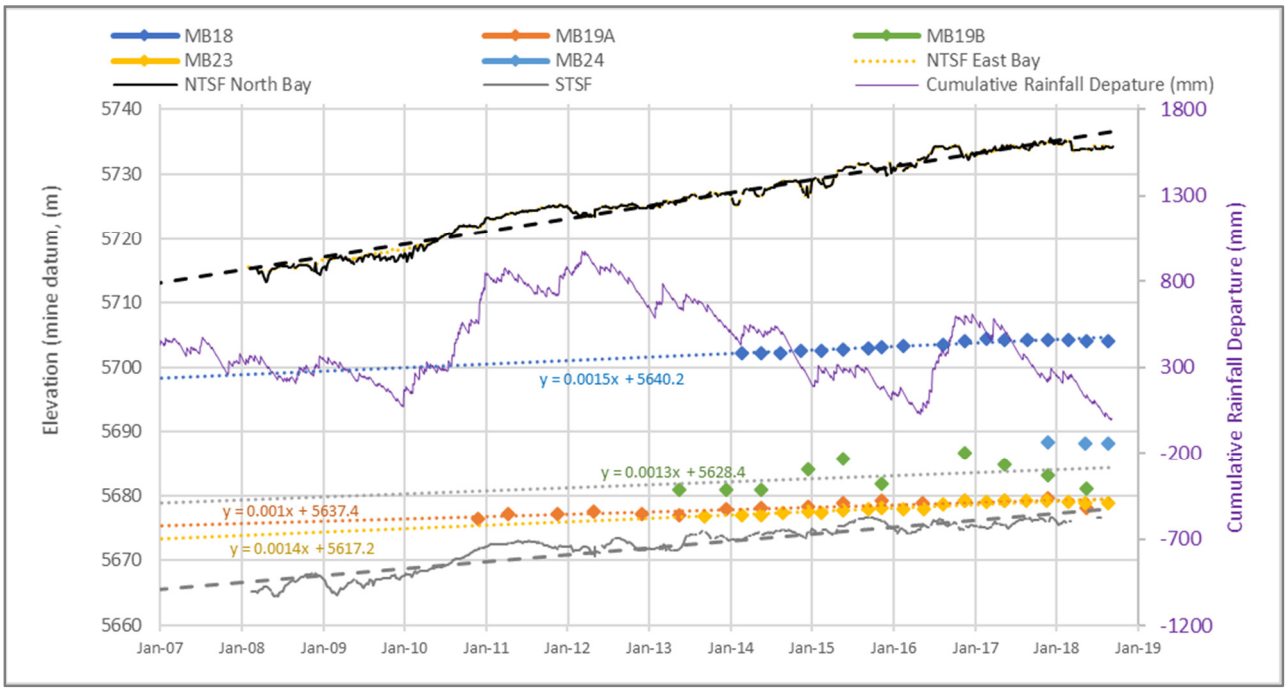

Figure 17: NTSF Proximal Foundation Head Monitoring, 2007 to 2018

Figure 18 shows a similar composite hydrograph, however, these are for sites slightly further away from the NTSF / STSF complex, to the west and south of the facilities. These bores are between 800 m and 1,700 m from the NTSF. In the lower section of the figure, the graphs have been reproduced to show detail for the cluster of bores between RL (5)640 and (5)660.

The long-term rising trends apparent in the proximal sites is not present in data from these more distal bores. Their response is considered more typical of that expected from groundwater unaffected by influences other than rainfall, with two sites (MB81 and MB25, and possibly MB85) of longer record showing a strong recharge and decline response to a period of prolonged above-average rainfall. Consistent with the current CRD trend, all distal bore hydrographs are now showing a steady rate of decline, which is in contrast to pond conditions in the NTSF and the STSF over the same period.

These data are indicating no translation of the NTSF / STSF pressure effects at distance, placing the likely lateral extent of NTSF pressure impact to be in the range of 500 m to 800 m from the TSF complex.

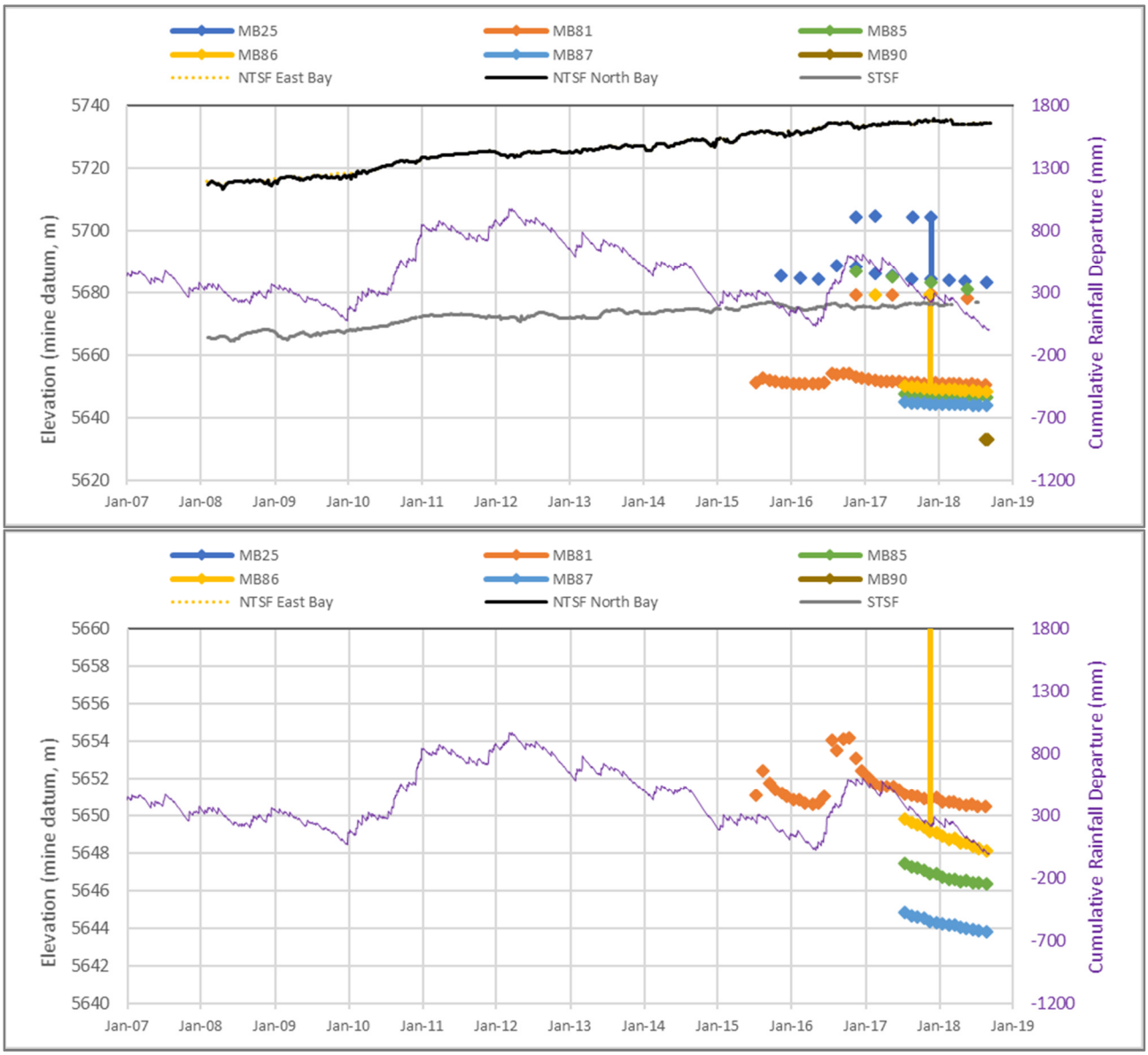

Figure 18: NTSF Distal Foundation Monitoring, 2007 to 2018

Figure 19 provides time series monitoring of piezometric conditions in the tailings and in the Tertiary basalt (from VWPs installed during the 2018 campaign). A section showing the relative location of these CE sites is also provided after Hatch (2019). Of the VWP's, location VWP-N03 is closest to these basalt VWP monitoring locations.

An observation from these data is the vertical head differential between the tailings and the basalt, particularly sites CE412 and CE430. These data indicate that seepage and head translation from the tailings to the underlying basalt is either (i) not significant compared to the basalt's ability to accommodate these flows, or (ii) absorbed by the basalts' ability to rapidly discharge this additional water. Because the conditions in the tailings do not indicate presence of drainage effects over the basalt, the former condition is considered more technically likely.

The gradient between the downstream basalt VWPs is also important for two reasons (i) it is relatively 'gentle' at ~1:30 (considering its proximity to the embankment), indicating seepage

contribution from the tailings which would be controlling features to the saturated section of the sequence are not significant, and (ii) the heads are below the interpreted top of the Tertiary basalt, indicating seepage from tailings into the basalt is not significant enough to pressurise the basalt, which in turn reduces its potential to create spring discharge back into the tailings (at this location)[1].

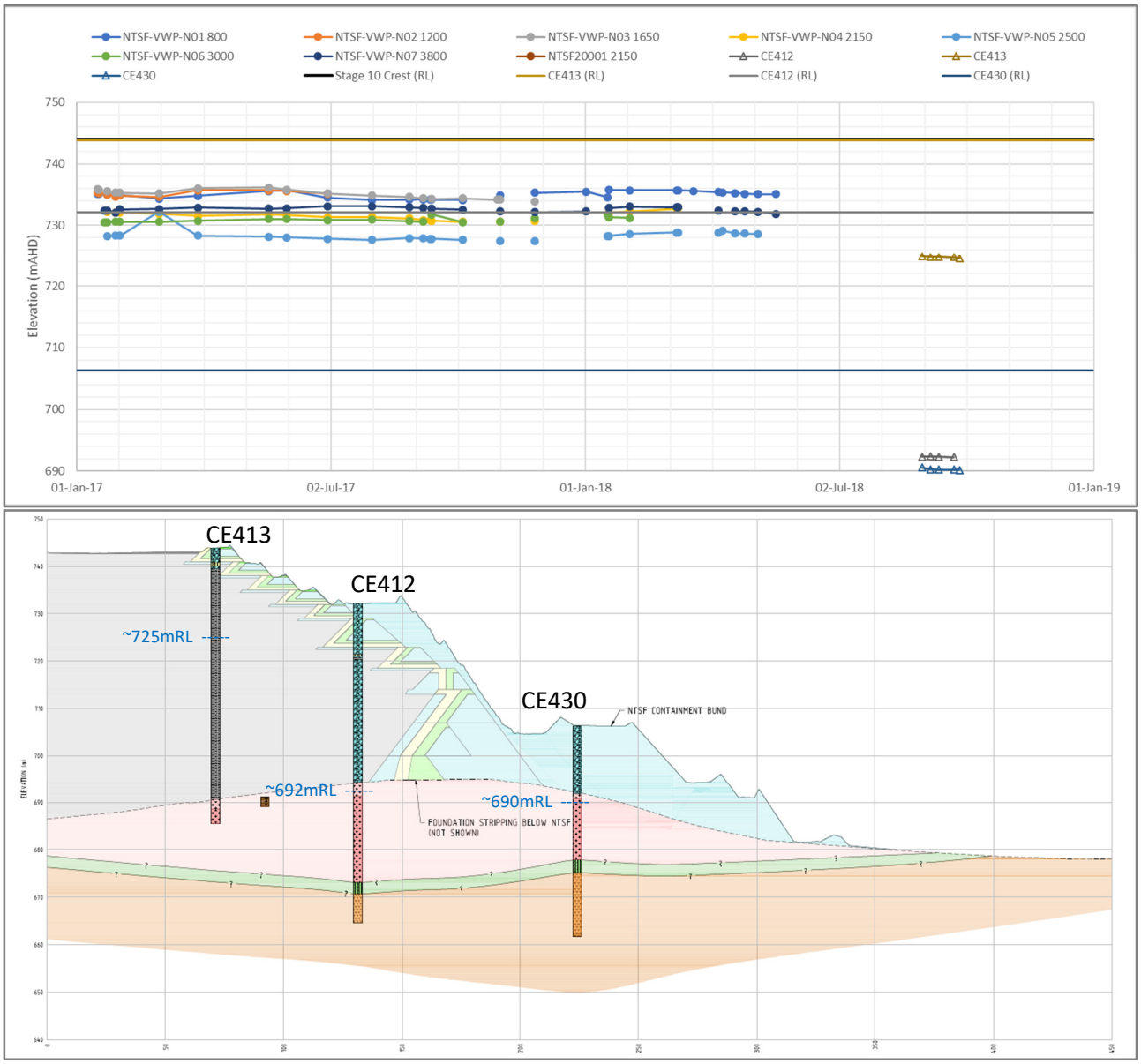

Figure 19: NTSF Internal Monitoring, Time Series Jan-2017 to May-2018, and 2018 Installed Tertiary Basalt VWPs, lower image location of CE series holes (Hatch, 2019)

[1] It is noted these observations are based on comparison of Tertiary basalt conditions measured after the slump event.

Equilibrium pore pressures (Figure 20) from pore pressure dissipation tests completed as part of the 2013 and 2017 CPTu investigations indicate a pressure gradient below hydrostatic at a number of test locations (Hatch, 2019). The pressure gradient is closest to hydrostatic along the western embankment (N1-2) and well below hydrostatic at sites N05 and N302, which are located on the southern embankment. At these sites the inferred water level is ~8m below the tailings surface, and 3-4m below the tailings surface elsewhere (Hatch, 2019).

The deeper groundwater surface in the vicinity of Ch2500 can also be seen in a longitudinal profile of the piezometric surface for a number of dates (Figure 21). This, and the pressure gradient less than hydrostatic, can most likely be attributed to downward drainage toward the Stage 1 underdrain system between Ch2300 and Ch2600 to assist in consolidation of the tailings (Hatch, 2019).

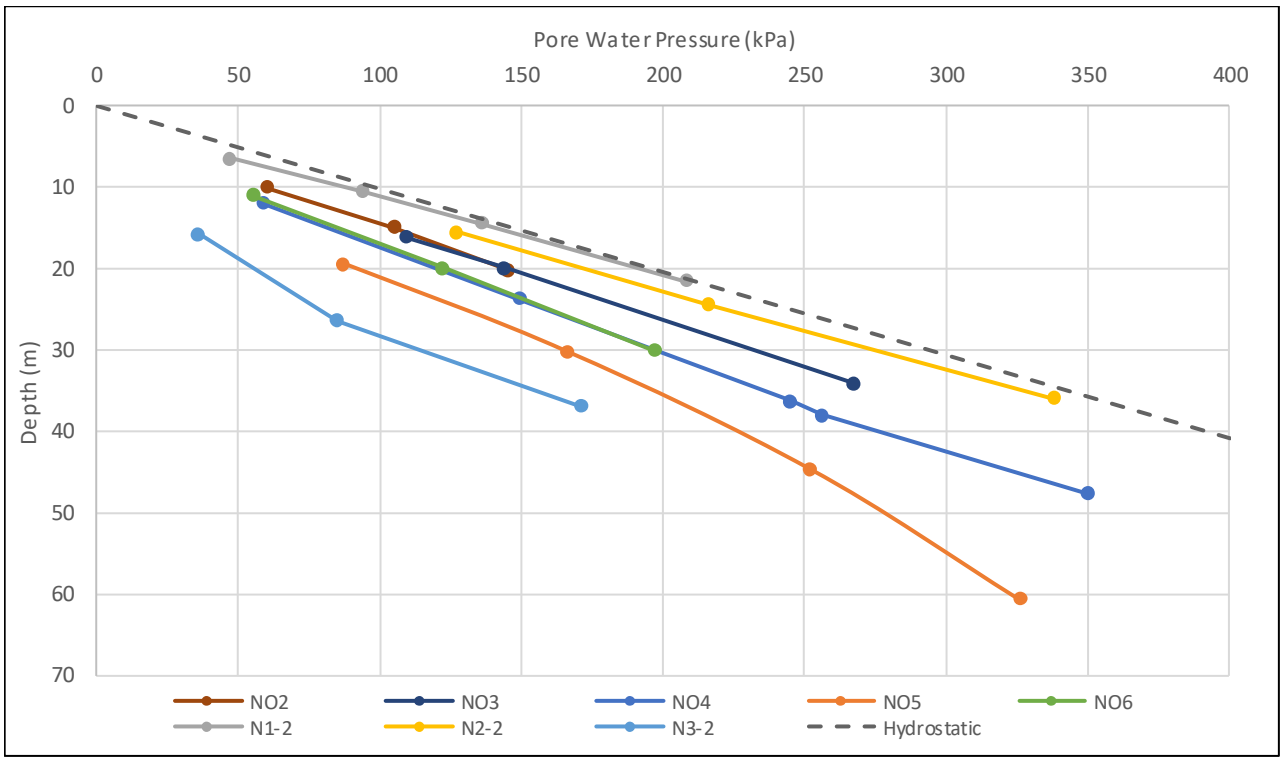

Figure 20: CPTu Pore Water Pressure Gradients (Hatch, 2019)

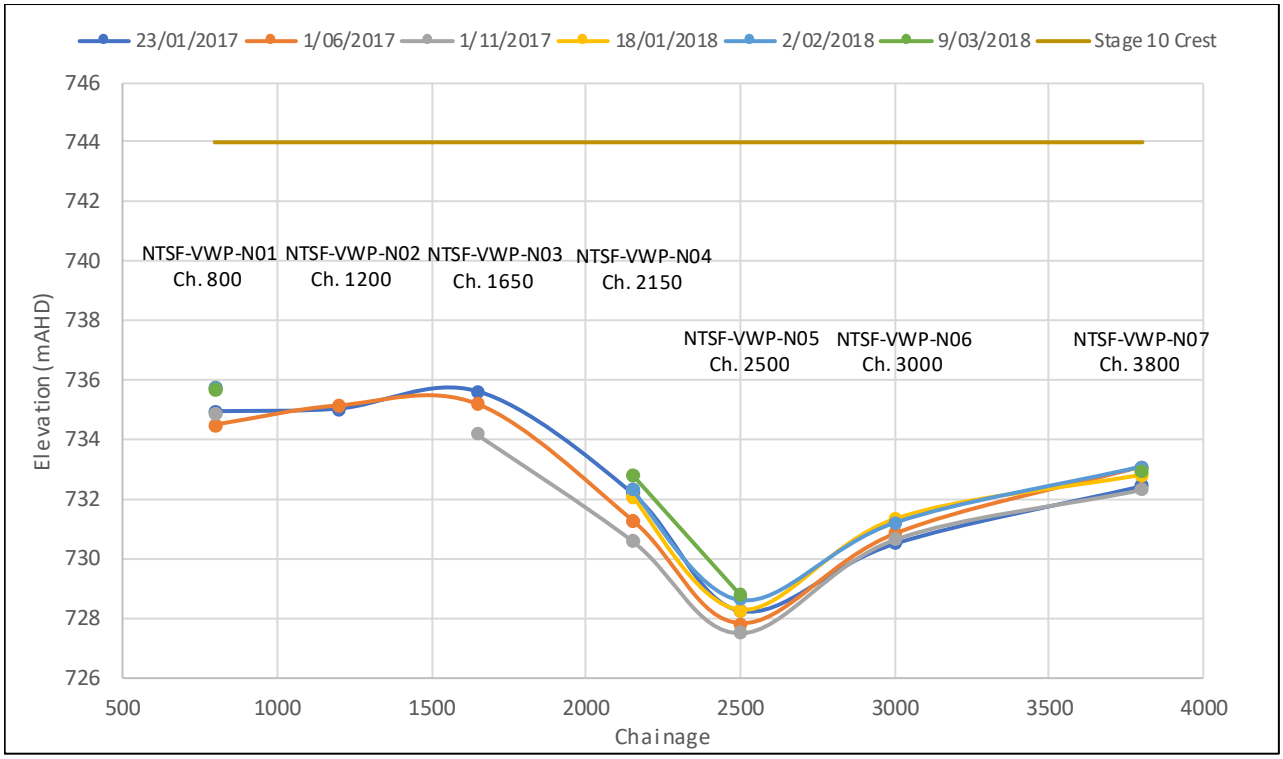

Figure 21: Longitudinal Profile of Piezometric Surface with Time (Hatch, 2019)

2.4.6 Springs

Numerous studies, including those related to the design, construction and performance assessment of the NTSF have acknowledged the presence and relevance of springs at the site. Examples of such references are provided in Table 3.

Table 3: Example Spring Referencing from Previous Technical Documentation

Reference	Comment
Woodward-Clyde (1995). *Cadia Project Tailings Disposal Study – Geotechnical; Investigation Report*	▪ Pg.5 "Baseflow appears to be recharged through leakage from basalts that outcrop within the upper reaches of the catchment, or through "Spring" flow fed from fault/fractured zones. ▪ Pg. 14 "Some groundwater springs have been observed from the boundary between the Tertiary basalt and the Silurian sediments"
Knight Piesold and PSM (1997). *NTSF1 Construction Report*	▪ Natural Springs (pg.9) ▪ Spring during construction (pg.10) ▪ Has recording of pore pressure during NTSF constructions (get copy of App C ref from Hatch*)
Newcrest Mining Limited (2000). *Geology of Southern Tailings Storage Facility Site, Rodd's Ck-Spring Dell-Wire Gully; Cadia Hill Gold Mine Region*	▪ Map ▪ "Dell Spring" which is STSF

Reference	Comment
Kalf (2000). *Ridgeway Project Groundwater Management. In: Ridgeway Project – Environmental Impact Statement, Appendix B*	▪ "Seepages emerging from the basalt at Ridgeway tend to occur at the head of drainage gullies." ▪ "Groundwater within the volcaniclastic rocks also emerges at the ground surface along gullies and this is thought to be controlled by local fracture systems associated with the drainage system." ▪ "In mid to second half of 1998 the area experienced very high rainfall which also recharged the groundwater system substantially (see Attachment B-B). These conditions have indicated the presence not only of baseflow but a substantial interflow component in the stream hydrographs (Gilbert and Associates, 2000)." ▪ "…there is also a significant interflow component where recharge water drains relatively quickly into the stream gullies after heavy rainfall."
Woodward-Clyde (2000). *Cadia Hill Gold Mine Tailings Storage Facility Surveillance Report*	▪ Pg. 19 & Pg.20 ▪ Natural Spring at CH1650 found during inspection ▪ Seepage cannot be separated from runoff (pg.11)
URS (2002). *Southern Tailings Storage Facility Construction Report (Memorandum)*	▪ Soft wet zones encountered during TSF foot print preparation (pg.15) ▪ Spring exposed in foundation of cut-off (pg.18)
Kalf & Associates (2004). *Ridgeway Deeps: Groundwater Model Simulation Update and Hydraulic Impact of Mining To -500 m RL (Draft)*	▪ Sec 2.2. Spring waters are predominately sodium bicarbonate type.
AGE (2009). *Cadia East Project Groundwater Assessment. In: Environmental Assessment Cadia East Project, Appendix G*	▪ Many mentions of "Spring". All not in zone of interest. Small seepage zone east of Rodd's creek (pg.30) ▪ Baseflow in Flyers Creek is partially maintained by an area of (Silurian) springs approximately 1,200 m downstream of Long Swamp Road. An individual spring in this area had a visually estimated flow of about 20 L/s in autumn 2007 (Gilbert & Associates, 2009). Monitoring bores MB47A/MB47B are located approximately 300 m to the north-west of the spring zone and were located to provide data on the strata which feed the springs and to act as long-term monitoring points. ▪ Spring census work completed by (AGE, 2009) focussed on the area to the north and north east of the mine, where the broader sequence of Tb is mapped. This work presents census results for 53 springs mapped, however these have little relevance to the NTSF area other than to assist in understanding the types of spring that may occur.
GHD (2015). *Southern Tailings Storage Facility Seepage Investigation Review Data*	▪ "Increasing groundwater levels near the STSF may be associated with seepage from the tailings dam and/or the influence of the STSF structure on localised flow within the fractured groundwater system" ▪ Study focussed on understanding seepage from the STSF – limited relevance to this investigation.
AGEC (2016). *Cadia Mine. Update to Groundwater Model. Ref.G1383C.*	▪ Represents interaction (numerical) between the groundwater system and a number of springs – the approach assumed springs are associated with drainage alignment and local discharge conditions.
ATC Williams (2017). *Cadia Valley Operations, Northern Surveillance Report 2017*	▪ Contains record of seepage, monitoring sites appears to be on embankment benches, post construction
GHD (2018). *Cadia Valley Operations – Tailings Storage Facilities. Seepage Management Options Study. Options Report.*	▪ Section 2.5, "In some places the basalt and volcanoclastic groundwater appears as springs along or near the drainage lines where the topography falls (Kalf and Associates, 2000; Newcrest, 2016)"

Cadia Spring Occurrence and Type

There are four general types of springs occurring across the Cadia area based on the notations provided in Table 3:

- Contact springs, located at the margins of the higher permeability Tertiary basalt, with seepage from the basalt discharging at the contact with the lower permeability rock beneath. As natural recharge raises the saturated profile in the basalt, discharge rates at the margins will increase;
- Baseflow springs for aquifers and aquitards which are incised from drainage development and where topographic lows intersect natural groundwater. These are also sensitive to the saturated profile in the aquifer / aquitard: in the case of Silurian and Ordovician strata, their generally low permeability limits the variability in spring flow rate. Spring discharge may not always be evident if discharge occurs into alluvial bedloads;
- Structurally derived springs, where regional or sub regional structure acts as either a:
  - conduit to flow, permitting higher heads to be laterally translated to lower elevation areas, or;
  - barrier to flow, with spring discharge occurring where the fault acts as a 'dam' to groundwater, locally raising heads which may discharge at surface.
- Shallow interflow springs, which represent short distance and duration springs caused from local rainfall recharge discharging in creek alignments or breaks in slope. This form of spring is effectively rejected recharge, short lived and closely related to rainfall conditions.

Based on the above the springs at Cadia are not believed to have deep seated sources. Variability in spring head and consequent flow are likely driven by local recharge events, with flow rate a result of the spring head and the permeability of the spring source aquifer. Although there are some substantial spring flows noted, these appear mostly related to the main outcrop of Tertiary basalt to the north of the mine, and are limited relevance to the NTSF performance.

NTSF Area Springs

All four of the spring mechanisms described above have the potential to occur in the NTSF area. The eastern flank of the Tertiary basalt beneath the western embankment may provide contact spring flow. The Werribee Fault strikes beneath the NTSF and is regional is scale – this feature may provide either of conduit or barrier to flow conditions. Baseflow and interflow springs are also possible and based on visual descriptions provided of observed springs are probably the main mechanism in place beneath the facility.

Some NTSF area observations include:

- Woodward-Clyde (1995): *"It is understood that creekflow is perennial. This baseflow appears to be recharged through leakage from basalts that outcrop with the upper reaches of the catchment, or through 'spring' flow fed from fault / fracture zones." And "The Tertiary basalt and trachyte flows are a known groundwater resource which are used for domestic and stock water supplies. Some groundwater springs are found at the contact between the Tertiary flows and underlying formations. Groundwater flows have been*

observed from the boundary between the Tertiary basalt and the Silurian Sediments / Angullong Formation in the catchment area of Rodds Creek."

- Knight Piesold and PSM (1997): Noted *"During construction of the Stage 1 embankment several small springs were encountered in the base of Rodds Creek both upstream and downstream of the Zone A core. Springwater trapped upstream of the core will be collected by the upstream drainage system and discharged to the drainage collection pond."* And *"…a small homogenous earthfill embankment was constructed in Rodds Creek to provide a seepage collection pond to trap any spring water seeping into the channel through the rockfill placed within the footprint."*
- Woodward-Clyde (2000): Photograph of a natural spring at Chh1650, noted to be very wet due to recent rain.

The observations at the NTSF and other references indicate that the springs observed are not large in yield, are not likely to have a substantial driving head, and their variability in flow appears related to local rainfall conditions rather than regional hydraulic stresses. The construction of the NTSF recognised the presence of these springs and included internal components to address water produced by the springs during and after construction (Section 2.4.2). The piezometric records shown throughout Section 2.4.5 indicates that the NTSF drain was operational and that potential increasing tailings saturation as a consequence (say) of unmitigated spring contributions does not appear to be apparent.

As the NTSF was progressively raised, the increased head over the springs would be expected to further reduce their ability to flow and contribute water to the base of the tailings. The occurrence of interflow or baseflow springs would be diminished due to this suppressing head, and also due to the loss or reduction of natural recharge which might be expected to be the source of their flow in the first instance.

2.5 Hydrogeological Processes Discussion

The following summarises the preceding content to provide a general description of the hydrogeology at the NTSF:

- There are four broad groundwater systems, being:
  - Low permeability Ordovician Volcanics of the Weemalla Formation and the Forest Reefs Volcanics.
  - Low permeability Silurian sediments of the Ashburnia Group, which comprise limestones, mudstones, siltstones, sandstones and shales[2].
  - Moderate to high permeability Tertiary basalt, which may include a buried palaeo channel sequence where vent flows infilled pre-Tertiary drainages. The main outcrop of this unit is north of the mine, however there is an elongate sequence of basalt which lies beneath and west of the western embankment of the NTSF

[2] Previous assessments have often considered the Ordovician and Silurian sequence as a singly hydrostratigraphic unit because of the similarity of conditions in each sequence, and their strong hydrogeological contrast to the Tertiary basalt and Quaternary alluvium (where developed).

  - Quaternary alluvium, which in the immediate study area is poorly developed. This is also of limited relevance to the performance of the NTSF due to foundation preparation activity as part of construction.

- Structurally, the Werribee Fault underlies the NTSF and is a regionally mapped north to north-northeast trending, westerly dipping thrust with a strike-slip component. Near to the Cadia Mine, it truncates several NNW trending faults indicating it may be a late stage feature. The structure has a damage zone 200-400m wide, and a vertical offset of about 300m. Local faulting and fracturing is likely and may cause localised areas of higher permeability in the Ordovician / Silurian basement rocks.
- Groundwater recharge of the Tertiary basalt is most likely through rainfall recharge. Recharge of alluvium will be a combination of rainfall, creek flow and spring / seep from underlying basement or flanking Tertiary basalt. Recharge into the Silurian / Ordovician will be via rainfall recharge and will also occur where saturated Tertiary basalt overlies these systems. Rates of recharge into the Silurian / Ordovician are expected to be low to negligible, and variable for the Tertiary basalt and Quaternary alluvium depending on their condition at surface. Groundwater discharge may occur from all units via springs and seeps. Additionally, bore abstraction may occur for permeable sequences such as the Tertiary basalt and alluvium of spatial and hydrogeological significance.
- The NTSF design recognised, and construction had accounted for, the presence of springs and the potential impacts of a high permeability aquifer beneath the western embankment. NTSF performance monitoring has indicated the underdrain installed during Stage 3 construction has performed as intended. Phreatic conditions within the tailings indicate downward drainage effects toward to the drain, and unsaturated tailings conditions of up to 8m below the tailings elevation at the upstream of the embankment. Foundation seepage loss appears to be low and does not appear to have pressurised the contrastingly permeable underlying basalt. Based on this observation, it is assumed that the Werribee Fault has also not been pressurised.

3 SEEPAGE MODELLING

3.1 Two-Dimensional Seepage Modelling

Two-dimensional (2D) seepage modelling was undertaken using Seep/W to test hydraulic concepts and to inform the construction requirement of boundary conditions and hydraulic stresses for the three-dimensional (3D) modelling.

3.1.1 2D Model Details

Two models were constructed:

- Section CH1950 across the NTSF dam with a section length of ~850 m (which is the same dimensions and alignment of the early Slope/W model), or the short section, and,
- An extended version of this section of Ch1950, extending the model in both directions (4,738m) to reach the northern decant pond and the upper level Rodd Creek Dam upstream of the NTSF – the long section.

Assigned model parameters are consistent with parameters used in the initial Slope/W simulations (reference) with judgement-based values assigned where additional input was required. A summary of the material parameters used in the 2D modelling is provided in Table 4.

Table 4: 2D Seep/W Sectional Models for Testing of Hydraulic Stressors

Geology / Strata	K_h(Sat) m/s	K_v/K_h	Porosity	Ss 1/m
NTSF with depth 0 to 3m	1.00E-05	0.1	0.35	9.80E-05
NTSF with depth 3 to 6m	5.00E-06	0.1	0.35	9.80E-05
NTSF with depth 6 to 10m	1.00E-06	0.1	0.35	9.80E-05
NTSF with depth >10m	1.00E-07	0.1	0.35	9.80E-05
Dam Core	1.00E-09	1	0.35	9.80E-05
DS Berm	2.00E-05	1	0.3	9.80E-05
DS Rockfill	2.00E-05	1	0.3	9.80E-05
2B Rockfill	2.00E-04	1	0.3	9.80E-05
2A Transition	1.00E-06	1	0.3	9.80E-05
Foundation	1.00E-07	1	0.35	9.80E-05
Weathered Rock	5.00E-08	0.1	0.2	9.80E-05
Bedrock	1.00E-08	0.1	0.1	9.80E-05
Tertiary basalt	1.00E-04	0.1	0.2	9.80E-05
Palaeo Pathway – Tb buried	1.00E-02	0.1	0.2	9.80E-05

3.1.2 2D Model Results

Model output are shown in Figure 22 and Figure 23.

For the short section model (Figure 22) phreatic conditions are largely controlled across the dam with drainage elements effectively maintaining partially drained conditions in the tailings upstream of the dam, consistent with general piezometric observations.

Foundation conditions in this model do not permit differentiation in material parameters, so the highly contrasting conditions of the Tertiary basalt are not able to be separately modelled, neither are pond conditions in the NTSF and their relative influence on phreatic conditions across the tailings.

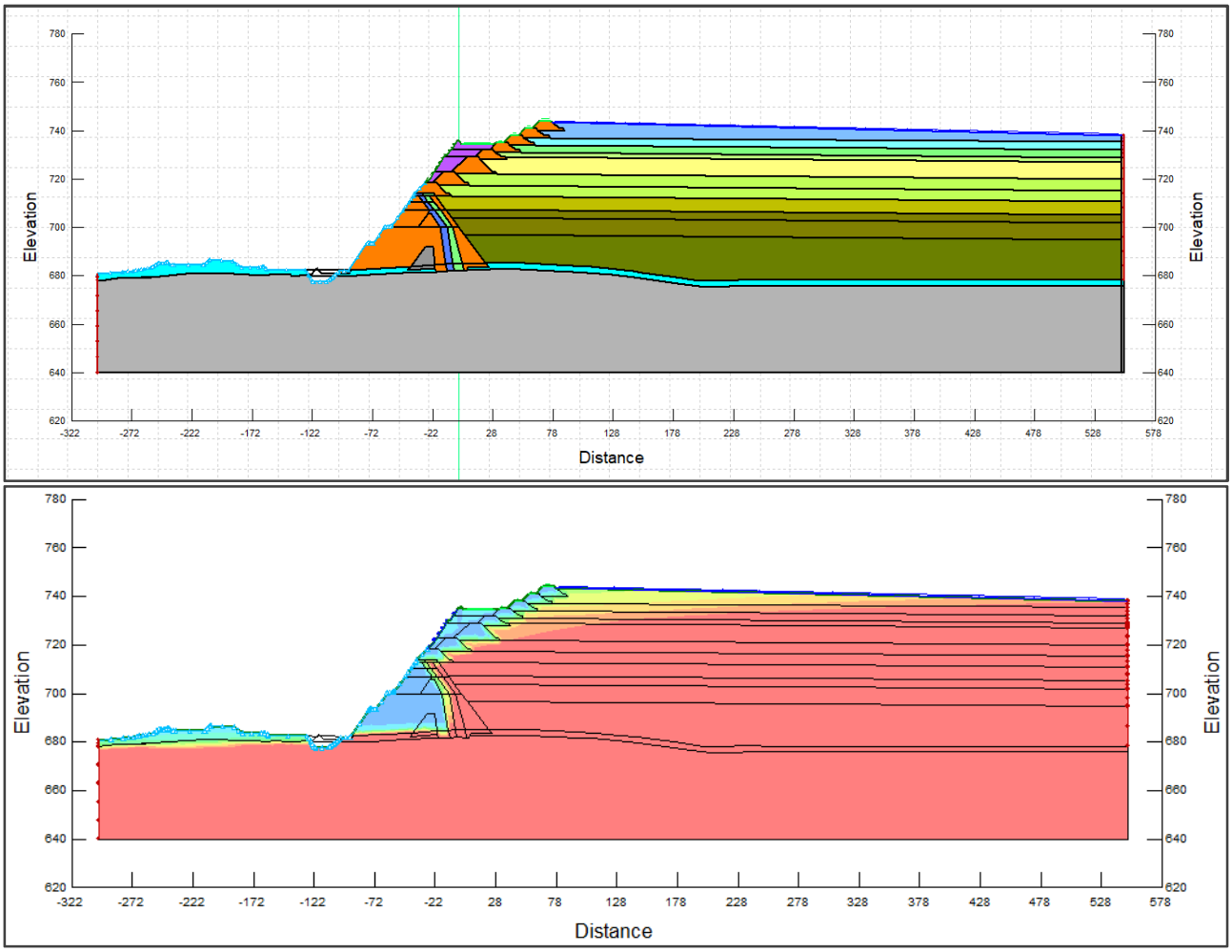

Figure 22: Short Section Model Domain (upper) and Modelled Phreatic Conditions (lower), Steady State

The long section model was developed to reduce the identified limitation in the short section model, and is shown in Figure 23. The modifications to this domain are extension upstream of the NTSF to permit inclusion of the NTSF pond and the potential effect of the Rodds Creek Dam, and increased layer partitioning of the foundation conditions to permit definition of the Tertiary basalt and a palaeo-alluvium sequence (between the base of the basalt and the underlying Silurian or Ordovician basement).

Three steady state scenarios are shown: the base case conditions (Silurian / Ordovician foundation materials), a Tertiary basalt (and palaeo-alluvium) sequence beneath and downstream of the dam,

and another version of this with the Tertiary basalt and palaeo-alluvium extending approximately 1/3rd upstream of the dam.

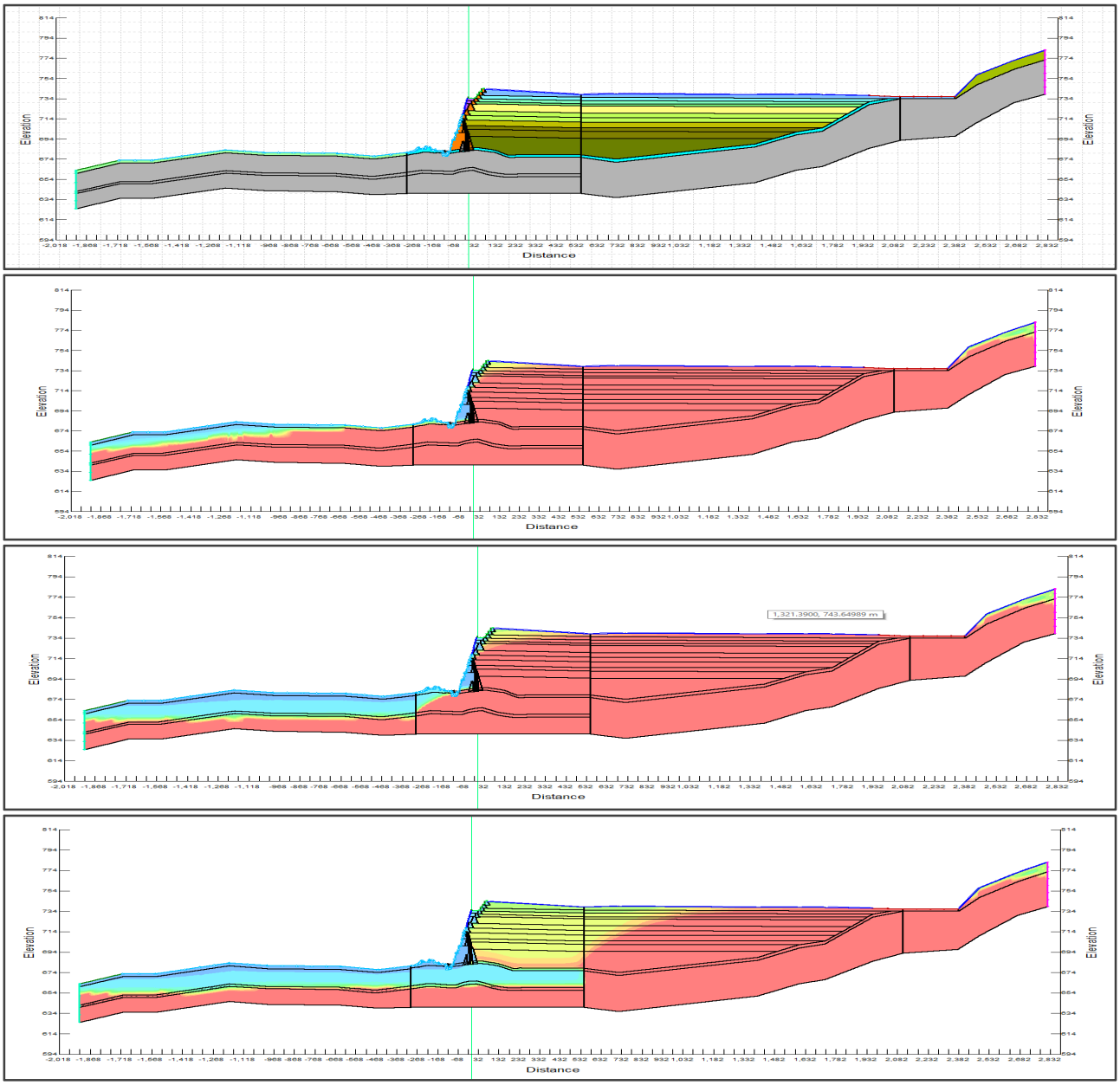

Figure 23: Long Section Model Domain (upper) and Modelled Phreatic Conditions a) Base Simulation Conditions, b) Tertiary basalt and palaeo-alluvium to Dam Toe, and c) Tertiary basalt and palaeo-alluvium to ~30% of Dam U/S of Crest

Discussion of the results of these three simulations is provided:

1. **Base Case Silurian / Ordovician foundation model case.**

   Similar results to the short section are observed, although this model gives a better appreciation of the relevance of the decant pond as a constant head source. With low permeability foundation materials, the model predicts largely saturated conditions at the

downstream toe of the dam, although the drainage elements within the dam appear to remain effective.

Resultant variability of the degree of saturation of the tailings is a combination of the applied boundary conditions at either end of the model – the decant pond elevation in the upstream area of the section, and drainage elements in the dam itself. Differing recharge rates across the tailings provided some variability in this saturation but was not the primary factor influencing saturation upstream of the dam.

2. **Tertiary basalt and palaeo-alluvium downstream of the NTSF model case.**

   This scenario showed that strong downstream drainage via the higher permeability basalt occurs. This prediction is consistent with observations shown in Figure 19, indicating that the underlying basalt allows the seepage to be distributed. These model results also suggest the rate of seepage into the Tertiary basalt for the section shown does not pressurise the system and that the geometry and material parameters of the basalt are sufficient to carry seepage water away.

3. **Tertiary basalt and palaeo-alluvium downstream and upstream of the NTSF model case.**

   This section was simulated to consider the drainage effect of the basalt (without seepage mitigation prevention) in contrast to the generally lower permeability material of the Silurian and Ordovician foundation and the tailings.

   This is intended to reflect conditions where the basalt underlies the dam and tailings with the potential to act as a high capacity drain. No clay cover of the basalt is modelled in this case.

   As expected under this scenario, the basalt is the dominant drainage material, pushing the upstream extent of saturation further upstream, and increasing the gradient in the tailings between the extent of basalt simulated and the decant pond. (This may also be a response to the steady state condition modelled.) This is not consistent with data observed (Section 2.4.5), which shows no such dominant drainage effects attributed to the basalt where it underlies tailings.

3.1.3 2D Model Discussion and Relevance to the 3D Domain

The following points are noted:

- The 2D system is sensitive to foundation permeability, decant pond conditions and dam drainage construction elements, and to a lesser extent rainfall infiltration on the NTSF beach. Spigot water contributions were not modelled in the 2D scenario.
- Lower foundation permeability limits the vertical losses from the NTSF, with removal of water and the shape of the phreatic condition within the tailings most influenced by the efficiency of the dam drainage construction elements and the location and elevation of the decant pond.
- The effect of the Tertiary basalt as a drain without preventative seepage measures is powerful, and does not appear present in observational data. Piezometric records indicate

dam construction methods to address the potential high drainage this unit may create as being effective. This concept should be carried to the 3D model domain.

- Hydraulic gradients within the basalt appear to dissipate relatively quickly downstream of the dam, consistent with observed (post slump event) data.
- Decant Pond – the elevation and location of the decant pond has a strong influence on the degree of saturation and the position of the fully and partially saturated tailings.;
- Staged TSF – field results suggest that the tailings do not exhibit strong reduction in permeability due to settlement / consolidation but do show a downward drainage effect. The effect of this drainage on conditions in the tailings needs to be replicated in the 3D model construction and calibration process.

3.2 Three-Dimensional Numerical Modelling

3.2.1 3D Modelling Preamble

Three-dimensional (3D) modelling was required to:

1. Predict NTSF seepage and phreatic conditions for the period leading up to the slump event in March 2018;
2. Account for the primary sources of potential hydraulic stress internal and external to the NTSF; being both construction elements of the facility and natural strata. In this regard the model is to reflect the conceptual system described in Section 2 of this report;
3. Represent pre-slump-event conditions with a suitable level of confidence in model calibration and predictive performance.
4. Provide predicted conditions to others for independent stability or deformation analysis.

A 3D domain is preferred over the 2D domain because of its ability to reflect the geometric uniqueness of the NTSF construction elements and the underlying geology, and it permits are more spatially calibrated condition to be achieved which can then be used for either 2D or 3D analysis by others.

The model does not assess potential failure of NTSF design elements, and is intended to reflect the as-built condition as close as possible, so that predictions of hydraulic conditions based on operational performance of design and construction, as is understood to be the case, can be carried forward to deformation and stability analysis by others.

3.2.2 Model Construction

Model Selection, Limits & Spatial Extent

The three-dimensional, finite-element model platform FEFLOW was selected to meet the objectives and requirements of this investigation.

The 3D NTSF model domain is shown in Figure 24, with key line-data which is used to develop nodal distribution (dam infrastructure and drainage) also shown. The domain includes the full domain of the NTSF and extends far enough west to capture the Tertiary basalt which underlies

the western embankment. To the south, the model domain extends far enough to capture the STSF ponding which is a critical boundary condition. The model domain covers a planar area of $1.39x10^7$ m^2 (~14 km^2), with model dimensions of 4.7 km x 4.0 km x 150m.

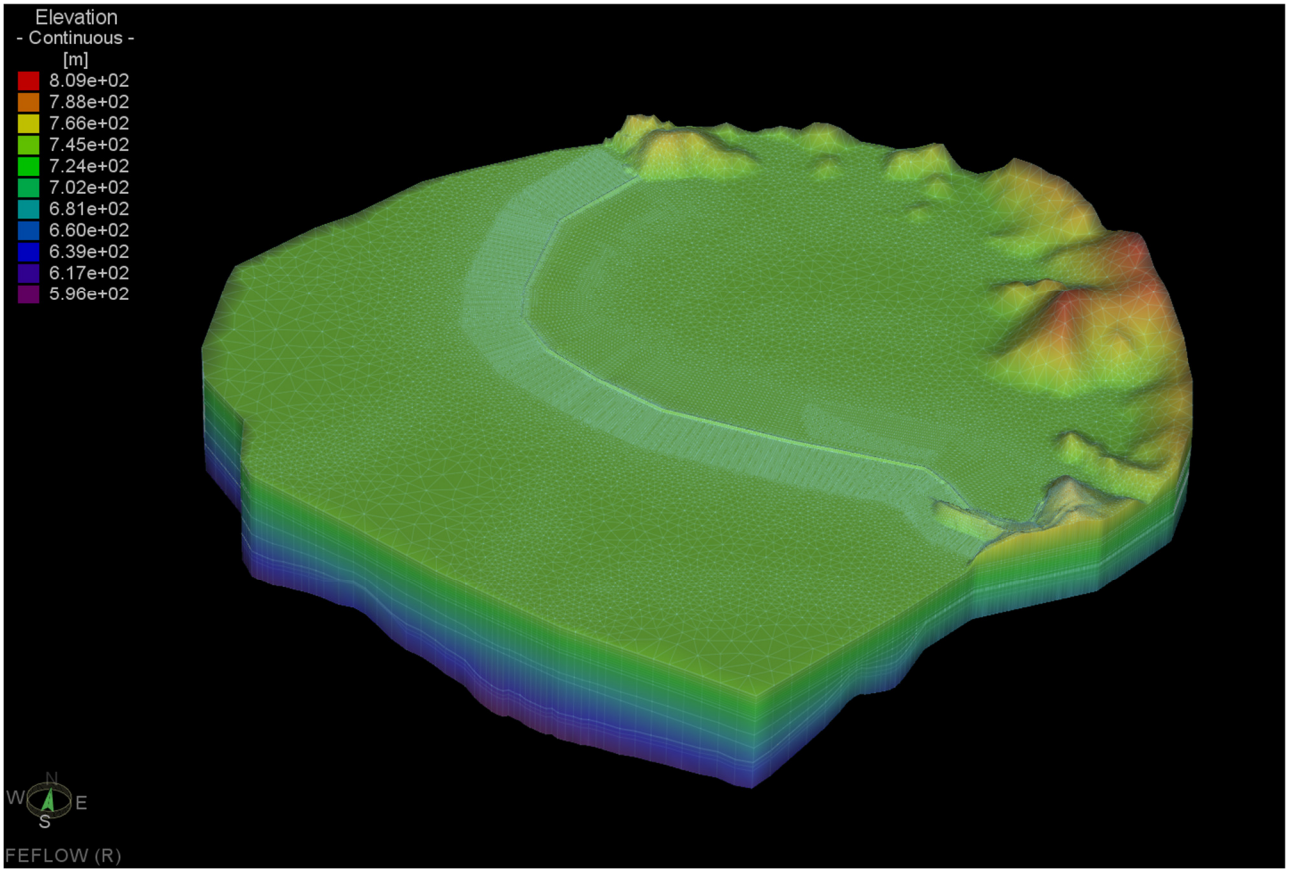

Figure 24: Cadia NTSF 3D Model Extent, Oblique View

Geological Basis

The model domain has been vertically extended to a nominal depth of ~5 x the maximum depth of the placed tailings. This is to provide sufficient depth definition to permit development of deeper groundwater flow regimes if required. Regional hydrogeology and dam construction have been represented consistent with the conceptual description provided in Section 2, and comprises:

- Dam Construction Elements:
  - Tailings, NTSF and STSF, with depth variability included in construction;
  - Dam Core;
  - Class 2B Fill;
  - Upstream clay liner;
  - Underdrain / gravel fill; and
  - Dam lifts (combined fill and lining).

- Geology:
  - Silurian / Ordovician, fresh and weathered;
  - Tertiary basalt, fresh and weathered;
  - Palaeo-alluvium where interpreted to exist;
  - Werribee Fault alignment; and
  - Top soil.

Calibrated material parameters are discussed in Section 3.2.3.

Domain / Nodes / Layers

The model was discretised using six-noded three-dimensional prism elements. A process of mesh refinement based on hierarchical areas of model interest was used to arrive at the final mesh configuration, which is shown in Figure 25.

There are ~73,000 elements per layer, across 19 layers for ~1.4M elements in total. Model layers 1-15 for the area of the NTSF are assigned for TSF construction and are aligned with the Stage development of the facility (e.g. model layer 5, is dam stage 5). Layer 15 is an allowance for engineering foundation transition conditions, and layers 16 to 19 represent natural strata. A summary of the model layering and NTSF staging is provided in Table 5.

Table 5: NTSF Construction Stage and Model Layer Development

Stage	Elevation	Layers
Natural geology	Variable	16-19
Engineering Layer/Top Soil	1m thickness	15
NTSF Stage 1	700	14
NTSF Stage 2A	707	13
NTSF Stage 2B/1	710.5	12
NTSF Stage 2B/2	714	11
NTSF Stage 3	718.5	10
NTSF Stage 4	723	9 and 8
NTSF Stage 5	729	6 and 7
NTSF Stage 6	732	5
NTSF Stage 7	735	4
NTSF Stage 8	738	3
NTSF Stage 9	741	2
NTSF Stage 10	744	1

This geometric arrangement resulted in reasonable model run times (generally ~2 hours for a quasi-steady state, and 1 hour for the 67-day transient with daily time steps), and relatively stable model simulations.

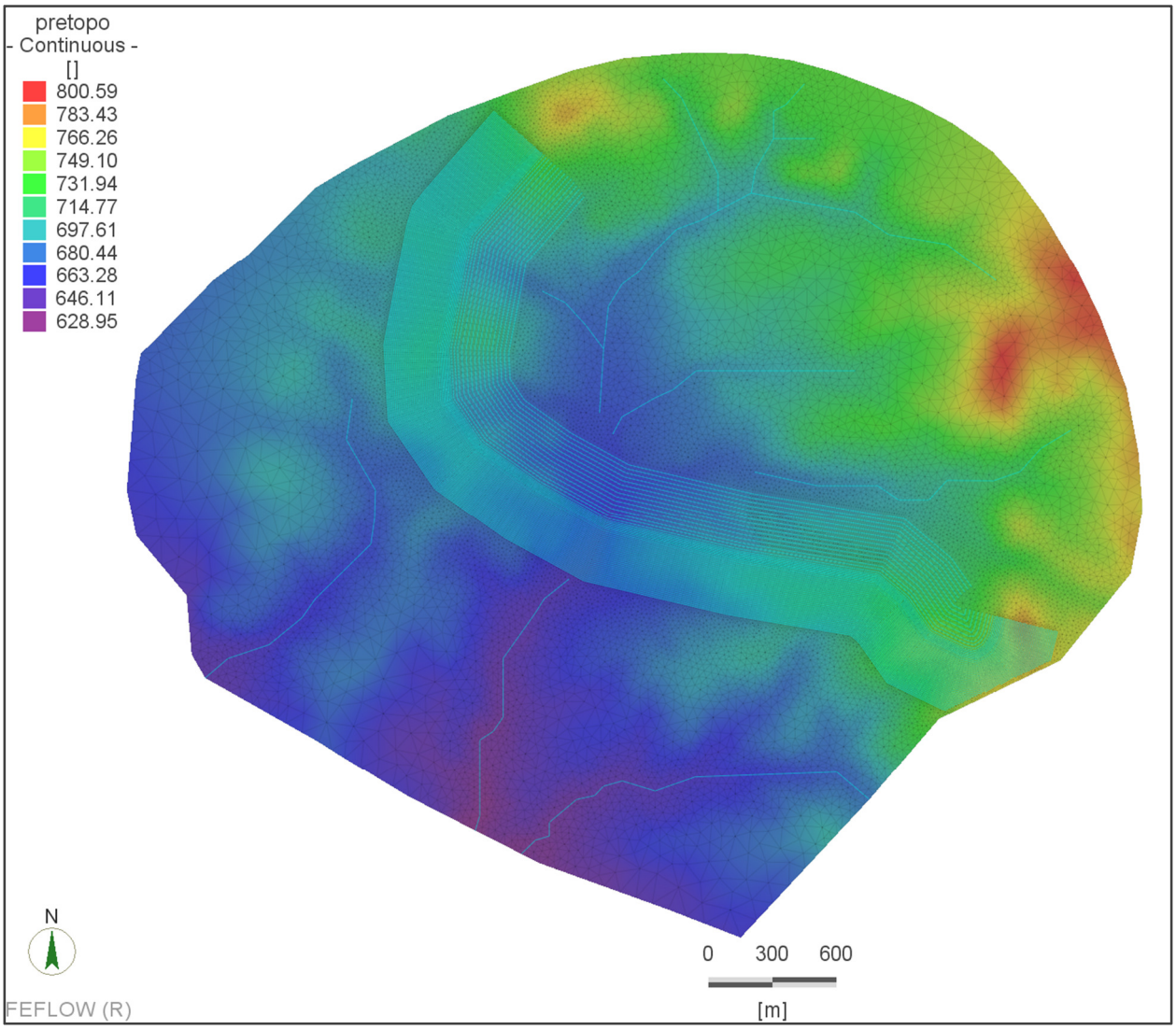

Figure 25: Cadia NTSF 3D Model Node Distribution

Model Boundary Conditions

Model boundary conditions comprise:

- Rainfall recharge, as a variable rate based on percentage of mean annual rainfall and dependant on the hydraulic properties of the upper most unit in the model;
- Decant pond area and elevation as a varying fixed head, for the NTSF and STSF, based on mapped extents and stage development of the tailings dam(s) and consequent ponded water levels (Figure 14);
  - Spigot water distribution across the NTSF beach was zoned based on distance from the dam crest and location to the pond. Rates were manually calibrated to assist in constructing a plausible water balance for the tailings, and were:
    - 400-600 mm/annum for the area up to 100m from the dam crest;
    - 100-200 mm/annum for beach areas 100 m to 400 m from the dam crest,
    - 30mm/annum for the balance, which is approximately equivalent to 4% of MAR.

- No flow boundary conditions were established at the model base and on the lateral limits of the model domain.

Constrained seepage face conditions were established across the face of the dam. The constraints on the seepage face dictate that once phreatic conditions intersect the top of the upper active layer in the model at the time of the simulation, water is removed from the system and reports to the water balance as an outflow. This representation of seepage faces is established to reflect the process of emerging seepage due to rising phreatic conditions "daylighting" at surface.

Drain discharge was measured from model output, no fixed heads were applied in forcing the model to exit excess water. The STSF southern outflow was modelled as a seepage face (665.0 to 671.0 mRL).

Model Timing & Stress Periods

Timing and evaluation of model calibration is discussed in Section 3.2.3

A steady state model of the Stage 9 NTSF condition was run and calibrated. This calibrated steady state model was then used to create starting conditions for the transient simulation of Stage 10 of the NTSF.

The Stage 10 model was constructed to run from 1-Jan-2018 to the 9-Mar-2018, for a 67-day period. Recharge on both the NTSF and the dam raise material was established as a daily time sequence based on actual conditions as recorded by site. Pond elevations reflected actual data, and model results were extracted for the final time step, which is coincident the slump event.

Results of this process are discussed in Section 3.2.4.

3.2.3 Model Calibration

Calibration Approach

The conceptualisation of the system, review of observation data and outcomes from the 2D sectional analysis indicate the NTSF has moderate to limited connectivity with foundation materials, and that the phreatic condition within the tailings are more dominated by dam construction elements and decant pond location. The calibration strategy was developed to reflect these system attributes with focus brought to NTSF observational data. Data outside the facility were still used, but were not considered the primary drivers to achieve a satisfactory level of model calibration.

Steady state model calibration was undertaken on the Stage 9 NTSF condition, with focus on three primary sets of observation data:

- CPTu Pore Water Pressure Gradients (Figure 20) measured in the NTSF, showing downward vertical gradient profiles within the tailings;
- 2017/18 piezometric data for tailings locations around the upstream area of the dam crest (Figure 21), which show the prominence of drain effects on the tailings profile;
- Measured drain flow between 2015 and 2018 (Figure 13), which for Stage 9 were generally between 40 L/min to 50 L/min.

Post-slump groundwater levels in the Tertiary basalt were also considered, however, it is noted these were measured after the event.

Initial calibration was manually completed modifying boundary condition and parameter ranges. Automated and manual calibration was then completed firstly on the foundation geology properties, and then on the permeability of the tailings inside the NTSF.

Calibration Results

A summary of model material parameters post calibration is provided in Table 6. Permeability modified during the calibration process is summarised in the following:

- Tertiary basalt Kh / 100 from the pre-calibration value
- Weathered rock Kh x 2.5 from the pre-calibration value
- NTSF Tailings Kh Variable, range 'tightened' and depth varying

As expected, the modification of tailings permeability had the greatest impact on model performance. A depth-variant hydraulic conductivity is included and is summarised in Figure 26. Tertiary basalt permeability was reduced; however, the basalt remains the unit with the highest permeability in both tailings and bedrock. High permeability underdrain materials and low permeability clay blanket conditions are the main controlling factors on the rate of water transfer vertically into foundation materials, and through the dam.

Table 6: Model Calibrated Hydraulic Parameters

Material	Kh (Sat) m/sec	Kv/Kh	Porosity	Ss 1/m
Bedrock	1.00E-08	0.1	0.1	1.00E-04
Faults	5.00E-09	1	0.1	1.00E-04
Lifts (Combined Fill and Liners)	1.00E-06	1	0.3	1.00E-04
2B Fill (Core side Fill)	2.00E-04	1	0.3	1.00E-04
Dam core	1.00E-09	1	0.35	1.00E-04
Basalt	1.50E-06	1	0.2	1.00E-04
Palaeo Pathway	1.50E-06	1	0.2	1.00E-04
Top Soil	2.00E-08	1	0.35	1.00E-04
Upstream Clay liner	1.00E-09	1	0.1	1.00E-04
Slotted piping/Gravel fill	1.20E-02	1	0.1	1.00E-04
Weathered Rock	2.00E-08	0.1	0.1	1.00E-04
NTSF	1.00E-7 to 2.65E-6	0.1	0.35	1.00E-04
STSF	5.00E-07	0.1	0.35	1.00E-04

Permeability modified during the calibration process is summarised in the following:

- Tertiary basalt Kh / 100 from the pre-calibration value
- Weathered rock Kh x 2.5 from the pre-calibration value

- NTSF Tailings Kh Variable, range 'tightened' and depth varying

The modification of tailings permeability had the greatest impact on model performance. A modified depth-variant hydraulic conductivity has been included in the model and is summarised in Figure 26. Reduction of two orders of magnitude of the basalt is also a noted significant modification. Initial estimates are considered more representative of the unit where it is more regionally mapped and recognised as an aquifer to the north. The modifications to ground conditions discussed in Section 2.4.2 may also contribute to a lowered value for this unit.

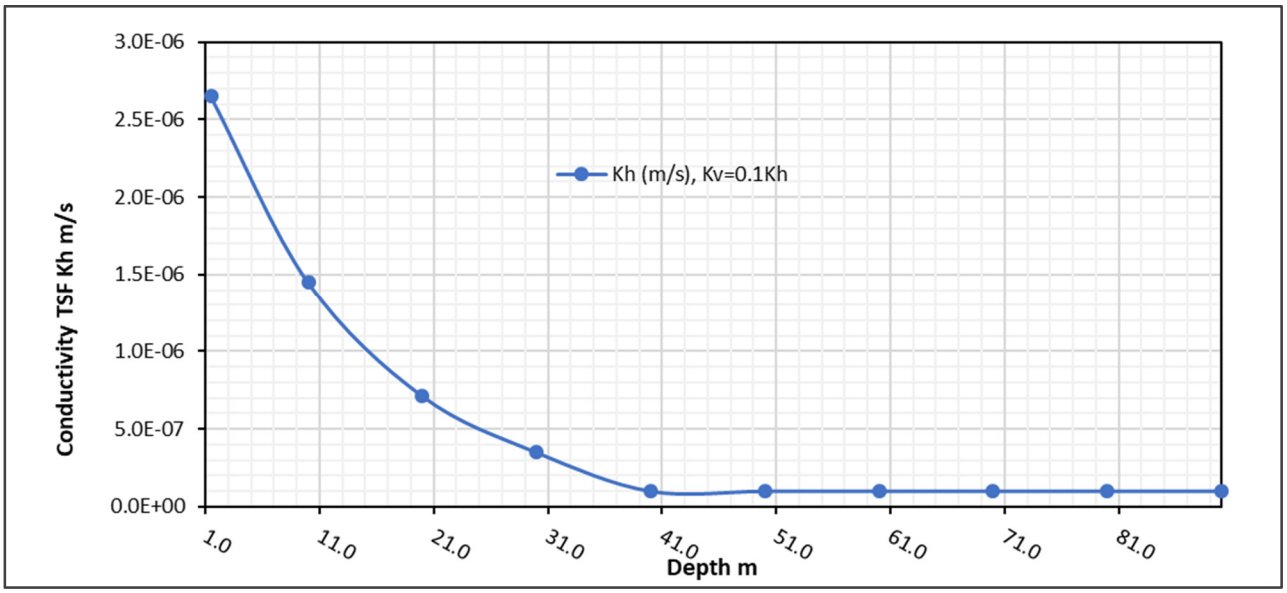

Figure 26: Inferred Tailings Permeability Modified Depth Variant Range

A summary of observed versus modelled head values for the calibrated Stage 9 model is provided in Table 7. Values used which post-date the event are shaded orange.

Table 7: Summary Observed versus Modelled Head Values, Calibrated Model

Name	Depth	Tip El. (m)	Observed Head m	Computed Head m	Observed Pressure kPa	Computed Pressure kPa	Head Residual (m)	Observation Date
VWP-N01	10.00	730.70	734.50	736.10	37.28	52.97	-1.60	2017-06-30
VWP-N02	10.00	731.20	735.10	735.02	38.26	37.44	0.08	2017-06-30
VWP-N02a	10.06	731.14	737.26	735.01	60.04	37.93	2.25	2017-xx-xx
VWP-N02b	15.00	726.20	736.90	734.17	104.97	78.18	2.73	2017-xx-xx
VWP-N02c	20.26	720.94	735.72	733.32	144.99	121.42	2.40	2017-xx-xx
VWP-N03	10.00	730.90	735.20	733.95	42.18	29.97	1.25	2017-06-30
VWP-N03a	16.11	724.79	735.90	732.75	108.99	78.12	3.15	2017-xx-xx
VWP-N03b	20.00	720.90	735.58	732.03	144.01	109.21	3.55	2017-xx-xx
VWP-N03c	34.09	706.81	734.03	726.85	267.03	196.63	7.18	2017-xx-xx
VWP-N04	16.00	724.40	731.30	733.01	67.69	84.47	-1.71	2017-06-30
VWP-N04a	12.01	728.39	734.40	733.76	58.96	52.67	0.64	2017-xx-xx
VWP-N04b	23.80	716.60	731.79	731.64	149.01	147.59	0.15	2017-xx-xx
VWP-N04c	36.35	704.05	729.02	726.18	244.96	217.14	2.84	2017-xx-xx
VWP-N04d	38.05	702.35	728.45	725.39	256.04	226.05	3.06	2017-xx-xx

Name	Depth	Tip El. (m)	Observed Head m	Computed Head m	Observed Pressure kPa	Computed Pressure kPa	Head Residual (m)	Observation Date
VWP-N04e	47.67	692.73	728.41	722.19	350.02	289.00	6.22	2017-xx-xx
VWP-N05	16.00	724.10	727.80	730.27	36.30	60.48	-2.47	2017-06-30
VWP-N05a	19.47	720.63	729.50	729.67	87.01	88.68	-0.17	2017-xx-xx
VWP-N05b	30.22	709.88	726.80	725.86	165.99	156.77	0.94	2017-xx-xx
VWP-N05c	44.66	695.44	721.13	718.45	252.02	225.75	2.68	2017-xx-xx
VWP-N05d	60.67	679.43	712.66	713.13	325.99	330.64	-0.47	2017-xx-xx
VWP-N06	16.00	723.00	730.80	731.67	76.52	85.05	-0.87	2017-xx-xx
VWP-N06a	11.07	727.93	733.54	732.39	55.03	43.73	1.15	2017-xx-xx
VWP-N06b	20.00	719.00	731.44	731.13	122.04	118.97	0.31	2017-xx-xx
VWP-N06c	30.07	708.93	729.01	728.60	196.98	193.00	0.41	2017-xx-xx
VWP-N07	16.00	723.00	733.10	732.26	99.08	90.83	0.84	2017-06-30
CE405	*30.25*	*657.58*	*682.68*	*677.26*	*246.23*	*193.09*	*5.42*	*2018-09-06*
CE406	*30.15*	*657.89*	*677.83*	*679.90*	*195.61*	*215.89*	*-2.07*	*2018-09-06*
CE407	*51.00*	*680.80*	*697.71*	*703.83*	*165.89*	*225.96*	*-6.12*	*2018-09-06*
CE408	*56.95*	*686.85*	*710.78*	*713.58*	*234.75*	*262.21*	*-2.80*	*2018-09-06*
CE412	*56.50*	*686.65*	*692.36*	*702.83*	*56.02*	*158.68*	*-10.47*	*2018-09-06*
CE413	*57.35*	*697.00*	*724.87*	*719.97*	*273.40*	*225.30*	*4.90*	*2018-09-06*
CE415	*25.00*	*661.16*	*684.77*	*687.22*	*231.61*	*255.67*	*-2.45*	*2018-09-06*
CE417	*12.40*	*688.60*	*691.21*	*694.03*	*25.60*	*53.29*	*-2.82*	*2018-09-06*
CE430	*26.15*	*680.17*	*690.57*	*698.44*	*102.02*	*179.22*	*-7.87*	*2018-09-06*

Contoured calibrated head conditions for Stage 9 are provided in Figure 27 for the NTSF tailings. A series of cross sections as shown on this figure, are provided for the calibrated model in Figure 28.

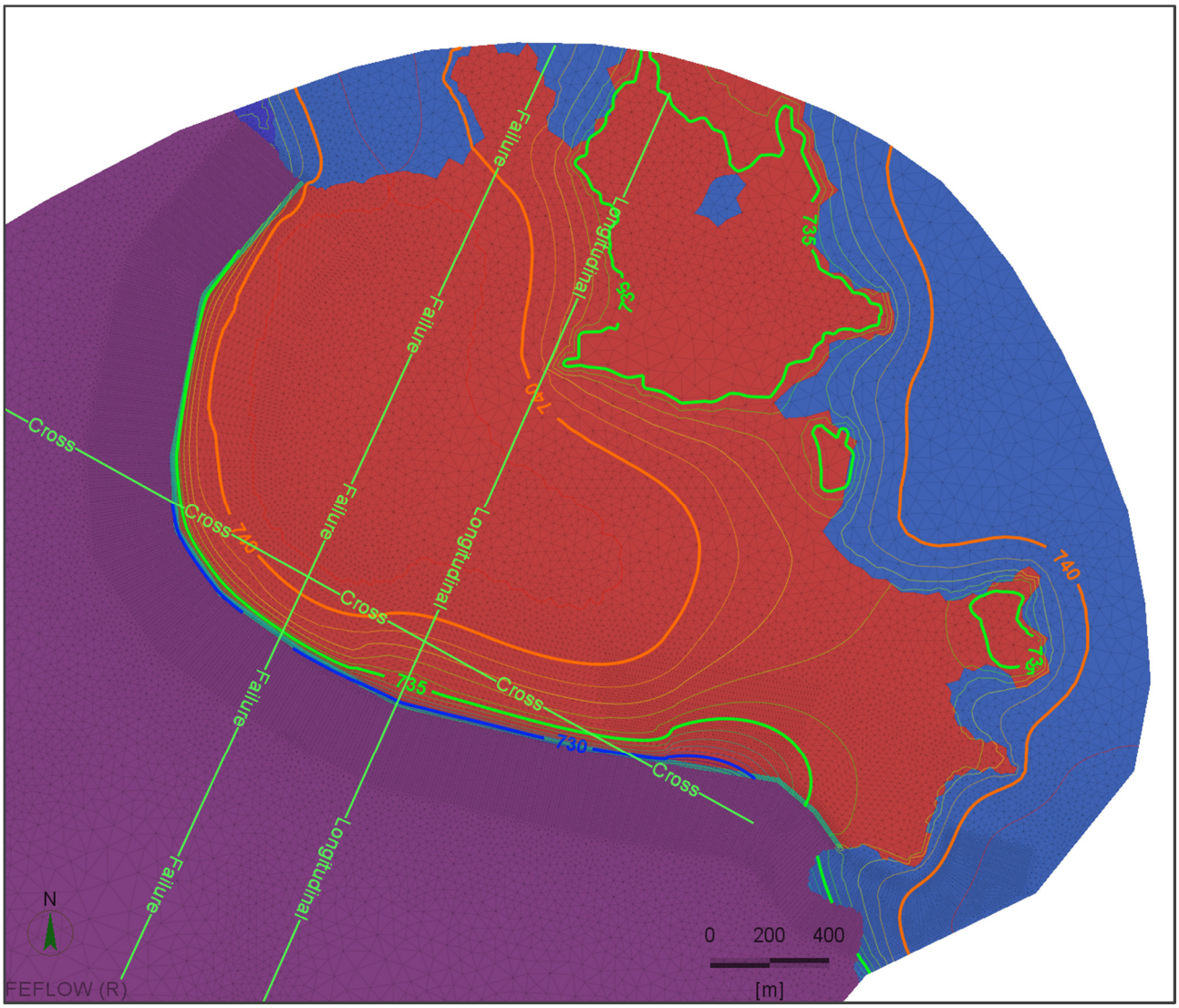

Figure 27: Calibrated Model Head Conditions, Tailings Conditions

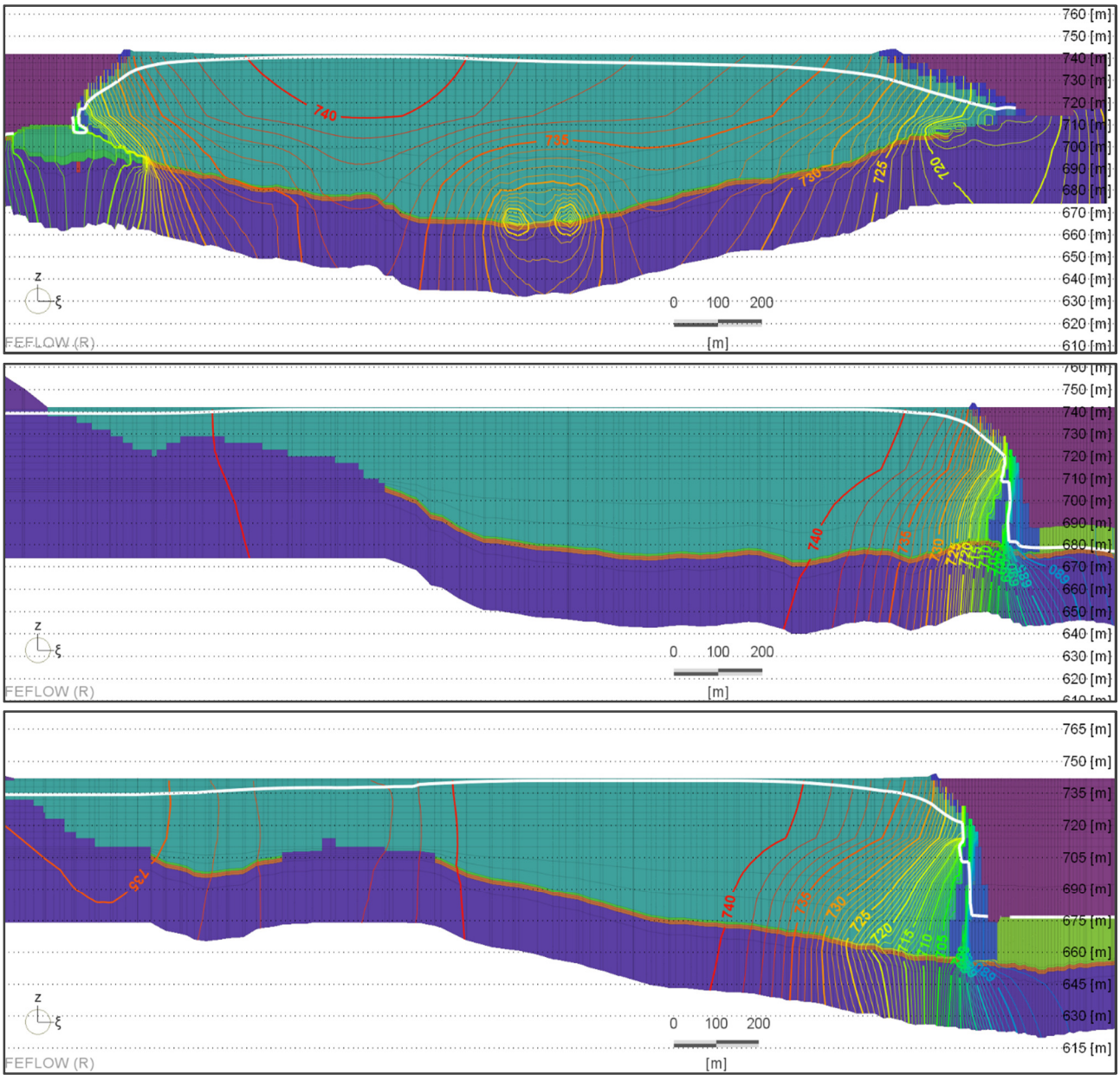

Figure 28: Calibrated Model Head Conditions, Model Sections: Cross (upper), Failure (middle), Longitudinal (lower)

Calibration Performance

Additional discussion of calibration performance is provided in the following sections and comprises review of the three components of the predictive model required to replicate the conceptual understanding of the performance of the NTSF, being: statistical measure of measured versus observed heads, replication of pore pressure response and downward gradient trends, prediction of drain flow discharge from the NTSF.

Measured versus Observed Conditions

Measured versus observed conditions for the Stage 9 model, for TSF VWPs are shown in Figure 29. Note this suite of data includes the 2018 installed CE sites at the base of the NTSF embankment.

Although these were installed post-slump-event, they are important in understanding the performance of the model to replicate key hydraulic stresses.

Calibration statistics are within industry accepted metrics. The correlation co-efficient between measured and modelled data is 0.95, the RMS error is ~3.69 m, and the mean error is -0.3m (indicating the model is computing heads slightly below measured). The scaled RMS is 6.2%, and the measured data has a 60 m vertical range between about 676 mRL and 736 mRL.

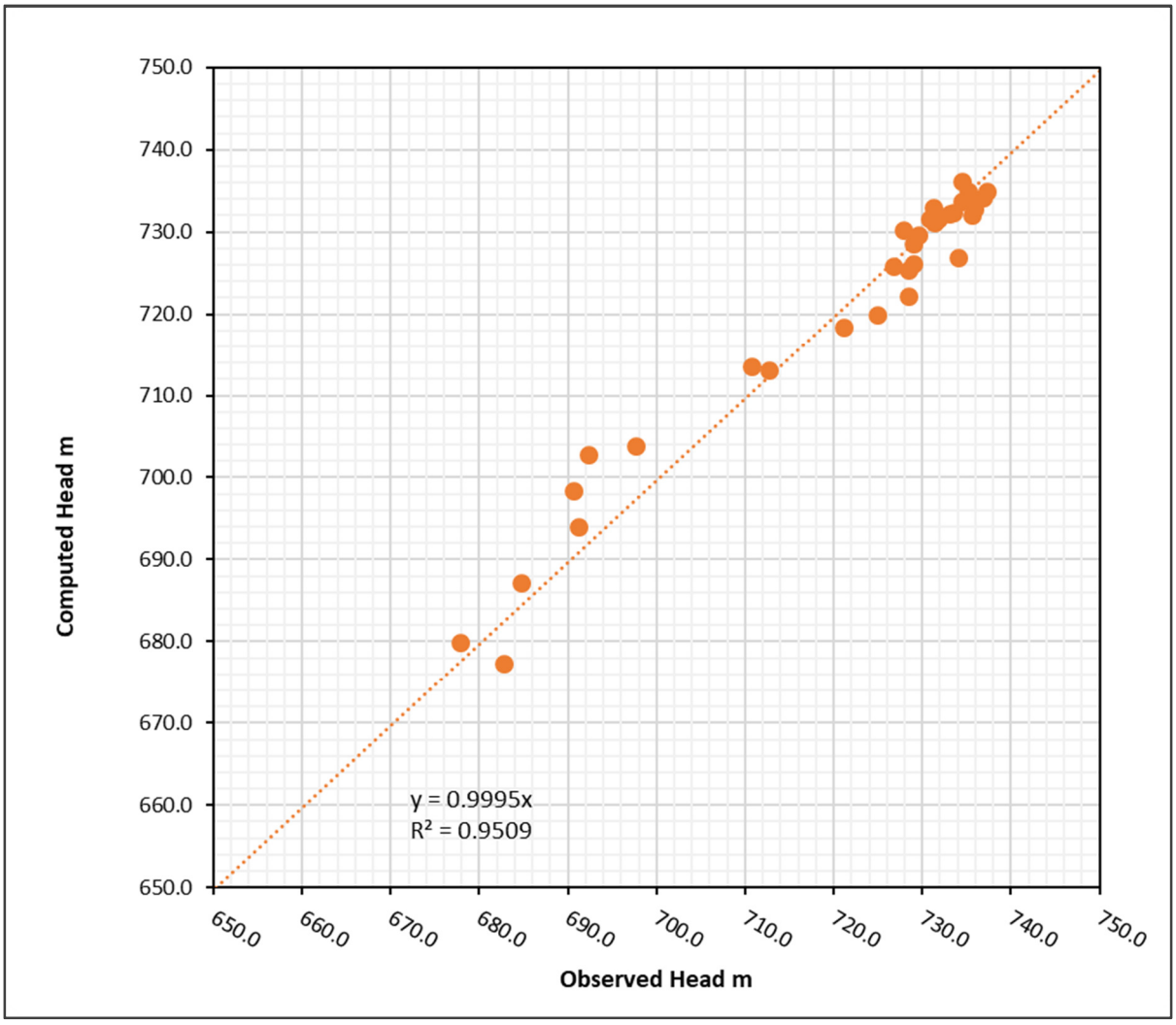

Figure 29: Measured versus Modelled Head Conditions, NTSF Tailings and Foundation Tb

Tailings Gradient Replication

CPtu derived pore water pressure data shown in Figure 20 are also used to assess whether the model is replicating the downward gradients observed in the field collected data. These results are shown in Figure 30. Visual comparison of these graphs indicates the model is replicating this process in all locations, at a similar scale to that observed.

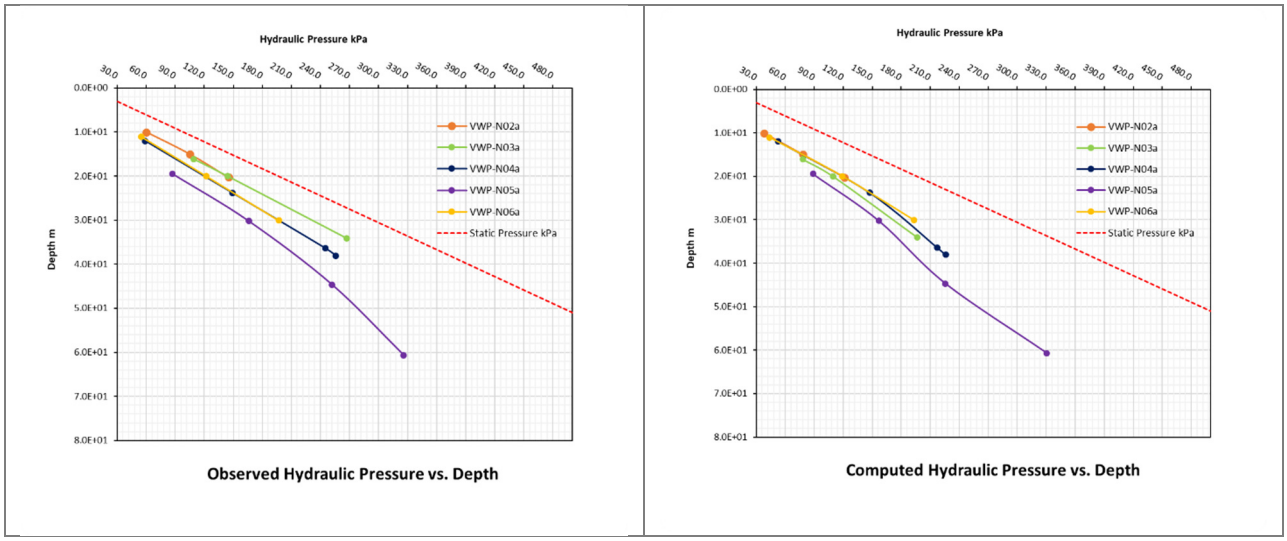

Figure 30: Comparison between Observed (left) and Computed (right) Tailings Gradients

NTSF Drain Flow Estimation

Model simulated total drain flow under steady state conditions for the calibrated model is estimated at 68.0 L/min. This is higher than 2018 measured data of 40 L/min to 50 L/min as the drain measurement does not collect all the seepage, whereas the modelled estimate captures seepage as a total loss form the model. The measured value therefore is considered to underestimates total. A summary of transient drain predictions from this feature is shown in Figure 31.

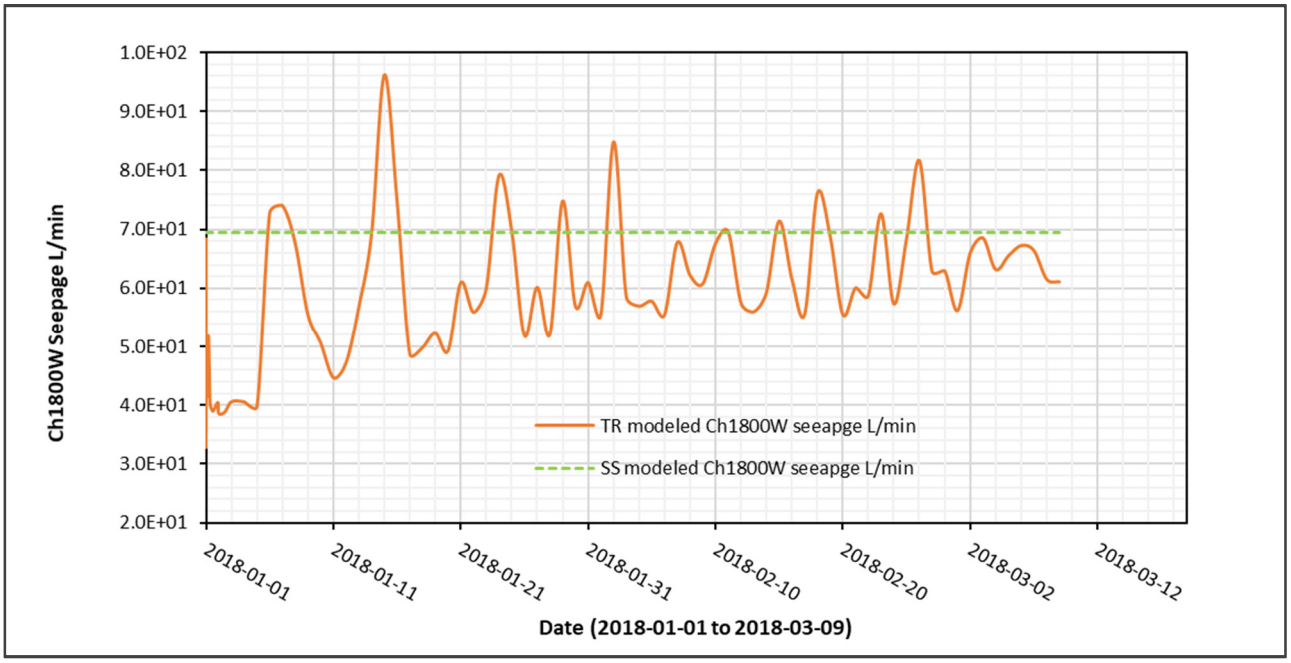

Figure 31: Transient Model Drain Flow Predictions, Ch1800W Drain

3.2.4 Model Results

3D Model Output

The results of the transient simulation are provided in a series of figures and cross sections between Figure 32 and Figure 37.

Generally, conditions are similar to those of the calibration model. Drainage via the Ch1800W drain remains a prominent visual component to phreatic conditions, particularly in the upper tailings sequence. The decant pond imposes a skew in these contours, and in lower levels of the model and foundation conditions the drainage effect of the Tertiary basalt becomes more prominent, as would be expected. The area of the slump event is located mid-way between the drainage effect to the east of the slump area, and the sub-crop of the Tertiary basalt.

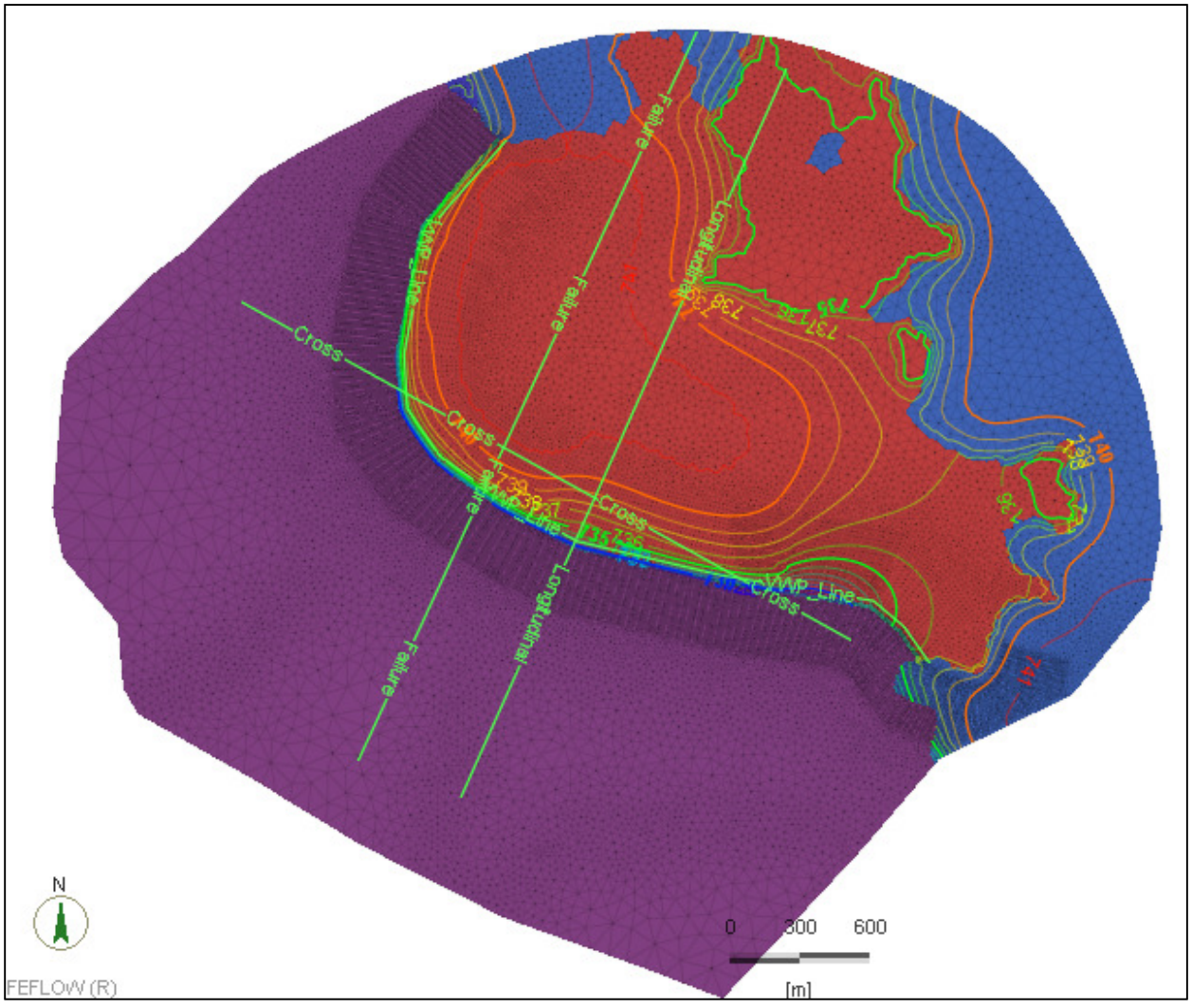

Figure 32: Transient 3D NTSF Model, Upper Layer Conditions, Time of Slump Event

A detailed image of the slump event failure section is provided in Figure 33. Modelling results suggest that the internal dam construction components appear to continue to perform as intended, with the phreatic surface predicted to be about 6-7 m below the Stage 10 dam crest,

and the phreatic condition above the Stage 3 crest elevation of about 718.5 m maintained behind (upstream) of the NTSF lifts.

Transient modelled drain discharge (Figure 31) fluctuates but remains within a relatively constant range for the six weeks or so preceding the failure date, and mostly below the steady state calibrated amount for this feature.

The climatic and dam raise conditions modelled do not appear to have created a disproportionate increase in either the phreatic condition of the tailings or drain flow estimation at the time of the slump event.

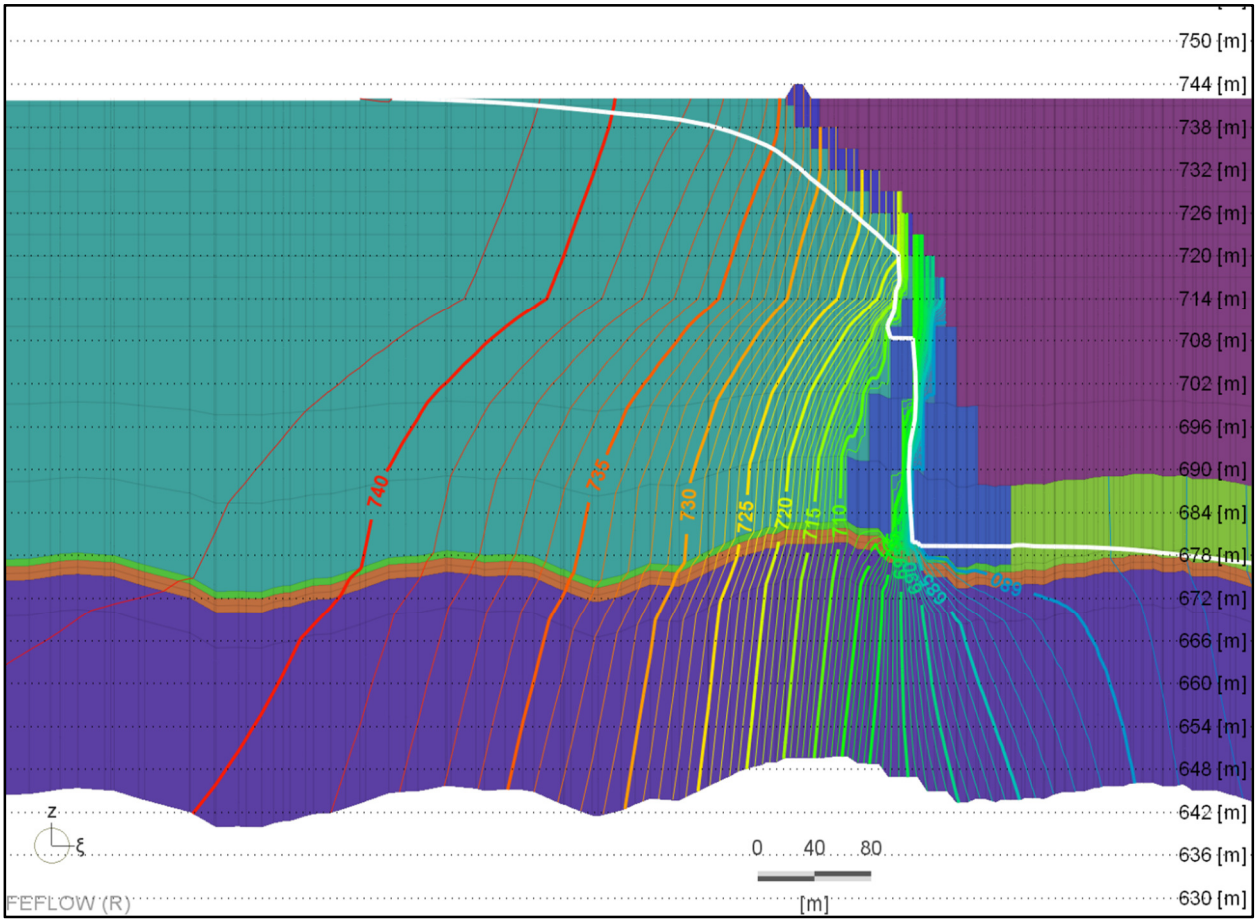

Figure 33: Detailed Piezometric Detail, Failure Section, Time of Slump Event

An important observation in Figure 32 is that visually the area of the slump coincides with the area of the NTSF which appears to experience the highest degree of saturation nearest to the dam (with exception of the western embankment). The detailed cross section (Figure 33) and the predicted drain discharge do not indicate that the phreatic condition has conceptually changed and has either encroached on the dam lifts or resulted in emergent seepage on the face. This is also consistent with the available monitoring data (Section 2.4.5) which confirms the same.

This area of the dam is simulated to have a higher degree of saturation than further to the east where drain effects are more prominent, but the dam construction elements built into the model appear to be continuing to manage the system. Further to the west, and around the western embankment, greater degrees of near dam saturation are noted, so this does not appear to be a

unique or singular observation, however it is visually prominent when compared with conditions toward the east.

The next four figures provide model predicted output for NTSF conditions in the lower sections of the system at the interface of the tailings system and the transition back into natural ground. The effect of the Tertiary basalt starts to be noted in layer 15 and is more visually prominent in lower layers; however due to the foundation preparation preventing this unit from creating a drainage effect in the tailings, as evident in NTSF performance data, this observation is relevant only below or downstream of the NTSF. The modelled phreatic conditions in the tailings, above the sub-crop of the Tertiary basalt, reflect the observation data and system performance discussed in Section 2.4.5

The Ch1800W drain which is a prominent feature throughout the tailings also increases in definition in lower elevations of the tailings as permeable strata associated with the pre-construction drainage assist in removing water from deeper areas of the system.

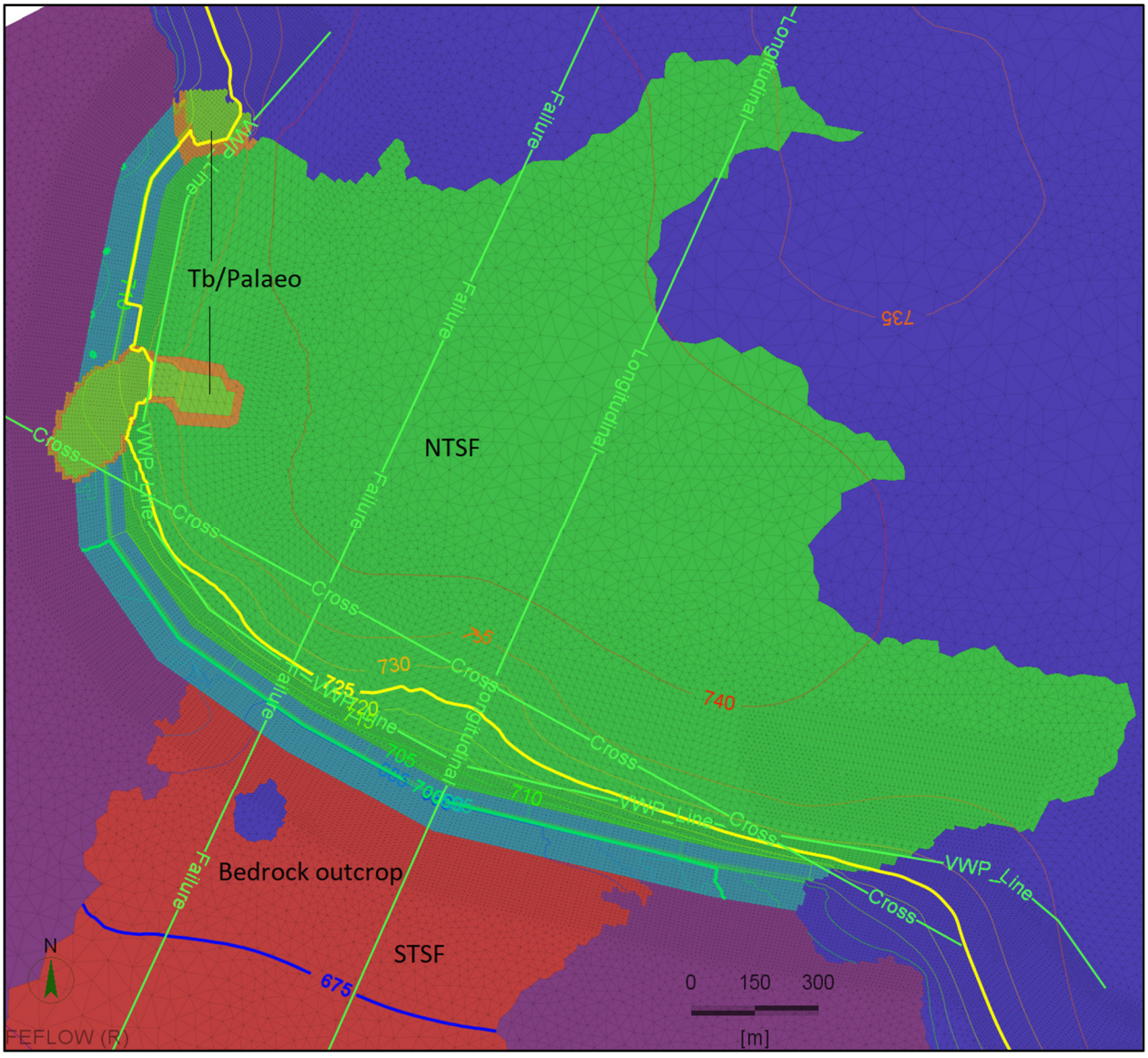

Figure 34: Transient Conditions & Geology, Layer 14, Base of NTSF, Time of Slump Event

Figure 35: Transient Conditions & Geology, Layer 15, Time of Slump Event

The imagery in Figure 34, Figure 35, Figure 36 and Figure 37 show predicted pressure conditions with increasing depth and transitioning geology, across model layers 14, 15, 16 and 17. The 725 m contour (yellow) and the 700 m contour (green) are useful visual guides in reviewing these figures to assess conditions with depth.

Below the tailings, underlying hydrogeological contrasts (for example, between the Tertiary basalt (high) and the Forrest Reef Volcanics, become dominant features on the shape of pressure conditions and the movement of groundwater. Tertiary basalt becomes more influential as a drain, as does the existing and covered Rodds Creek channel. Pressure contours indicate very little change in vertical gradients in the area of the slump.

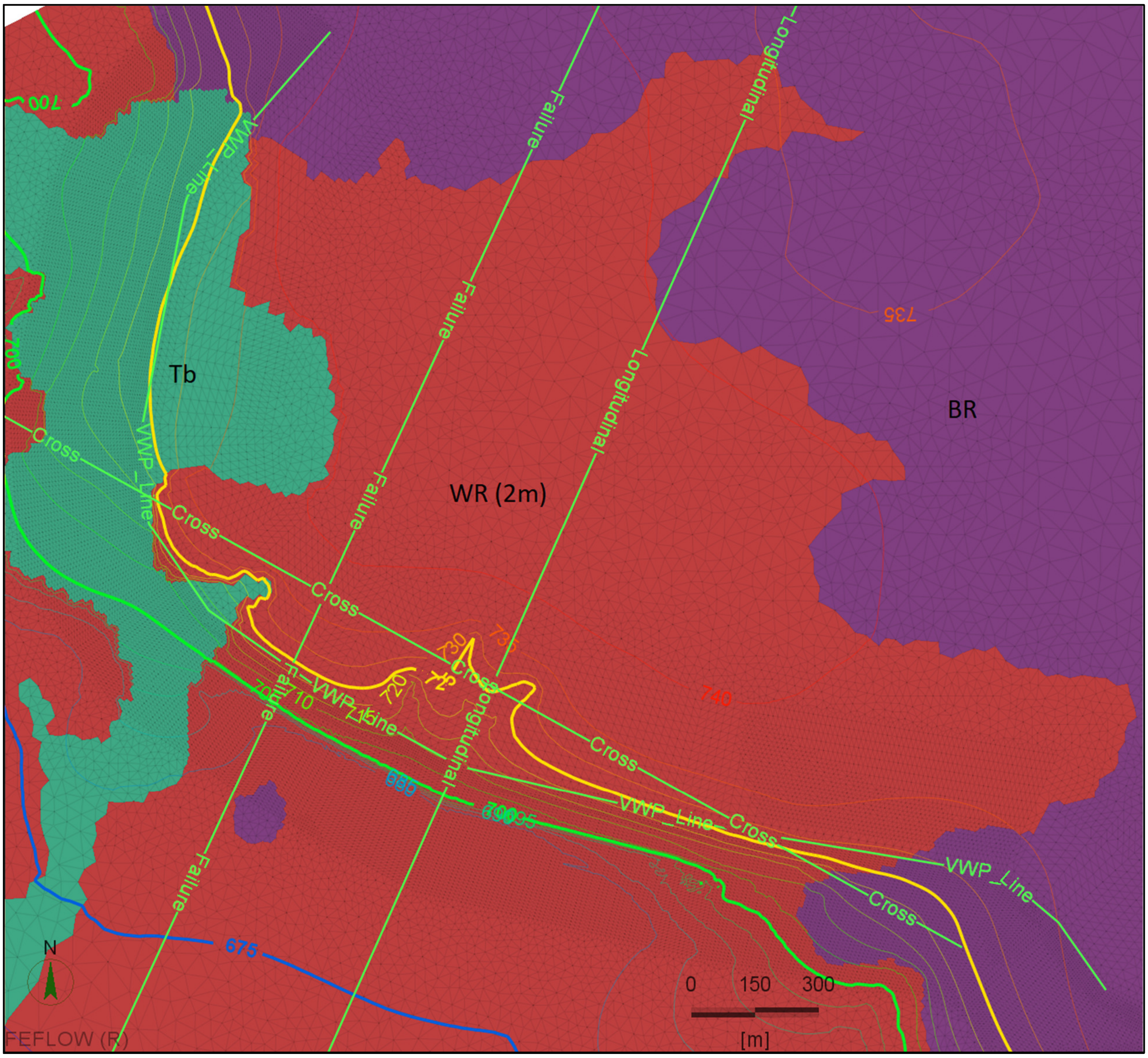

Figure 36: Transient Conditions & Geology, Layer 16, Time of Slump Event

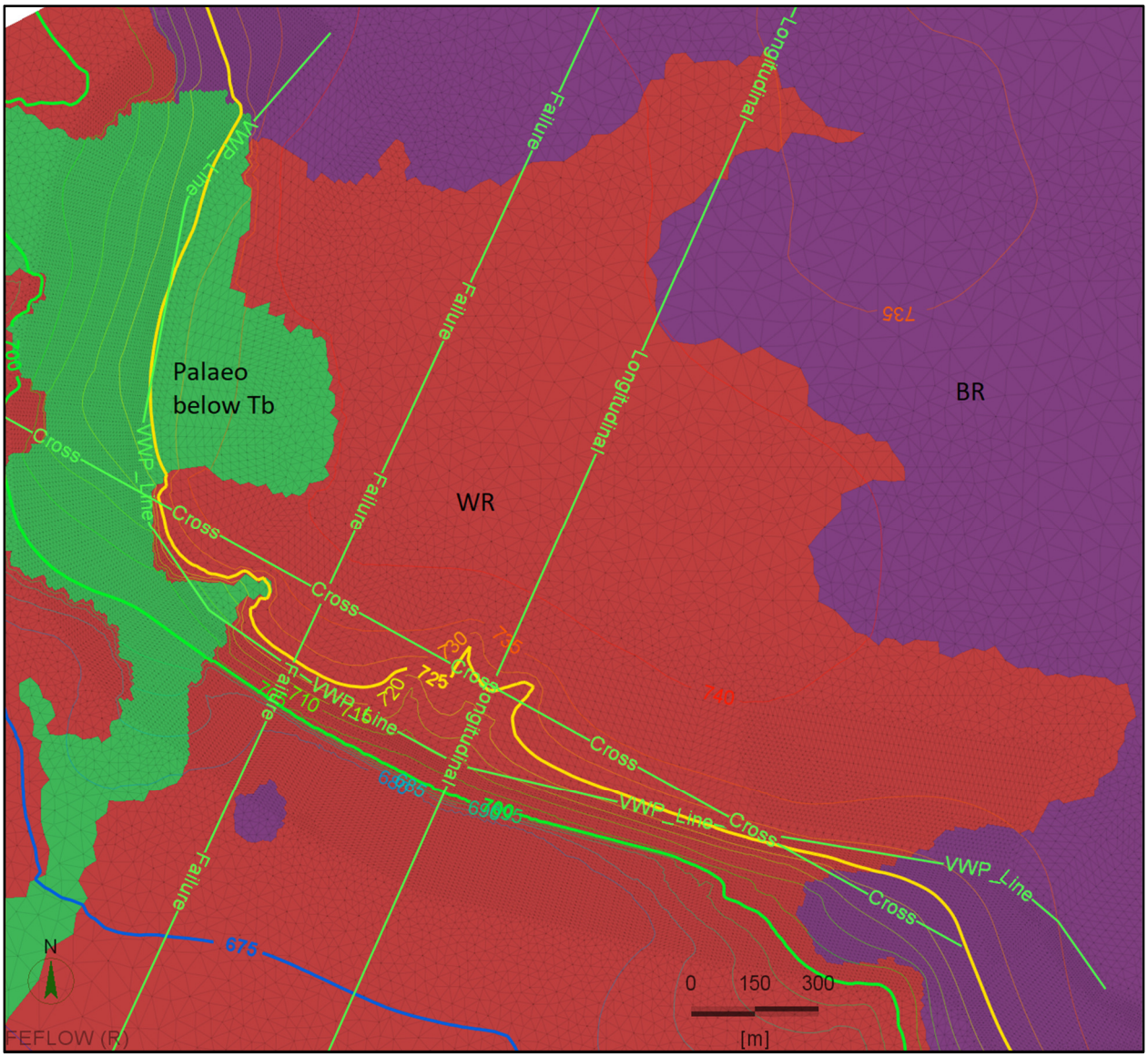

Figure 37: Transient Conditions & Geology, Layer 17, Time of Slump Event

3.3 3D Modelling Summary

A 3D model has been constructed to replicate performance of the NTSF in the period leading up to the slump event that occurred in March 2018. The model was constructed based on the conceptual understanding of the site described in Section 2 and informed through 2D modelling to assess prominent hydraulic concepts of greatest relevance to prediction of conditions inside the NTSF.

The model was calibrated to three primary performance criteria: piezometric conditions of the tailings, vertical gradients within the tailings derived from CPtu testing, and estimation of drain flow emerging from the Stage 3 underdrain. The model calibration was able to replicate each of these criteria through a manual and automated calibration process, and the model was then set up to simulate the Stage 10 construction from 1-January-2018 to the time of the slump event, under transient conditions.

During the period of transient simulation, no significant rainfall or creek flow was noted, pressure conditions within the tailings did not exhibit any abnormal trends compared with prior or recent data, and the decant pond elevation was not substantially increased. Model simulated conditions for the time of failure do not indicate any occurrence of new or abnormal seepage emergence on the dam face, and the effect of the Stage 3 underdrain maintained phreatic conditions upstream of the dam lifts. Review of deeper predicted pressure conditions does not indicate generation of higher pressures at the area of the slump.

The data from this simulation were compiled and forwarded for use in other elements of the study. The simulation did not consider failure of any element of the dam construction and modelled the conditions as close to actual as possible. No sensitivity or uncertainty analysis has been completed.

4 REGULATORY QUESTION RESPONSE

Two points in relation to the seepage and hydraulic performance of the NTSF have been raised by the regulator. These, and comments addressing each, are provided in the following, noting some section reproduction is provided in the following to permit the response to be located in one location:

4.1 Question 1

> ***"an assessment as to the contribution that seepage has had on the integrity of the NTSF wall at the site of the wall slump event"***

4.1.1 Groundwater Modelling Analysis

Groundwater modelling was undertaken to construct a best estimate of phreatic conditions in the NTSF at the time of failure. A 3D model was constructed and calibrated to NTSF performance observations, and then run under transient conditions using true meteorological records to estimate phreatic conditions and seepage at the location of the slump, at the time of the event.

This work is documented in detail in this report, with the modelling results discussed in Section 3.2.4. A summary, specifically related to seepage at the NTSF wall at the site of the slump event, is provided:

- The climatic and dam raise conditions modelled do not appear to have created a disproportionate increase in either the phreatic condition of the tailings or drain flow estimation at the time of the slump event.
- Visually, although the area of the slump coincides with the area of the NTSF which appears to experience the highest degree of saturation, dam construction elements intended to manage water and built into the model appear to be continuing to manage the system. In this regard, the model results do not indicate that saturated conditions have either encroached on the dam lifts or resulted in new emergent seepage on the dam face.
- Model simulated conditions for the time of failure do not indicate any occurrence of new or abnormal seepage emergence on the dam face, and the effect of the Stage 3 underdrain maintained phreatic conditions upstream of the dam lifts.

4.1.2 Monitoring Data Analysis

Piezometric records form a substantial component of base information to this investigation, through informing the assessment of the conceptual system, and calibrating the 3D groundwater modelling. A detailed review of piezometric data is provided in Section 2.4.5, with data recorded for the period leading up to the slump event inside the NTSF reproduced for about 15 months preceding the slump event shown in Figure 38. Decant pond elevation for the same period is also shown:

- VWP-001 & VWP-002 are located along the western embankment. Levels in VWP-002 do not include the immediately preceding period of the slump. VWP-001 shows a rise in levels coincident with decant pond elevation increase.

- VWP-003 is located west of the slump event and over Tertiary basalt. The record stops in November 2017 on a downward trend. This site may have experienced a rise in levels after this time as observed in other locations.
- VWP-004 is located close to and east of the slump. Pressure ranges between 730.5 mRL and 732.8 mRL, with the high value about 11 m below the Stage 10 crest. This site indicates a change of 2m rise from October to March 2018, which may be responding to two stresses resulting from the same trigger (decant pond elevation):
  - Decant pond increases over this period to a high of about 735 mRL, and,
  - Secondary response to increase in levels across the TSF which is noted along the western embankment and upstream of this site in VWP-N005, with a high of about 735.8 mRL. The rate of rise between this VWP and VWP-003 is very similar. A rise is also noted in VWP-005 although this site remains strongly affected by the drain discharge.
- VWP-005, VWP-006 and VWP-007 are located further to the east, with VWP-005 closest to the main area of drain impacts.

All sites with 2018 data observed a similar rising trend in the 6 months of late 2017 / early 2018, probably attributed to the progressive rising of the NTSF decant pond and the resulting re-saturation of the general tailings profile throughout the system. VWP levels generally show 1-2 m of vertical variance, and all remain 8-14 m below the Stage 10 crest elevation. For those VWPs with early time data, the elevation of conditions at the time of the slump event are similar to their conditions at the earlier 'high' in early 2017, when the crest elevation and the decant pond operating level were both lower.

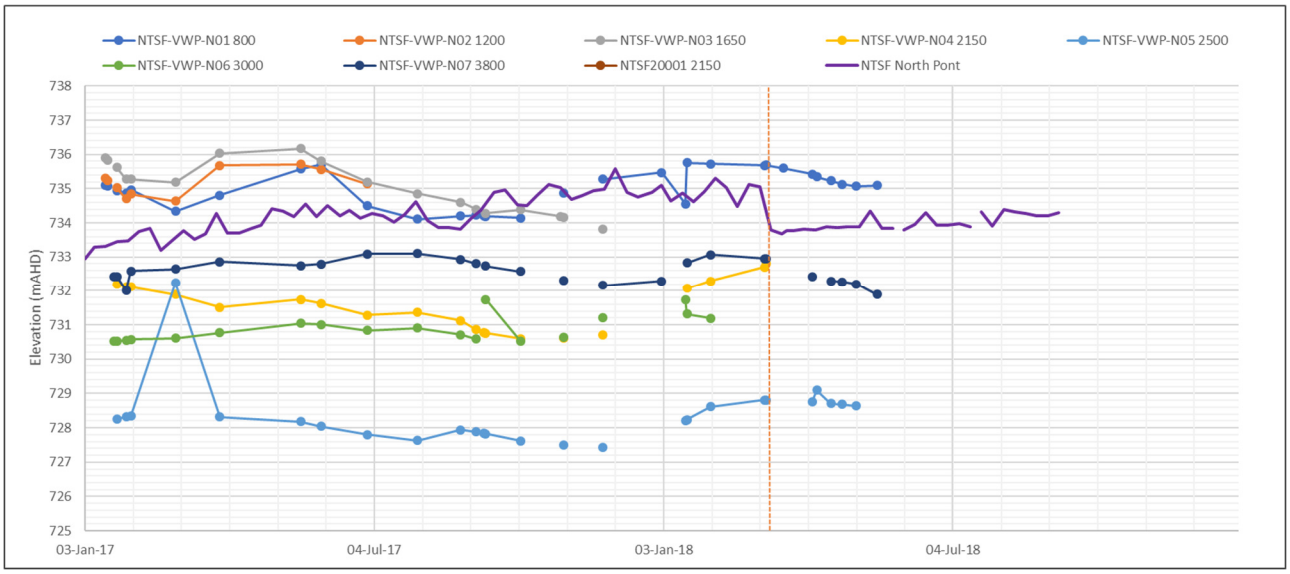

Figure 38: VWP Data NTSF, 2018 and 2018, and NTSF Decant Pond Elevation

In the months preceding the slump, no substantial rainfall was noted (Figure 7), and creek flows measured at the mine did not exhibit any significant events (Figure 8). Changes to conditions discussed above in the VWPs are consistent with pond elevation increases and re-saturation of the tailings profile across the whole NTSF. This hydraulic response mechanism also reinforces the

relevance of the decant pond elevation as a key boundary condition in the modelling reported earlier.

4.1.3 Question Response Summary

Summary points from this discussion are:

1. Modelling, informed by monitoring data and detailed conceptualisation of the tailings and foundation conditions, does not predict additional emergent seepage on the dam face at the time of the slump. This modelling also does not predict development of phreatic conditions or drain flows which have not been previously observed at the site;
2. Piezometric observation data shows the tailings system responding to decant pond level. Pressure elevations in VWPs at the time of the slump are similar to elevations observed in early January 2017, when the dam crest was 3 m lower, and the decant pond 2m lower, than conditions at the time of the slump.

4.2 Question 2

"an assessment of historical piezometer data for the NTSF and the contribution that groundwater levels has had on the integrity of the NTSF wall at the site of the wall slump event"

Understanding the potential impact of groundwater levels on the stability of the dam, at the location of the slump event, is very difficult because of the hydrogeological influence of the STSF on conditions at and near the site.

This question is addressed in three parts: observation of conditions inside the NTSF as they relate to the NSTF and STSF decant ponds, observation of groundwater level responses in proximal and distal monitoring bores as reported elsewhere in this report, and consideration of hydrogeological conditions as they relate to the construction of the NTSF at the slump location.

4.2.1 Groundwater Modelling Analysis

The groundwater model was constructed in a manner to permit review of predicted conditions at the time of the slump event in deeper, natural geology. These results are shown and discussed earlier in this report in Section 3.2.4. Table 8 provides a numerical summary of results with deepening strata at three locations near the slump. These data indicate that head differentials across layers are generally small, further locational observation discussion on these is provided:

- Upstream, downward gradients are maintained across both layer transitions
- At the dam, an upward gradient with a head differential of about 1.3 m is noted from layer 16 into layer 15 (weathered rock to the base of tailings / clay liner). Fresh rock to weathered rock contact indicates a downward gradient with a head differential of 0.15 m.
- At the downstream area, the gradient between layer 15 and 16 is almost negligible, very weakly downward gradient of <0.01 m, and an upward gradient from fresh rock into weathered rock of ~0.07 m head differential is predicted.

- The scale of these model predicted head differentials are well within the range of measured pressure changes within the NTSF tailings, and naturally fluctuating groundwater conditions for proximal and distal monitoring locations.

Table 8: Summary Pressure Conditions with Depth, 9-March-2018, NTSF Slump Location

Location	Model Layer	Computed Head (m)	Vertical Gradient (down +ve, up -ve)	Node Locations
Upstream	15	715.2535	L15 > 16, +0.2966 m L16 > 17, +0.1621 m	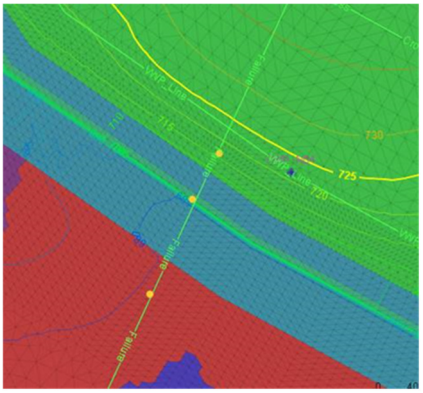
	16	714.9569		
	17	714.7948		
Dam	15	693.3675	L15 > 16, -1.2872 m L16 > 17, +0.1525 m	
	16	694.6547		
	17	694.5022		
Downstream	15	679.2957	L15 > 16, +0.0039 m L16 > 17, -0.0695 m	
	16	679.2918		
	17	679.3613		

4.2.2 Monitoring Data Analysis

Figure 39 shows post-slump-event performance of the dam construction components as they relate to foundation geology conditions in the Tertiary basalt. Dam construction components and the relative head of VWP data at these locations indicate the dam continued to manage the seepage, and that water into the basalt was not causing problematic or high-pressure conditions in that sequence. This is consistent with the concept that the basalt will act as a natural drain to water which enters it from the NTSF, as long as the recharge from the NTSF does not overcome the ability of the basalt to naturally drain.

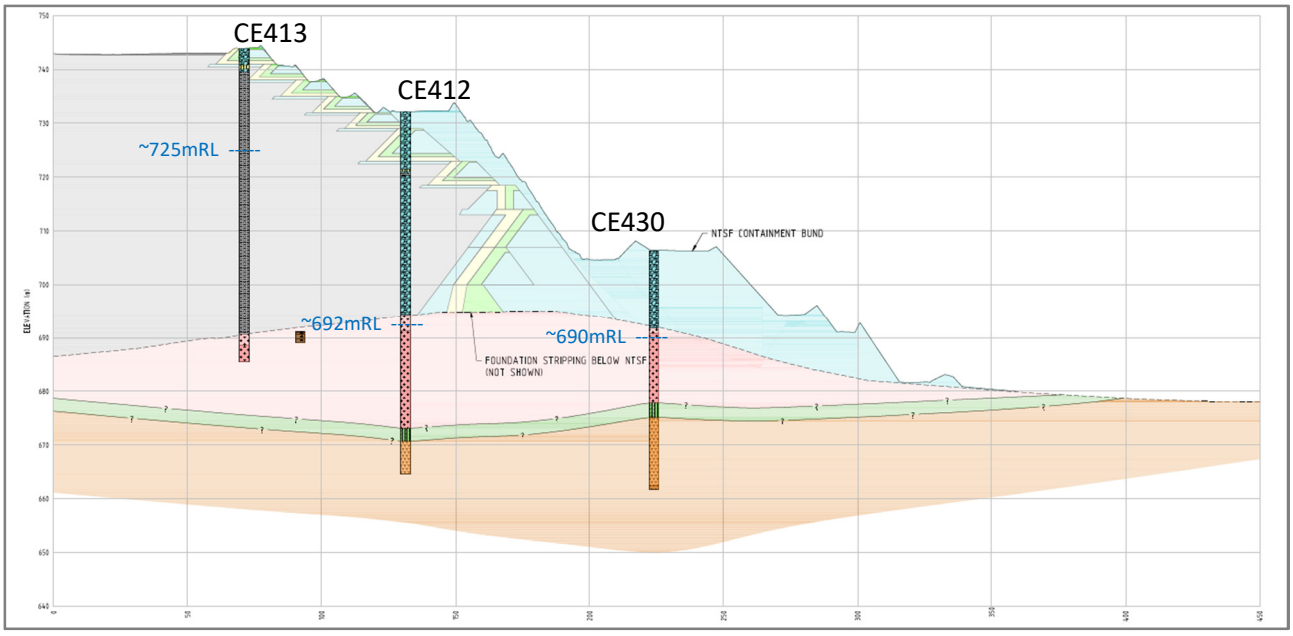

Figure 39: 2018 Installed Tertiary Basalt VWPs, CE series holes (Hatch, 2019)

Decant pond conditions in the STSF have observed a much slower rate of rise than those of the NTSF. In the 2 years preceding the slump, the STSF decant pond has observed 2.2 m of rise, while the NTSF has observed 4.4 m. During 2018 in the period leading up to the slump event, the STSF decant pond varied across a range of 0.58 m: the maximum elevation of STSF decant pond levels for this period is 676.6 m, which is below the starter dam for the NTSF (Figure 40), and approximately 14 m lower than the piezometric conditions observed in CE430. These levels are also lower than three Forrest Reefs Volcanics VWPs installed after the slump, at CE405, CE406 and CE415, which have a range of pressure elevations between 678 m and 685 m, which are 1-10 m below their installed collar elevations. These values although similar, are not consistently close to pond elevation in the STSF, and they do not indicate direct and efficient connectivity into the underlying volcanics.

There are five hydrographs presented for bores completed in natural strata and proximal to the NTSF. These are MB18, MB19A/MB19B, MB23 and MB24 and their hydrograph data are reproduced in Figure 40. These bores are immediately west and south west of the NTSF, close to the abutment of the STSF into the southern NTSF embankment. All the bores are within 500 m of the toe of the western or southern embankment of the south west corner of the NTSF.

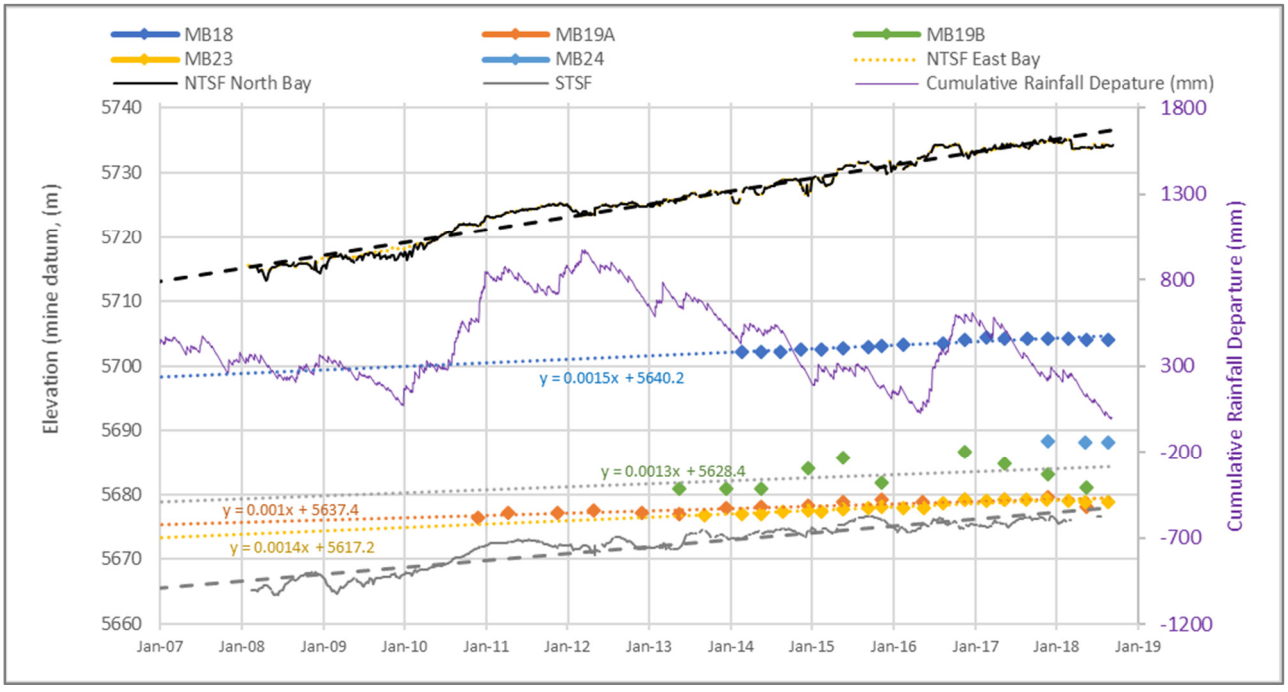

Figure 40: NTSF Proximal Foundation Head Monitoring, 2007 to 2018

Long term trends for four of these bores are shown and indicate a consistent head increase of 0.35 m to 0.55 m per year. This trend appears to be present for several years for a number of the bores and may be attributed to either or both of the NTSF and STSF operations. No unique spikes in the record due to sudden recharge events such as rainfall or creek flow are evident, although this may be a function of the gap between records. These data indicate translation of the developing pressure response from raising of the NTSF (and the STSF) into local groundwater conditions within the Silurian and Ordovician strata.

The absence of local peaks in the data (exception being MB19B which is the shallowest completion at 7.6 m) and the large difference in vertical elevations between the bores and the decant pond elevation in the NTSF (30 m-50 m), indicates that this trend is a muted pressure response to the TSF's presence rather than an indicator of direct and efficient hydraulic continuity. There do not appear to be any late time increases in the trends in these data either – sites MB18, MB19A and MB23 may be observing a flattening of their response in 2018.

A similar exercise was conducted for a series of distal bores and is discussed earlier in this report. All of these distal bores however experienced trends consistent with regional conditions and did not show the same pressure response as the proximal bores to the tailings dams. These data are indicating no translation of the NTSF / STSF pressure effects, placing the likely lateral extent of NTSF pressure impact to be in the range of 500 m to 800 m from the TSF complex.

To bring this into context and to consider the potential for TSF operations to impact conditions in natural groundwater, a summary of depth to water records is provided for both the proximal and distal data (Table 9). Over the past three years, all the distal bores experienced an increase in the depth of water from collar, consistent with the regional trend of below average rainfall conditions. Pressure translation from the TSFs has not only not occurred, but groundwater levels have fallen.

For the proximal sites, three of the five locations have experienced a rise in groundwater levels of between 0.4 m and 1.3 m between 2015 and 2018, lower than the rate of rise of either of the TSFs. None of these bores are approaching artesian conditions, two are observing a decline in groundwater level.

Table 9: Averaged Depth to Water Records, 2015 and 2018

Bore		Ground Elevation	2015 Depth To Water Average (mbCol)	2018 Depth To Water Average (mbCol)	Change (+ve = rise -ve = fall)	Notes
MB18	Proximal	722	19.6	18.3	1.3	
MB19A		688.12	9.4	10.3	-0.9	
MB19B		688.14	4.6	7.3	-2.7	
MB23		703.49	26	24.9	1.1	
MB24		696.44	9.7	9.3	0.4	
MB25	Distal	668.9	14.2	15.8	-1.6	
MB81		657.48	6.5	7.4	-0.9	
MB85		676.50	15.8	16.7	-0.9	First reading 15/7/17
MB86		685.650	13.4	14.7	-1.3	First reading 15/7/17
MB87		693.56	18.4	19.2	-0.8	First reading 15/7/17
MB90		644	30.4	30.4	0	First reading 17/8/18

4.2.3 Question Response Summary

Summary points from this discussion are:

1. Modelling, informed by monitoring data and detailed conceptualisation of the tailings and foundation conditions, does not predict generation of substantial vertical pressure gradients across the area of the slump at the time of the event.

2. Focussed review of conditions from the model at the area of the slump indicate head conditions with depth do not vary substantially, a mix of upward and downward gradients are predicted, with their scale within the range of regional groundwater monitoring and NTSF tailings head variability.

3. Monitoring indicates that natural groundwater conditions in low permeability strata are experiencing a muted response to TSF operations at the NTSF and the STSF, observed as a consistent increase in their levels over a long period of time. None of these sites appear in direct and efficient hydraulic connection with either of the NTSF or STSF decant ponds, and none are artesian in hydrogeological nature.

4. Monitoring data (post slump event) indicates that natural groundwater conditions in the Tertiary basalt near the slump event are currently not under confining pressure, and that the basalt appears to be operating as an effective drain to seepage which does bypass the dam components designed for seepage and pressure control.

5 CLOSURE

This report is an instrument of service of Klohn Crippen Berger Ltd. The report has been prepared for the exclusive use of Ashurst Australia (Client) for the specific application to the Newcrest - ITRB Report on NTSF Embankment Failure Hydrogeology Assessment. The report's contents may not be relied upon by any other party without the express written permission of Klohn Crippen Berger. In this report, Klohn Crippen Berger has endeavoured to comply with generally-accepted professional practice common to the local area. Klohn Crippen Berger makes no warranty, express or implied.

Yours truly,

KLOHN CRIPPEN BERGER LTD.

Chris Dickinson, RPGeo (Hydrogeology)
Principal Hydrogeologist

CD:CD

REFERENCES

AGE. (2009). *Cadia East project Groundwater Assessment, prepared for Cadia Holdings Pty Limited.* Ref: G1383/D.

AGE. (2013). *Cadia East Mine Uodate of the Groundwater Model.*

Hatch. (2018). *Cadia Mine NTSF Apprndix B, NTSF History.*

Newcrest Mining Ltd. (2016?). *Cadia Architeecture (5-slide Power Point Presentation).*

NGMA. (1998). *Bathurst 1:250,000 Geology sheet SI55-8, 2nd Ed.*

Pogson D.J. & Watkins J.J. (1998). *Bathurst 1:250,000 Geological Survey Sheet SI/55-8: Explanatory Notes.* Geological Survey of New South Wales, Sydney, xiv + 430 pp.

Wilson, A. (2003). *The Geology, Genesis and Exploration Context of the Cadia Gold-Copper Porphyry Deposits.*